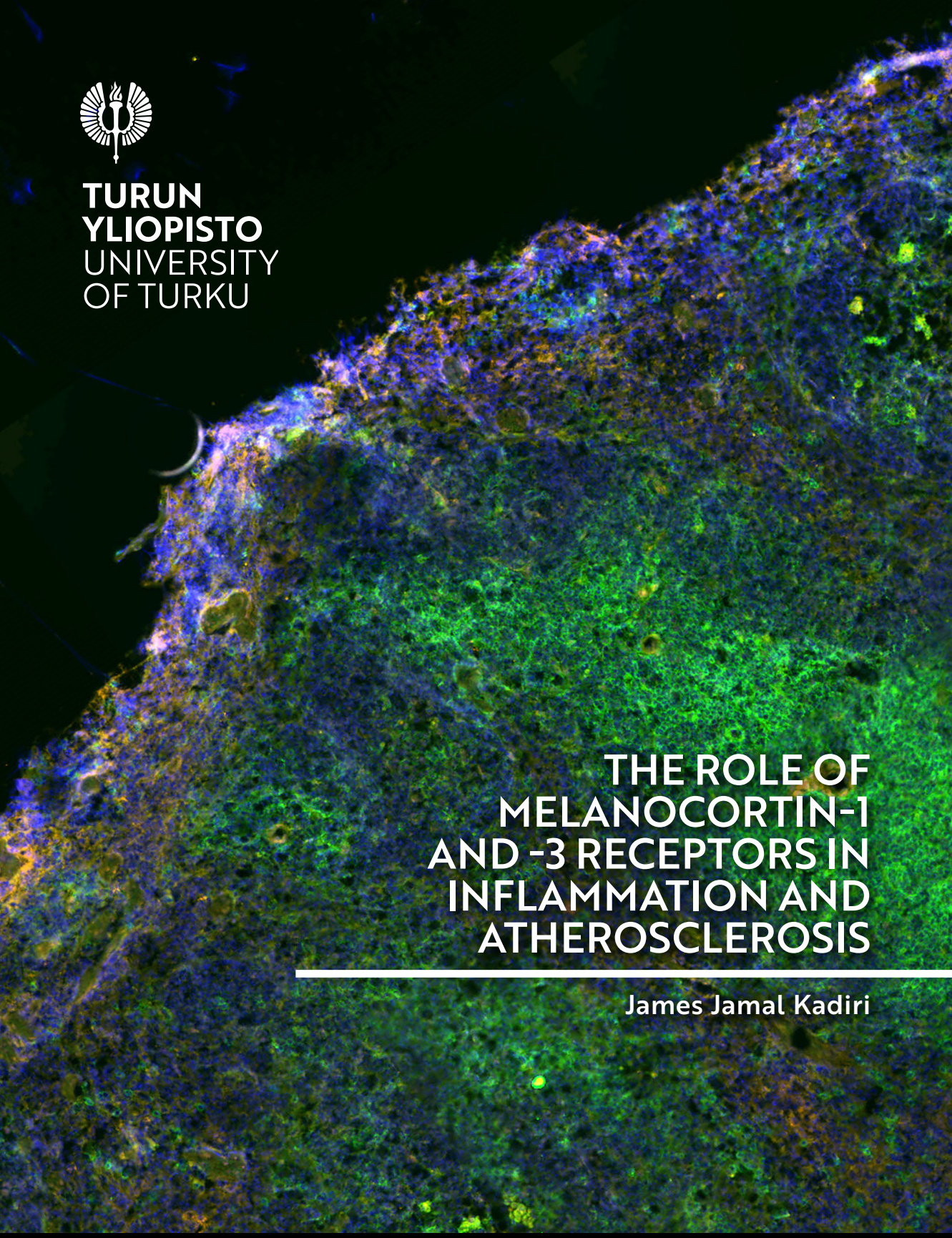

TURUN YLIOPISTO
UNIVERSITY OF TURKU

THE ROLE OF MELANOCORTIN-1 AND -3 RECEPTORS IN INFLAMMATION AND ATHEROSCLEROSIS

James Jamal Kadiri

TURUN YLIOPISTON JULKAISUJA – ANNALES UNIVERSITATIS TURKUENSIS
SARJA – SER. D OSA – TOM. 1705 | MEDICA – ODONTOLOGICA | TURKU 2023

TURUN
YLIOPISTO
UNIVERSITY
OF TURKU

THE ROLE OF MELANOCORTIN-1 AND -3 RECEPTORS IN INFLAMMATION AND ATHEROSCLEROSIS

James Jamal Kadiri

TURUN YLIOPISTON JULKAISUJA – ANNALES UNIVERSITATIS TURKUENSIS
SARJA – SER. D OSA – TOM. 1705 | MEDICA – ODONTOLOGICA | TURKU 2023

University of Turku

Faculty of Medicine
Institute of Biomedicine
Pharmacology, Drug Development and Therapeutics
Drug Research Doctoral Programme

Supervised by

Docent Petteri Rinne, PhD
Institute of Biomedicine
University of Turku
Turku, Finland

Professor Eriika Savontaus, MD, PhD
Institute of Biomedicine
University of Turku
Turku, Finland

Reviewed by

Doctor Trinidad Montero-Melendez
Queen Mary University of London
The William Harvey Research Institute -
Faculty of Medicine and Dentistry
London, United Kingdom

Professor Jaana Rysä
University of Eastern Finland
Faculty of Health Sciences
School of Pharmacy
Kuopio, Finland

Opponent

Adjunct Professor Katariina Öörni
Wihuri Research Institute
Atherosclerosis Group
Helsinki, Finland

The originality of this publication has been checked in accordance with the University of Turku quality assurance system using the Turnitin OriginalityCheck service.

Cover image: James Jamal Kadiri

ISBN 978-951-29-9242-3 (PRINT)
ISBN 978-951-29-9243-0 (PDF)
ISSN 0355-9483 (Print)
ISSN 2343-3213 (Online)
Painosalama, Turku, Finland 2023

“Seek for knowledge and wisdom, or whatever the vessel from which it flows,
you will never be the loser”
(Muhammad pbuh)

UNIVERSITY OF TURKU
Faculty of Medicine
Institute of Biomedicine
Pharmacology, Drug Development and Therapeutics
JAMES JAMAL KADIRI: The role of melanocortin-1 and -3 receptors in inflammation and atherosclerosis
Doctoral Dissertation, 156 pp.
Drug Research Doctoral Programme
April 2023

ABSTRACT

The melanocortin system comprises the endogenous melanocortin peptides adrenocorticotropic hormone (ACTH) and melanocyte-stimulating hormones (α-, β- & γ-MSH) as well as their five cognate receptors (MC1R – MC5R). These peptides are post-translational products of the proopiomelanocortin precursor hormone and mediate multiple biological processes including skin pigmentation, energy homeostasis and inflammation. Melanocortins elicit potent anti-inflammatory actions by activating MC1R and MC3R, which are widely expressed in different leukocyte subsets. Atherosclerosis is a chronic inflammatory disease characterized by lipid and leukocyte accumulation in arterial walls that leads to the development of atherosclerotic plaques and eventually to acute complications such as stroke and myocardial infarction. Melanocortins have been previously shown to suppress inflammation in experimental atherosclerosis. The primary aim of this thesis was to investigate the specific roles of MC1R and MC3R in experimental atherosclerosis and its associated inflammatory processes.

To address this objective, the contribution of MC1R to the development of atherosclerosis was investigated in apolipoprotein E deficient (*Apoe*$^{-/-}$) mice, a widely used mouse model of atherosclerosis. *Apoe*$^{-/-}$ mice carrying a mutated and dysfunctional MC1R (*Mc1r*$^{e/e}$) globally showed accelerated atherosclerosis that was associated with enhanced arterial monocyte accumulation and perturbed cholesterol metabolism. Secondly, the specific contribution of leukocyte MC1R to atherosclerosis was examined *via* transplantation of *Mc1r*$^{e/e}$–derived bone marrow into *Apoe*$^{-/-}$ mice. Leukocyte-specific MC1R deficiency significantly increased total leukocyte counts and particularly $CD4^+$ T cells in the spleen and blood, but it did not affect the development of atherosclerosis or plaque vulnerability. Thirdly, the therapeutic effects of selective activation of MC3R were explored in *Apoe*$^{-/-}$ mice. Chronic treatment with the potent MC3R agonist [D-Trp^8]-γ-MSH suppressed systemic inflammation and reduced leukocyte counts in the blood and aorta.

In conclusion, this thesis work advances our understanding of the significant roles of MC1R and MC3R in modulating lipid metabolism, inflammatory responses and leukocyte behavior in the context of experimental atherosclerosis.

KEYWORDS: melanocortin, melanocortin receptor, atherosclerosis, inflammation, leukocytes

TURUN YLIOPISTO
Lääketieteellinen tiedekunta
Biolääketieteen laitos
Farmakologia, lääkekehitys ja lääkehoito
JAMES JAMAL KADIRI: Melanokortiini-1 ja -3 reseptoreiden merkitys ateroskleroosissa ja siihen liittyvissä tulehdusvasteissa
Väitöskirja, 156 s.
Lääkekehityksen tohtoriohjelma
Huhtikuu 2023

TIIVISTELMÄ

Melanokortiineihin lukeutuvat α-, β- ja γ-melanosyyttejä stimuloiva hormoni (MSH) sekä adrenokortikotropiini (ATCH), jotka säätelevät tärkeitä fysiologisia toimintoja kuten ihon pigmentaatiota, elimistön energiatasapainoa ja tulehdusvasteita sitoutumalla G-proteiinikytkentäisiin melanokortiinireseptoreihin, joita on tunnistettu 5 eri alatyyppiä. Näistä alatyypeistä erityisesti melanokortiini 1 (MC1-R) ja 3 (MC3-R) reseptorin aktivaatio hillitsee elimistön tulehdusvasteita ja suojaa tulehduksellisia sairauksia kuten valtimotautia eli ateroskleroosia vastaan, jossa keskeisenä sairautta edistävänä tekijänä on pitkittynyt tulehdustila valtimoiden seinämässä. Tämän väitöskirjatutkimuksen tavoitteena oli tutkia tarkemmin MC1-R ja MC3-R alatyyppien merkitystä ateroskleroosin kehittymisessä sekä siihen liittyvien tulehdusvasteiden säätelyssä.

Hyödyntämällä ateroskleroosille herkkää apolipoproteiini E poistogeenistä (*Apoe*$^{-/-}$) hiirimallia havaittiin, että MC1-R:n geneettinen puutos tässä mallissa voimistaa ateroskleroottisten plakkien muodostusta sekä muokkaa niiden rakennetta hauraammaksi. Tätä ilmiasua selittävät osaltaan verenkierron sekä valtimoiden kohonneet valkosolutasot sekä häiriintynyt kolesterolin ja sappihappojen aineenvaihdunta. Toisessa osatyössä MC1-R:n geneettinen puutos kohdennettiin veren valkosoluihin luuydinsiirron avulla ja tutkittiin sen vaikutusta ateroskleroosin kehittymiseen. Valkosoluihin kohdennettu MC1-R:n puutos nosti merkittävästi valkosolujen ja erityisesti lymfosyyttien määrää verenkierrossa ja muissa kudoksissa vaikuttamatta kuitenkaan ateroskleroottisen plakkien muodostumiseen. MC1-R:n puutos myös heikensi valkosolujen liikkumiskykyä tulehdusalueille, mikä saattaa selittää sen, että veren kohonnut valkosolumäärä ei vaikuttanut ateroskleroosin kehittymiseen tässä hiirimallissa. Kolmannessa osatyössä tutkittiin MC3-R alatyyppiin kohdennetun lääkehoidon terapeuttisia vaikutuksia *Apoe*$^{-/-}$ hiirimallissa ja havaittiin sen madaltavan veren ja aortan valkosolumääriä sekä verenkierron tulehduksellisia merkkiaineita. Lääkehoito ei kuitenkaan vaikuttanut ateroskleroottisten plakkien muodostumiseen tai niiden rakenteeseen. Kokonaisuudessaan väitöskirjatyön löydökset syventävät ymmärrystämme melanokortiinien ja niiden reseptorien vaikutuksista tulehdusvasteiden sekä valkosolujen määrän ja niiden toiminnan säätelyssä. Nämä löydökset lisäksi tukevat melanokortiineihin liittyvää lääkekehitystyötä tulehduksellisissa sairauksissa ja auttavat ymmärtämään melanokortiinireseptoreiden potentiaalia lääkekehityskohteena ateroskleroosin hoidossa.

AVAINSANAT: Melanokortiinit, melanokortiinireseptori, ateroskleroosi, tulehdus, valkosolut

Table of Contents

Abbreviations

ABC	Adenosine triphosphate-binding cassette transporters
ACTH	Adrenocorticotropic hormone
Apo	Apolipoprotein
ASCVD	Atherosclerotic cardiovascular disease
BM	Bone marrow
BMT	Bone marrow transplantation
cAMP	Cyclic adenosine monophoshate
CAD	Coronary artery disease
CD	Cluster of differentiation
CLIP	Corticotrophin-like intermediate peptide
CVD	Cardiovascular disease
[D-Trp^8]-γ-MSH	[D-Trp^8]-gamma-melanocyte-stimulating hormone
END	Endorphin
HFD	High-fat diet
i.p	Intraperitoneal injection
JP	Junctional peptide
LDL	Low-density lipoprotein
LPH	Lipotropic hormone
Ly6C	Lymphocyte antigen 6 complex
MC	Melanocortin
MCR	Melanocortin receptor
MSH	Melanocyte-stimulating hormone
MT-II	Melanotan-II
NF-κB	Nuclear factor kappa B
oxLDL	Oxidized low-density lipoprotein
PC	Pro-hormone convertase
PKA	Protein kinase A
PKC	Protein kinase C
POMC	Pro-opiomelanocortin
RCT	Reverse cholesterol transport
SMC	Smooth muscle cell
WT	Wild type

List of Original Publications

This dissertation is based on the following original publications, which are referred to in the text by their Roman numerals:

I Rinne P, Kadiri JJ, Velasco-Delgado M, Nuutinen S, Viitala M, Hollmen M, Rami M, Savontaus E, Steffens S. Melanocortin 1 Receptor Deficiency Promotes Atherosclerosis in Apolipoprotein $E^{-/-}$ Mice. 2018 Feb;38(2):313-323. doi: 10.1161/ATVBAHA

II Kadiri JJ, Tadayon S, Thapa K, Suominen A, Hollmen M, Rinne P. Melanocortin 1 Receptor Deficiency in Hematopoietic Cells Promotes the Expansion of Inflammatory Leukocytes in Atherosclerotic Mice. Front Immunol. 2021 Nov 19;12;774013. Doi: 10.3389/fimmu.2021.774013

III Kadiri JJ, Thapa K, Kaipio K, Cai M, Hruby VJ, Rinne P. Melanocortin 3 receptor activation with [D-Trp8]-γ-MSH suppresses inflammation in apolipoprotein E deficient Mice. Eur J Pharmacol. 2020 Aug 5;880:173186. doi: 10.1016/j.ejphar.2020.173186

1 Introduction

Cardiovascular diseases (CVDs), among the non-communicable diseases, are the leading cause of death in the world (Dahlöf, 2010; W.H.O, 2020). CVDs account for 31% of global mortality. In economically developed countries, coronary artery disease (CAD) arising from atherosclerosis is the prevalent type of CVD (British Heart Foundation, 2022; Lloyd-Jones, 2010). The luminal narrowing of the major coronary arteries conducting blood supply to the heart is a deleterious risk factor for the development of CAD and its associated complications, namely myocardial infarction (MI). The arterial narrowing is largely provoked by damage to the endothelial lining of arteries, which enhances the accumulation of lipids within the arterial wall (Mundi et al., 2018). Various leukocyte subsets and endothelial adhesion molecules regulate and influence this process. The persistent chronic inflammation drives infiltration and accumulation of various leukocyte subsets into the developing atherosclerotic plaques. Eventually, lipid and leukocyte accumulation may lead to the formation of unstable plaques that are characterized by a thin fibrous cap and a large necrotic core. Unstable plaques are prone to rupture causing thrombosis and myocardial infarction or stroke (Badimon et al., 2012). Presently, the available therapeutics for managing atherosclerosis disease are targeted toward the treatment of predisposing conditions such as hypertension, hyperlipidemia and/or to prevent thrombotic complications. These treatment options, however, are not directly aimed at the underlying inflammatory mechanisms promoting atheroprogression. Therefore, there is an unmet medical need to investigate and develop new disease-modifying strategies for treating atherosclerosis disease.

The melanocortin system is known to regulate diverse physiological functions including skin and hair coloration, energy homeostasis, blood pressure and inflammation (Catania et al., 2004; Cone, 2005; Eves et al., 2006; Gantz & Fong, 2003; Getting, 2006; Ignar et al., 2003; Kadekaro et al., 2006; Luger et al., 2003; Tatro & Sinha, 2003; Wessells et al., 2003). This biological system consists of the melanocortin peptides including adrenocorticotropic hormone (ACTH) and α-, β-, and γ-melanocyte-stimulating hormone (α-, β-, γ-MSH) and their cognate receptors named melanocortin receptors (MCRs). The melanocortin peptides are products of the post-translational cleavage of the common precursor hormone

proopiomelanocortin (POMC). POMC is expressed in various tissues of the periphery and the central nervous system. Melanocortin peptides interact with MCRs to induce their biological activities. These receptors consist of five closely related G protein-coupled receptors named MC1R to MC5R. The activation of these receptors primarily evokes their coupling to the stimulatory G_s protein subunits, which stimulate the adenylate cyclase-cyclic adenosine monophosphate (cAMP) pathway (Wikberg & Mutulis, 2008). In addition, MCRs may activate the inositol trisphosphate (IP_3)/ extracellular Ca^{2+} influx, protein kinase C (PKC), mitogen-activated protein (MAP) kinase and Janus kinase pathways (Catania et al., 2004).

Over the past decades, it has become evident that melanocortins mediate potent immunomodulatory and anti-inflammatory actions by activating their target receptors in multiple cell types. For example, the activation of MC1R and MC3R exhibits anti-inflammatory effects in various inflammatory disease models such as arthritis, inflammatory bowel disease, brain and kidney ischemia, dermatitis, contact hypersensitivity, fever, acute respiratory distress syndrome and atherosclerosis (Getting et al., 2002; Kalden et al., 1999; Kannengiesser et al., 2008; Maaser et al., 2006; Rinne et al., 2014). α-MSH-mediated stimulation of MC1R and MC3R reduces inflammation through multiple mechanisms including downregulation of adhesion molecules, pro-inflammatory cytokines and chemokines and stimulation of anti-inflammatory cytokine production (Wang et al., 2019). Therefore, activation of these two melanocortin receptor subtypes, MC1R and MC3R has therapeutic potential for the management of inflammatory disorders.

Monocytes and macrophages are the main leukocyte subtypes governing atherosclerosis-linked inflammation (Swirski et al., 2007; Xu et al., 2019). These cells, along with other leukocytes, express MC1R and MC3R (Brzoska et al., 2008; Cooper et al., 2005; Lam et al., 2005, 2006). The activation of these receptors on macrophages induces anti-inflammatory and pro-resolving effects through an NF-κB-dependent mechanism that limits pro-inflammatory cytokine synthesis and upregulates anti-inflammatory cytokine production (Patel et al., 2011). Aside from the regulation of inflammation, MC1R was recently found to promote reverse cholesterol transportation (RCT) and to reduce the uptake of oxidized low-density lipoprotein (oxLDL) particles in macrophages (Rinne et al., 2017), which are preventive mechanisms against the development of atherosclerosis. Furthermore, the treatment of *Ldlr*$^{-/-}$ (low-density lipoprotein receptor knockout) atherosclerotic mice with a nonselective melanocortin agonist limited plaque inflammation and improved arterial function (Rinne et al., 2014). These studies highlight that targeting the melanocortin receptors MC1R and MC3R might also protect against atherosclerosis, which is characterized and driven by chronic inflammation.

This thesis aimed to build on the previous data demonstrating the favorable effect of nonselective targeting of MCRs in a mouse model of atherosclerosis. The exact

contributions of MC1R and MC3R and the underlying mechanisms have however remained unexplored and therefore, the main objective of this thesis was to address these knowledge gaps. Specifically, the thesis explored the role of MC1R in the regulation of leukocyte trafficking and its possible implications in atherosclerosis using two different MC1R loss-of-function mouse models (*Mc1r*$^{e/e}$) on the atherosclerotic background (Study I & II). In Study III, the pharmacological effects of selective MC3R activation on inflammation and atheroprogression were investigated in *Apoe*$^{-/-}$ (apolipoprotein E knockout) mouse model. The data herein highlights the important roles of MC1R and MC3R in regulating leukocyte behavior and inflammatory processes in atherosclerosis.

2 Review of the Literature

2.1 Atherosclerosis

Atherosclerosis is a chronic inflammatory disease of medium- and large-sized arteries initiated by endothelial dysfunction and lipid accumulation. It is the number one risk factor for other CVDs, in particular, CAD and cerebrovascular disease leading to MI and stroke, respectively (Hansson, 2005). CVDs are the number one cause of death in the world with 8 million associated deaths annually (British Heart Foundation, 2022). The paradigm of atherosclerosis as a disease of gradual lipid accumulation in arteries has shifted as we continue to probe the pathogenesis of this complex disease. It is now well-established that the pathogenesis of atherosclerosis involves lipid accumulation and its cross-talk with the immune system. As the understanding of the immune system evolved in the last decades, more is being uncovered on the role of inflammation in atherosclerosis. For instance, the detection of adhesion molecules on endothelial cells and characterization of mechanisms controlling leukocyte transmigration into atherosclerotic plaques lend support to the inflammation theory of atherosclerosis (Hansson & Hermansson, 2011).

2.1.1 Pathogenesis of atherosclerosis

Atherosclerosis is characterized by plaque development in the arteries, which may clinically manifest into severe stenosis and eventually into thrombosis. The disease progress is initiated by lipid accumulation in the subendothelium of arterial walls (Libby, 2021). The accumulation of lipids in the subendothelium is stimulated by risk factors such as dyslipidemia, diabetes mellitus, obesity, hypertension, tobacco smoking and a sedentary lifestyle. Other non-modifiable risk factors include a family history of CAD, male gender and advanced age. The presence of these risk factors is thought to induce mechanical damage to the endothelium layer of arteries, thus promoting the passage of circulating lipids to the subendothelial space (Mundi et al., 2018). The distortion in the structural and functional properties of the vascular endothelium is generally known as endothelial dysfunction. The damage to the endothelium is one of the earliest detectable changes observed in lesion-prone areas

of the vasculature in the onset of atherosclerosis (Jebari-Benslaiman et al., 2022). Endothelial dysfunction drives the permeation, trapping and chemical modification of circulating lipoprotein particles in the intimal space (**Fig. 1**). Modified lipids and other atherogenic factors stimulate an increase in adhesion and infiltration of monocytes and other leukocytes into the arterial intima. This results in the activation of signaling pathways driving inflammation and the formation of fatty streaks, an early indicator of atherosclerotic lesions.

During the initiation and progression of atherosclerosis, circulating monocytes are recruited to the arterial intima, where they transform into phagocytotic macrophages and internalize modified lipoprotein particles to become foam cells. Accumulation of lipids within the foam cell induces the local synthesis of pro-inflammatory cytokines (e.g. tumor necrosis factor alpha, TNF-α; and interleukin-1, IL-1). Modified lipids can also directly activate endothelial cells and smooth muscle cells (SMCs), which in turn, promotes the expression of chemoattractants (monocyte chemoattractant protein-1, MCP-1) and adhesion molecules (intercellular adhesion molecule 1, ICAM-1; vascular cell adhesion molecule 1, VCAM-1; E-selectin and P-selectin). Together, these molecules stimulate the diapedesis of monocytes and the recruitment of T lymphocytes as well as other leukocyte subsets to the arterial wall (Deshmane et al., 2009).

The activated endothelium and monocyte-derived macrophages provoke also the release of various chemokines and growth factors that stimulate the neighboring SMCs to proliferate and release extracellular matrix components resulting in the formation of a fibrotic plaque (Mach et al., 2020). Migration of SMCs from the media to the luminal side of arteries mediates also the formation of a collagen-rich fibrous cap that stabilizes the plaque. The developing lesions, however, progressively undergo structural remodeling and form a lipid-rich necrotic core that contains oxidized lipids and crystallized cholesterol and cellular debris from dead cells (**Fig. 1**) (Bäck et al., 2019). The integrity of the fibrous cap is concomitantly compromised by foam cells, which synthesize collagen-degrading matrix metalloproteinases (MMPs) (Louis & Zahradka, 2010). Eventually, the degradation of the extracellular matrix together with hemodynamic stress exerts pressure and increases the risk of fibrous cap rupturing. A ruptured fibrous cap can release pro-thrombotic molecules from the lipid core and precipitate acute thrombus formation (Watson et al., 2018). Thrombus could occlude the arterial lumen and manifest as acute coronary syndrome (ACS). Notwithstanding, thicker fibrous plaque promotes stable plaque formation marked by reduced rupture-propensity compared to a thinner, more fragile and rupture-prone plaque (i.e. vulnerable plaque).

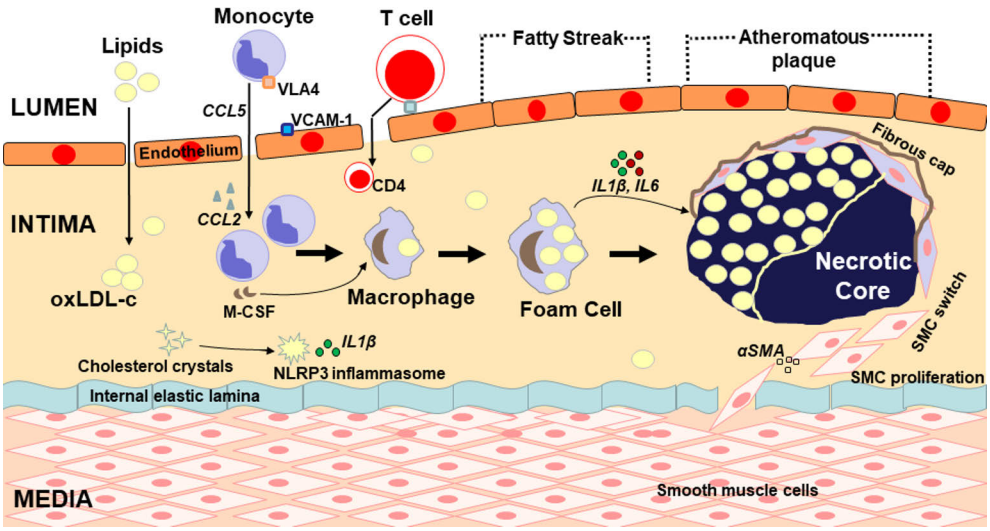

Figure 1. Pathogenesis of atherosclerosis. Endothelial dysfunction allows transmigration of immune cells and accumulation of chemokines and cholesterol in the subendothelium of arteries, thus promoting atheroprogression. A physical or chemical insult to the endothelium causes injury to the membrane allowing LDLc as well as monocytes other leukocytes (via adhesion molecules) to migrate into the subendothelium. Monocytes differentiate into macrophages to phagocyte the oxidized LDL particles and transform eventually into foam cells. Furthemore, T lymphocytes adhere to the damaged endothelium, migrate into the atherosclerotic plaque and secrete cytokines/chemokines that stimulate smooth muscle cell (SMC) proliferation. Over time, lipids, leukocytes, SMCs progressively accumulate in the lesions, which then leads to the formation of advanced and complex plaques characterized by a necrotic core and thin fibrous cap. oxLDLc (oxidize low-density lipoprotein cholesterol), CCL5 (chemokine (C-C motif) ligand 5), CCL2 (chemokine (C-C motif) ligand 2), VLA4 (very late antigen-4), M-CSF (macrophage colony-stimulating factor), CD4 (cluster of differentiation 4), VCAM-1 (vascular cell adhesion molecule 1), NLRP3 (NLR family pyrin domain containing 3), IL1β (interleukin-1 beta), IL6 (interleukin 6), αSMA (alpha smooth muscle actin).

2.1.2 Lipoprotein metabolism

Lipoproteins are complex macromolecules that transport different types of lipids including cholesterol in the plasma. These macromolecules are characterized and categorized by their physical and chemical properties and possess varying density, size, composition and function (**Fig. 2**). Thus, based on their density, there are four major classes of lipoproteins in the blood: chylomicron (CM), very low-density lipoprotein (VLDL), low-density lipoprotein (LDL) and high-density lipoprotein (HDL) (Mach et al., 2020). The density classification shows that lipoproteins with a higher fat-to-protein ratio are larger but less dense (CM, VLDL) (**Table 1**). While VLDL conveys synthesized triglycerides (TGs) from the liver to adipose tissue for storage and other tissues for energy production, CM transports gastrointestinal TGs to various tissues (Borén et al., 2020).

The lipid content of lipoproteins is composed of phospholipids, TGs, free cholesterol and esterified cholesterol (Öörni et al., 2019). TGs and cholesterol esters form the hydrophobic core of lipoproteins, which is surrounded by an outer shell, composed of amphipathic phospholipids and smaller consignments of proteins and free cholesterol. At any given time, lipoproteins convey hundreds to thousands of TGs and free cholesterol particles linked to their core (Borén et al., 2020). Lipoproteins express surface proteins known as apolipoproteins, which facilitate lipid core solubilization and transportation of lipoprotein particles. Principally, apolipoproteins aid in lipid metabolism by acting as co-factors in enzymatic reactions. In addition, apolipoproteins serve as ligands for lipoprotein receptors and support the structural integrity of lipoproteins (Öörni et al., 2019). For instance, lipid-free apolipoprotein A1 (ApoA1) solubilizes plasma membrane phospholipids and cholesterol thereby aiding cholesterol transportation from the periphery to the liver, whereas ApoB100, the main protein constituent of VLDL and LDL, stimulates the secretion of these lipoproteins (VLDL, IDL and LDL) from the liver. The ApoB48 subtype is a condensed form of ApoB100 and it facilitates the secretion of CMs from the small intestine (Mach et al., 2020).

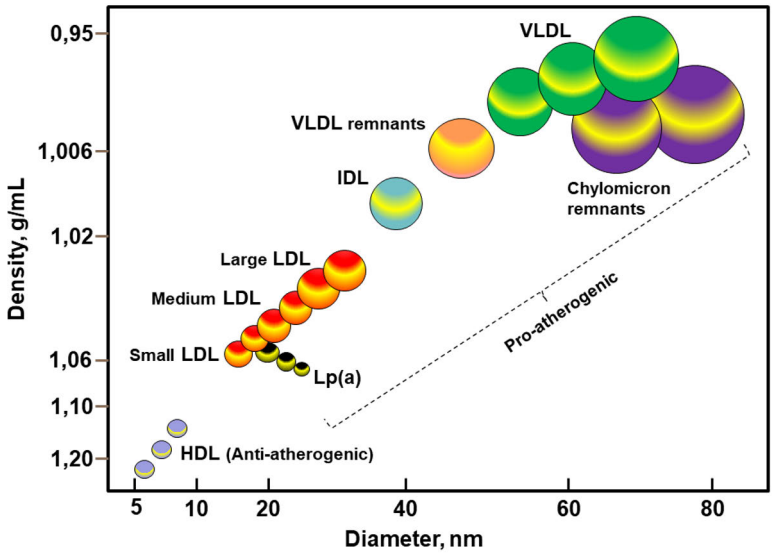

Figure 2. The size distribution, density and atherogenicity of major classes of lipoprotein particles. The metabolism of LDL particles affects their size and composition (small, medium and large LDL). The smaller LDL particles are highly potent atherogenic molecules. LDL (low-density lipoprotein), HDL (high-density lipoprotein), IDL (intermediate-density lipoprotein),VLDL (very-low-density lipoprotein), Lp(a) lipoprotein (a). [Adapted & modified from (Feingold, 2000)]

HDL is a dense lipoprotein with high protein content. HDL generally collects lipids from the cells and transports them to the liver for further processing. A higher concentration of HDL cholesterol (HDLc) usually signifies a healthier blood vessel and a lower risk of atherosclerosis (Tall & Yvan-Charvet, 2015). LDL however has a lower protein-to-fat ratio compared to HDL. LDL is essential for the transport of cholesterol, phospholipids and TGs (Öörni & Kovanen, 2021). An increased plasma concentration of LDL cholesterol (LDLc) and TGs, in particular, are markers of cardiovascular diseases, as there is a positive correlation between the plasma levels of these lipids and the incidence of atherosclerosis and CAD (Libby, 2015, 2021). LDL particles are not homogenous, since, in the course of their metabolism, their size and composition are altered. The smaller particle size LDLs, in particular, are readily absorbed into the subendothelial space, where they are retained due to their binding to extracellular matrix proteoglycans and exposed to various modifications (**Fig. 2**). LDL, CM remnants, VLDL, intermediate-density lipoprotein (IDL) and lipoprotein (a) (Lp(a)) in the plasma are considered pro-atherogenic (Libby, 2021).

Table 1. Lipoprotein classes, their size and molecular components. [Adapted & modified from (Feingold, 2000)]

Lipoproteins	Major apoproteins	Major lipids	Lipid/ protein ratio	Density (g/mL)	Size (nm)
Chylomicrons	ApoB48, ApoC, ApoE, ApoA	Triglycerides	99:1	<0.9	75–1200
VLDL	ApoB100, ApoE, ApoC	Triglycerides	90:10	0.9–1.0	30–80
IDL	ApoB100, ApoE, ApoC	Triglycerides Cholesterol	85:15	1.0–1.02	25–35
LDL	ApoB100	Cholesterol	80:20	1.02–1.06	18–25
HDL	ApoAI, ApoAII, ApoC, ApoE	Cholesterol Phospholipids	50:50	1.06–1.21	5–12
Lp(a)	ApoB100, Apo(a)	Cholesterol		1.06–1.09	~30

2.1.3 Cholesterol metabolism

Cholesterol plays important physiological roles in maintaining plasma membrane fluidity, metabolic regulation in the endoplasmic reticulum, embryonic signaling and cellular proliferation. Being the most important sterol in mammals, cholesterol serves as the precursor for oxysterols, steroid hormones and bile acid synthesis. Cholesterol biosynthesis is a tightly regulated process, as excess cholesterol in the cell can be toxic. Accordingly, the rate of cholesterol production and uptake is controlled by a negative feedback mechanism (Luo et al., 2020). Cholesterol is a major driver of atherosclerotic lesion formation. An increase in dietary intake or

de novo synthesis from acetyl coenzyme A (acetyl Co-A) and peripheral or genetic alteration in cholesterol homeostasis increases plasma cholesterol levels, leading to hypercholesterolemia. This, in turn, leads to the accumulation of cholesterol in the subendothelial space of medium- and large-sized arteries and promotes the development of atherosclerosis.

Cholesterol from dietary sources is absorbed in the intestine by Niemann–Pick C1-Like 1 (NPC1L1) protein on the enterocytes by clathrin-mediated endocytosis (Jia et al., 2011). Acetyl Co-A acetyltransferase 2 (ACAT2) enzyme in the enterocyte catalyzes the esterification of excess cholesterol and amasses this cholesterol into CMs. CMs are transported via the lymphatic system to the liver where they are assembled in VLDL particles and released into circulation. VLDL particles and CMs are enzymatically hydrolyzed by lipoprotein lipase (LPL) into higher-density products including LDL particles and CM remnants. While the CM remnants are taken up by the liver, cholesterol-rich LDL particles deliver cholesterol to tissues via LDL receptor (LDLr) (Luo et al., 2020). In the arteries, atherosclerosis is initiated in the subendothelial space where LDL particles are modified by acetylation, aggregation or oxidation and ingested by macrophages via scavenger receptors class A type 1 (SR-A1), low-density lipoprotein receptor-1 (LOX-1) and the cluster of differentiation 36 (CD36) (Moore et al., 2018; Öörni & Kovanen, 2021). The accumulation of cholesterol in macrophages promotes foam cell formation. Consequently, the modified lipoprotein particles and foam cells in the intima exert a pro-inflammatory effect and provoke a multitude of immune responses (Libby, 2021). The surplus cholesterol within the lesional macrophage is extricated from the foam cells via a counter-regulatory mechanism initiated mainly by adenosine triphosphate-binding cassette transporters type A1 and G1 (ABCA1/ABCG1). These macrophage efflux proteins interact with nascent lipid-poor HDL and mature HDL particles to deliver cholesterol back to the liver using scavenger receptor class B type 1 (SR-B1), a process known as reverse cholesterol transportation (RCT) (Bäck et al., 2019). The liver stores excess cholesterol converts it into bile acids or secretes it into the gallbladder via ABCG5/ABCG8 transporters.

2.1.4 Inflammation in atherosclerosis

Atherosclerotic inflammation is activated by endothelial injury and the accumulation of lipids within the subendothelium, which stimulate leukocyte infiltration into the atherosclerotic plaque. This inflammation contributes significantly to the disease pathobiology. Inflammation is crucial to elicit innate immunity, which in turn stimulates the priming of adaptive immunity and facilitates the effector phase of the immune response. However, in atherosclerosis, persistent undesired and non-resolving systemic inflammation promotes the

progression of the disease. Recent animal and clinical studies have enhanced the understanding of inflammation as a driver of atherosclerosis. In many animal studies, plaque development and disease progression are considerably halted when crucial inflammatory mediators such as *Il1b* and *Ifng* pathways are silenced (Kirii et al., 2003; Major et al., 2002; Reardon et al., 2001; Zhou et al., 2000; Zhou et al., 2006). In the late 1980s and 1990s, supporting evidence that identified the release of inflammatory mediators from vascular endothelial cells and monocytes was reported (Libby et al., 1986; Lipton et al., 1995). The identification of different cell types and various inflammatory cytokines and their involvement in human and animal atherosclerosis lends further support to the inflammation hypothesis of atherosclerosis. The earliest recognizable atherosclerotic lesions (fatty streaks) in rabbits, nonhuman primates and humans were found to contain lipid-rich macrophages (foam cells) and T lymphocytes (Faggiotto et al., 1984; Rosenfeld et al., 1987; Ross & Glomset, 1976; Stary, 1989). These immune cells, alongside SMCs and endothelial cells, contribute to the cellular mediation of atherosclerotic inflammation (Jebari-Benslaiman et al., 2022).

The chronic, low-grade release of C-reactive protein (CRP) in atherosclerotic patients helps to substantiate the role of inflammation in atherosclerosis (Ridker et al., 2000; Ridker & Lüscher, 2014). CRP is synthesized in the liver and induced by IL-1, IL-6 and TNF-α, hence it is a downstream biomarker for these pro-inflammatory cytokines and a risk indicator for atherosclerosis (**Table 2**) (Badimon et al., 2018). There is a prognostic association between heightened plasma CRP concentration and CVD events such as acute MI (Badimon et al., 2018; Hassan et al., 2020; Ridker & Lüscher, 2014). In addition to CRP, the concentration of lipid parameters in the blood contributes to atherosclerosis risk diagnosis (**Table 2**) (Mach et al., 2020).

Table 2. Risk of atherosclerosis - plasma lipid concentrations and non-lipid parameters [Adapted & modified from (Mach et al., 2020; Nehring et al., 2022)]

Lipid parameters	Desirable concentration	High concentration
LDLc	<3 mmol/L	>4 mmol/L
HDLc	≥1 mmol/L	
Triglycerides	<4 mmol/L	>5 mmol/L
Lp(a)		>105 nmol/L
Total cholesterol	<5 mmol/L	>6 mmol/L
Nonlipid parameters		
C-reactive protein	≤1 mg/dL	>3 mg/dL

As alluded to in the earlier section **2.1.1**, monocyte-derived macrophages are the central cellular regulator of inflammation and plaque development. Lesional macrophages originate from the proliferation of resident cells in the arterial wall or from infiltrating circulating monocytes (Hilgendorf et al., 2015; Woollard & Geissmann, 2010). Monocytes recruited from the circulation are the predominant source for plaque macrophages in the early phases of atherosclerosis, which also feeds the continuous accumulation of macrophages during plaque formation. Monocyte accumulation is enhanced in proportion to lesion size and their recruitment to the plaque is exacerbated by hypercholesterolemia (Hilgendorf et al., 2014; Swirski et al., 2006). Therefore, monocyte and macrophage expansion in the atherosclerotic plaques is progressive and proportional to the extent of the disease.

The identification of lymphocytes (T and B cells) in human atherosclerotic plaque suggest also the involvement of adaptive immunity in atherosclerosis (Hermansson, 2011; Hansson & Libby, 2006). In addition, the presence of other systemic inflammatory diseases could enhance the risk of atherosclerosis, further supporting the role of inflammation in the pathogenesis of the disease. Autoimmune diseases such as psoriasis, rheumatoid arthritis, multiple sclerosis and systemic lupus erythematosus have been linked to increased cardiovascular and atherosclerotic risk (Conrad et al., 2022; Vila et al., 2021)

2.1.4.1 Monocytes and macrophages in inflammation of atherosclerosis

Monocytes are an important contributor to the pathobiology of atherosclerosis. They originate from differentiated and proliferating hematopoietic stem and progenitor cells of the bone marrow. In experimental atherosclerosis, monocyte count in the circulation is increased in hypercholesterolemic rodents, rabbits and swine (Murphy et al., 2011). These circulating monocytes migrate unselected into tissues such as the spleen and lymph nodes and differentiate into macrophages or dendritic cells. Monocytes play an active role in atherosclerosis and studies have shown that circulating monocytes derived from the bone marrow populate atherosclerotic lesions (Kim et al., 2020; Swirski et al., 2006). Monocytes exhibit heterogeneity and while still in the circulation, they are believed to commit to a specific function such as cytokine production and antigen presentation (Kim et al., 2020).

Based on the expression of chemokine receptor patterns on the cell surface, monocytes can be subdivided into two main subsets: $CCR2^{+}CX_3CR1^{+}GR1^{+}$ ($Ly6C^{high}$) and $CCR2^{-}CX_3CR1^{++}$ $GR1^{+}$ ($Ly6C^{low}$) monocytes in mice. In short, Ly6C glycoprotein expression may also be used for this classification and $Ly6C^{high}$ monocytes are considered the classical monocytes and $Ly6C^{low}$ as non-classical monocytes. The human equivalent of $Ly6C^{high}$ monocytes expresses $CD14^{++}$ $CD16^{-}$, while $Ly6C^{low}$ expresses $CD14^{+}CD16^{+}$ in humans (Swirski et al., 2007). Mouse and

human monocyte subsets share similar phenotypes and homing properties. The classical mouse Ly6C^{high} and human CD14^{++} CD16^{-} monocytes are short-lived. They transport tissue antigens to the lymph nodes and are actively recruited to inflamed tissue where they accumulate (Geissmann et al., 2003; Jakubzick et al., 2013). The majority of total monocytes are classical monocytes with pro-inflammatory potential, which differentiate into macrophages and dendritic cells (Xu et al., 2019). The non-classical Ly6C^{low} (human: CD14^{+} CD16^{+}) monocytes, on the other hand, are longer-lived, patrol the blood vessel, respond faster to infection and modulate endothelial integrity (Auffray et al., 2007; Carlin et al., 2013). This subtype of monocytes possesses M2-like characteristics and counterpoises the actions of classical monocytes (Geissmann et al., 2003). The non-classical type of monocytes phenotypically also possesses differing migratory properties in the circulation (Geissmann et al., 2003). An intermediate subset of monocytes (CD14^{++} CD16^{+}) that account for about 5% of total monocytes has also been reported (Askari et al., 2021; Xu et al., 2019). However, it is the classical monocyte subset that populates the blood during atherosclerosis and invades atherosclerotic lesions, which promotes plaque development (Dutta et al., 2012; Murphy & Tall, 2016). Intermediate monocytes have been also linked to atherosclerotic plaque thinning and CVD events (Biessen & Wouters, 2017).

When infiltrated into inflamed tissues, monocytes differentiate into macrophages or dendritic cells. In the context of atherosclerosis, circulating monocytes infiltrate the arterial wall and transform into lesional macrophages in the presence of macrophage colony-stimulating factor (M-CSF). Monocyte recruitment and influx contribute significantly to macrophage accumulation during early lesion development, while the majority of macrophage accumulation (~90%) in established plaque arises from local proliferation (Biessen & Wouters, 2017; Moore et al., 2018). Lipid uptake by macrophages is engineered through the expression of various scavenger receptors including SR-A, LOX-1, SR-B1, CD36, and toll-like receptors (TLRs). The latter also exacerbates plaque inflammation through the interaction with oxLDL that stimulates TLR signaling (Kim et al., 2020; Moore et al., 2018; Westerterp et al., 2014).

Of note, not only does the quantity of macrophages matter in atherosclerotic inflammation but also the quality affects plaque phenotype. The classification of macrophages is not limited to but includes M1- and M2 -type subsets (Farahi et al., 2021). The ‘classical’ M1-type macrophages are activated by the T helper 1 (Th1) cytokine or interferon-gamma (IFN-γ) and promote inflammation along with plaque development. The ‘alternatively’ activated M2-type macrophages, on the other hand, are induced by the Th2 cytokines IL-4 and IL-13 and elicit anti-inflammatory responses, thus counterpoising the development of atherosclerotic plaques and promoting plaque stability (Bäck et al., 2019; Tabas & Bornfeldt, 2016). M1 and M2

macrophage classification is however simplistic since various overlapping macrophage phenotypes are likely to exist in atherosclerotic lesions (Farahi et al., 2021; Lin et al., 2021).

Macrophages, in the context of atherosclerosis, internalize modified lipids, which turn them into foam cells. As the disease progresses, macrophage function extends to phagocytotic clearance of apoptotic foam cells and other cells (efferocytosis), which promotes the resolution of inflammation (Bäck et al., 2019). Macrophage foam cells eventually lose their ability to clear apoptotic cells, which leads to secondary necrosis and the formation of the necrotic core as well as to amplification of a pro-inflammatory environment (Lin et al., 2021). An impaired resolution sustains plaque inflammation and increases immune cell infiltration. The disruption in efferocytosis has a consequential effect, particularly in advanced plaques. However, in the early phase of atherosclerotic plaque development, macrophage efferocytosis capacity is sufficient to clear inflammatory cells from lesions. Specialized lipid-derived mediators of inflammation resolution (e.g. lipoxins, resolvins, protectins and maresins) contribute to plaque stability by counteracting the effect of impaired efferocytosis (Fredman & Tabas, 2017). In advanced lesions, the amount of these resolution mediators is reduced, which favors the development of vulnerable plaque.

2.1.4.2 Hypercholesterolemia and monocytosis, drivers of inflammation in atherosclerosis

An imbalance in cholesterol metabolism and/or excessive intake of dietary cholesterol provokes hypercholesterolemia and early onset of atherosclerosis. Amongst the potent pro-inflammatory host molecules, which are abundantly present in atherosclerotic lesions, are modified and aggregated lipids or lipoproteins such as crystalline cholesterol and oxLDL molecules. This provides a link between cholesterol accumulation and inflammation in the vasculature. An increase in plasma cholesterol is an independent risk factor for atherogenesis and significantly induces atherosclerosis-linked inflammation (Mach et al., 2020). Interestingly, plasma cholesterol level also influences the number and function of circulating leukocytes. In a hypercholesterolemic state, the number of circulating leukocytes, particularly the classical monocytes, drastically increases. This also correlates with the accumulation of these cells in atherosclerotic lesions and the extent of atherosclerosis (Chistiakov et al., 2018). The expansion of circulating and lesional monocytes results from their increased survival and sustained proliferation rate. In addition, impaired $Ly6C^{high}$ to $Ly6C^{low}$ conversion also contributes to monocyte expansion (Swirski et al., 2007). Conversely, the cholesterol-lowering drug statin reduces the number of systemic and splenic $Ly6C^{high}$ monocytes (Swirski et al., 2007), suggesting a clear

link between high plasma cholesterol levels and monocytosis in experimental atherosclerosis. Therefore, monocyte count is considered an independent risk marker for CAD and MI (Askari et al., 2021).

Hypercholesterolemia may also induce defects in the management of cholesterol in immune cells, causing phenotype differentiation and mal-signaling of these immune cells. Moreover, the handling of cholesterol in leukocytes contributes to lesion progression independently of hepatic cholesterol regulation or circulating cholesterol levels. Furthermore, the proliferation and mobilization of hematopoietic stem cells and neutrophils as well as T cell activation and monocyte priming are affected by plasma cholesterol levels (Bäck et al., 2019; Drechsler et al., 2010; Tall & Yvan-Charvet, 2015; Tolani et al., 2013). More specifically, cholesterol crystals, a common feature of advanced lesions, induce lysosomal damage in macrophages/foam cells and reinforce the continuous plaque inflammation by activating inflammasome (Duewell et al., 2010; Rajamäki et al., 2010). Inflammasomes are cytoplasmic caspase-1-activating protein complexes that contribute to the maturation and secretion of the pro-inflammatory cytokines IL-1β and IL-18. Thus, they play a crucial role in innate immunity regulating atherosclerotic plaque initiation, progression and rupture. The NOD-, LRR- and pyrin domain-containing protein 3 (NLRP3) inflammasome, in particular, is activated by various endogenous danger signals such as cholesterol crystals and oxLDL that are abundantly present in atherosclerotic lesions (Sharma & Kanneganti, 2021). The activation of NLRP3 by cholesterol crystals causes also defective resolving mechanisms via the increase in the synthesis of IL-1β and IL-6 cytokines that contribute to atherogenesis and the formation of vulnerable plaques (Peter Libby, 2021). In contrast, the inhibition of the NLRP3 receptor abrogates cholesterol crystal-induced IL-1β activation in macrophages, thus indicating that NLRP3 inflammasome is the cholesterol crystal-responsive element (Hoseini et al., 2018; Rajamäki et al., 2010).

2.1.4.3 T and B cells in atherosclerosis

T cells have been identified as important players in the inflammatory processes of atherosclerosis. They are selectively recruited to nascent atherosclerotic plaque following their activation. Lesional T cells influence disease progression by secreting mediators regulating plaque development. T cell expression on the human atherosclerotic plaque was described by Jonasson *et al* (Jonasson et al., 1985) followed by the identification of major histocompatibility complex (MHC) class II antigens that are a prerequisite for antigen presentation and facilitate T cell activation within the atherosclerotic plaque (Hansson et al., 1989). Although their frequency in the atherosclerotic lesion is lower compared to monocytes and macrophages, T cells

are crucial regulators of the immune response in atherosclerotic plaques. For instance, the adoptive transfer of T cells into immunodeficient mice aggravates atherosclerosis (Zhou et al., 2000; Zhou et al., 2006). Immunohistochemistry (Hansson et al., 1988; Jonasson et al., 1986), cytometry by time-of-flight/ CyTOF (Cole et al., 2018; Winkels et al., 2018) and single-cell RNA-sequencing (Winkels et al., 2018) studies have estimated that approximately 25-38% of all leukocytes present in mouse and human atherosclerotic plaques, especially, around the fibrous cap are of the $CD3^+$ T cell subset. About 10% of these cells are $CD3^+CD4^+$ T helper cells. The recruitment of T cells to the plaque is orchestrated through C-C chemokine receptor type 5 (CCR5) and C-X-C chemokine receptor type 6 (CXCR6). In particular, $CD4^+$ T cell homing to the atherosclerotic plaque is facilitated by CCR5 (Saigusa et al., 2020). CCR5 is one of the receptors for chemokine (C-C motif) ligand 5 (CCL5), which plays a role in atherogenesis by aiding monocyte arrest on the endothelium thereby promoting infiltration of immune cells to the atherosclerotic lesion (Gencer et al., 2021). $CD4^+$ T cells induce numerous effector functions in adaptive immune response and possess the ability to differentiate into different T helper effector subsets. These effector subsets exhibit distinct functions and exert either pro- or anti-inflammatory effects on resident tissue.

T cell response is stimulated upon encountering antigen-presenting cells (APCs) displaying T cell-specific antigens (e.g. MHC class I → $CD8^+$ T cell; MHC class II → $CD4^+$ T cell). In human lesions, the vast majority of T cells are effector or memory T cells, which are upregulated in proportion to the severity of CAD (Saigusa et al., 2020). Particularly, $CD4^+$ T and $CD8^+$ T cells are abundantly expressed in mice and human atherosclerotic plaques (Fernandez et al., 2019). $CD4^+$ T cells are activated by epitopes of oxLDL presented by APCs such as dendritic cells and macrophages. Naïve $CD4^+$ T cells differentiate into different Th effector cells depending on the stimulatory cues. Th cell subsets with distinct functional characteristics have a specialized role in atheroprogression. The Th1 subset of $CD4^+$ T cells promotes inflammation and accounts for the majority of T cells in an atherosclerotic lesion. Th2 response in atherosclerosis is still ambiguous. Generally, Th17 and regulatory T cells (Treg) convey pro-inflammatory and anti-inflammatory effects, respectively. Tregs, in particular, confer atheroprotection by suppressing inflammation and by inactivating dendritic cells (Ait-Oufella et al., 2006; Fernandez et al., 2019). Taken together, the balance between T cell subsets influences lesion formation and characteristics (Saigusa et al., 2020).

Activated T cells can also affect atherosclerosis by stimulating B cells in lymphoid organs to synthesize and release antibodies into the blood. B cells, in turn, secrete inflammation-regulating cytokines and stimulate other immune cells such as proatherogenic Th1 cells and promote the activation of myeloid cells by stimulating the production of granulocyte-macrophage colony-stimulating factor (GM-CSF)

(Pattarabanjird et al., 2021). Conversely, other B cell subsets (B regulatory/B_{reg}) induce anti-inflammation via IL-10 secretion and induction of Treg cells. The number of B cells in atherosclerotic plaques is lower compared to T cells (Winkels et al., 2018). However, B cells are upregulated in the spleen under hypercholesterolemic conditions (Nus et al., 2017). B cells can also be categorized into B1 and B2 cells. The B1 subtype of B cells secret immunoglobulin M (IgM) antibody that recognizes oxLDL and inhibits its uptake by macrophages in mice (Pattarabanjird et al., 2021). In contrast, the proatherogenic B2 subtype synthesizes IgG and IgE and activates T cells (Upadhye et al., 2020). It is, however, important to point out that the role of B cells in human atherosclerosis is not completely defined, but innate B1 response is generally atheroprotective, while adaptive B2 responses appear to promote atherogenesis. Thus, reducing the number of B2 cells and increasing or preserving the B1 cell population would likely result in atherosclerotic plaque regression.

2.2 Animal models of atherosclerosis

Animal models are important preliminary tools to mimic the atherosclerosis disease milieu in humans. They facilitate a better understanding of the pathogenesis, diagnosis, prevention and treatment of the disease. Since the classical experiments by Ignatowski (1908) and Anitschkow (1913), which showed that feeding rabbits a cholesterol-rich diet causes atherosclerosis, the use of mice in atherosclerosis studies has been evolving. The ease in genetic manipulation of laboratory mice to elucidate the pathogenetic stages and causalities in atherosclerosis has interested investigators in the use of smaller animals such as rodents in probing the biology of the disease. The therapeutic and mechanistic exploration of various mouse models has significantly improved our understanding of the mechanisms behind atherogenesis and the identification and development of novel therapeutic options. In particular, genetically modified mice have been pivotal to the ongoing progress and they are still the most extensively used animal model in atherosclerosis research.

Although mouse models of atherosclerosis have some similarities to human disease, they are not a 100% representation of atherogenesis in humans. Hence, the results obtained from mouse models do not directly translate to humans. Atherosclerosis development in humans is a spontaneous phenomenon. In mice, however, gene manipulation techniques are required to induce atherosclerotic disease (Wang et al., 2021). More importantly, wild-type mice are generally resistant to diet-induced atherogenesis and they typically express a high level of HDLc (~70% of total plasma cholesterol), which is largely explained by the deficiency of cholesteryl ester transfer protein (CETP) activity in mice (Oppi et al., 2019). Furthermore, human atherosclerosis develops over a long period and is usually

associated with lower lipid levels in comparison to mouse models of atherosclerosis. In addition to the differences in cholesterol and lipoprotein metabolism between mice and humans, there are important distinctions in the inflammatory processes and reverse cholesterol transportation (Oppi et al., 2019). Mouse atherosclerotic lesions are physiologically and anatomically distinct. In addition to the apparent size difference, the medial layer of mouse arteries consists of only 2 to 3 layers of SMCs and the arterial endothelium is situated directly on the internal elastic lamina compared to humans (Hopper et al., 2021). Accordingly, caution must be exercised when extrapolating data from a mouse model of atherosclerosis to human atherosclerosis. However, despite clear limitations in the validity of mouse models, they are still currently the most widely used experimental models to study atherosclerosis.

2.2.1 *Apoe*$^{-/-}$ mouse model of atherosclerosis

Apolipoprotein E (ApoE), like other apolipoproteins, is a structural apoprotein that aids with lipid solubilization and maintains the structural integrity of lipoprotein particles in circulation. ApoE is a surface component of lipoprotein particles synthesized primarily in the liver and acts as a ligand for lipoprotein receptors to facilitate the clearance of cholesterol and TGs, thus protecting against atherosclerosis. ApoE is the main lipoprotein involved in cholesterol metabolism where the different isoforms (E2, E3 and E4) interact specifically with lipoprotein receptors to regulate cholesterol metabolism. In the periphery, ApoE mediates the binding and internalization of lipoprotein particles to facilitate the uptake of phospholipids, TGs, cholesterol and cholesterol esters into cells (Getz & Reardon, 2016). The genetic alteration in ApoE receptor binding in human and experimental atherosclerosis impairs the clearance of circulating atherogenic lipoproteins (CM and VLDLs), resulting in early atherosclerosis development due to hypercholesterolemia.

The *Apoe*$^{-/-}$ mouse is one of the most widely used genetically modified mouse models to study atherosclerosis. It was the first atherosclerotic murine model where the target gene was successfully deleted (Plump et al., 1992; Zhang et al., 1992). As a consequence, *Apoe*$^{-/-}$ mice exhibit impaired lipoprotein clearance and increased plasma cholesterol level (400 – 600 mg/dl) due to the accumulation of chylomicron and VLDL remnants rich in free cholesterol and esterified cholesterol (Plump & Breslow, 1995). Hypercholesterolemia in these mice is further exacerbated by feeding them a cholesterol-rich diet.

With lesions formed throughout major arteries (Oppi et al., 2019), *Apoe*$^{-/-}$ mice produce extensive and reproducible atherosclerotic lesions. At 5-6 weeks of age, early lesion formation appears with monocytes adhering to the endothelium and

migrating to the subendothelial space. At about 10 weeks of age, fatty streaks develop followed by the appearance of foam cells and spindle-shaped SMCs in these early lesions. An additional advantage of the *Apoe*$^{-/-}$ mice over most genetically modified mouse models of atherosclerosis is the formation of fibrous plaque with a necrotic core covered by a fibrous cap consisting of SMCs, elastic fibers and collagen after 20 weeks of age. Beyond 20 weeks, fibrous plaques progress into advanced lesions that may become calcified or result in an aneurysm and partly occlude the arteries. However, such advanced lesions are not prone to rupture and are thus devoid of thrombosis as commonly observed in human atherosclerosis (Golforoush et al., 2020). Therefore, the mouse models engineered to mimic human atherosclerosis are models of atherogenesis and not models of advanced atherosclerosis and atherothrombosis. Several mouse models exhibiting plaque rupture have been however generated using *Apoe*$^{-/-}$ and *Ldlr*$^{-/-}$ mice, but the mechanistic resemblance to human plaque rupture is still debated (Getz & Reardon, 2016; Wang et al., 2021).

Although circulating ApoE is primarily derived from the liver, it is also synthesized in other cell types including macrophages. Regulation of ApoE synthesis in macrophages appears to be important in maintaining the balance between cholesterol intake and efflux in this cell type and therefore, contributes to foam cell formation and atherogenesis. The introduction of wild-type hematopoietic cells into an *Apoe*$^{-/-}$ recipient mice via bone marrow transplantation revealed the detection of ApoE in the serum of the recipient mice and serum cholesterol level was normalized, thus preventing atherosclerosis (Boisvert et al., 1995; Linton et al., 1995). Similarly, transgenic expression of local ApoE in the arterial wall or macrophages curtails atherosclerosis via cholesterol efflux, an effect independent of the cholesterol-lowering influence of ApoE (Bellosta et al., 1995; Shimano et al., 1995). Therefore, it is important to take into account the extrahepatic origin of ApoE, when planning bone marrow transplantation experiments using *Apoe*$^{-/-}$ mice.

Ultimately, animal models of atherosclerosis, particularly *Apoe*$^{-/-}$ mice, equip researchers with unique tools and models to investigate the disease. This model confers benefits such as low cost, spontaneity in atherosclerosis development, reproducibility and the accessibility of transgenic methodologies. Gene manipulation techniques such as tissue-specific gene targeting techniques, recombinase technology and bone marrow transplantation are modern alternate techniques to aid the understanding of the mechanisms underlying atherosclerosis. Accordingly, this encourages the translation of the observed data into clinical progress.

2.2.2 Other mouse models of atherosclerosis

The dietary models of atherosclerosis in mice were first developed in late 1960 when mice were fed a high-fat diet (HFD) containing 5% cholesterol, 30% fat and 2% cholic acid (Poznyak et al., 2020). This type of diet effectively induced hypercholesterolemia and the formation of fatty streaks in the vasculature. Diet alone, however, does not promote the formation of more advanced lesions and therefore, genetic modifications, in addition to HFD feeding, are needed to better model atherosclerosis (**Table 3**). *Ldlr*$^{-/-}$ mice and other transgenic and knockout mouse models have been generated to model atherogenic dyslipidemia and associated atherosclerosis.

Ldlr$^{-/-}$ mice, in comparison with *Apoe* $^{-/-}$ mice, demonstrate only a mild increase in plasma cholesterol concentration when fed a normal chow diet (Golforoush et al., 2020). Hypercholesterolemia and lesion development in *Ldlr*$^{-/-}$ mice is however exacerbated with a cholesterol-rich diet (Oppi et al., 2019; Poznyak et al., 2020). In *Ldlr*$^{-/-}$ mice, lipoprotein clearance is impaired resulting in increased plasma LDLc. Genetic alteration in the *Ldlr* gene is common in humans and results in familial hypercholesterolemia and early atherosclerosis. *Ldlr*$^{-/-}$ mice are also a relevant model to study atherosclerosis-linked comorbidities such as obesity and diabetes since *Ldlr*$^{-/-}$ mice are more prone to develop insulin resistance than *Apoe* $^{-/-}$ mice (Oppi et al., 2019). Overall, *Ldlr*$^{-/-}$ and *Apoe* $^{-/-}$ mice are useful and relevant for investigating the role of immune cells in the development of atherosclerosis, since different leukocyte subsets are abundantly present in the atherosclerotic plaques of both models (Saigusa et al., 2020; Winkels et al., 2018).

Table 3. A table of selected mouse models of atherosclerosis showing different characteristicsin the atherogenic stimuli, lesion types, lesion stages and area of lesion development in the artery.

Mouse	Atherogenic stimulus	Lesion type	Lesion stage (I–VI)	Area of lesion characterization
Inbreed strains				
C57BL/6	VLDL, LDL	Fatty streak (aortic leaflet)	I	Aortic root, aorta
Transgenic				
ApoB100	LDL	Fatty streak	I–III	Aortic root
Single gene deletion				
Ldlr$^{-/-}$	IDL, LDL	Fatty streak, necrotic core	I–IV	Aortic root, aorta
Apoe$^{-/-}$	Chylomicron, VLDL remnants	Fatty streak, necrotic core, fibrous plaque	I–V	Aortic root, aorta

2.3 Treatment of atherosclerosis

The disease burden of atherosclerosis remains a challenge in the realm of cardiovascular diseases. Available treatments such as high-dose statin pharmacotherapy and other standard therapies have yet to meet the treatment needs of the disease. The residual burden of events, for example, recurrent events in MI survivors require novel treatment modalities to treat patients unresponsive to currently available therapies. The gold standard for the treatment of atherosclerotic cardiovascular disease (ASCVD) remains the use of cholesterol-lowering statins in combination with other lipid-lowering therapies such as proprotein convertase subtilisin-kexin type 9 inhibitor (PCSK9i), ezetimibe, fibrates or omega-3 fatty acids. However, the current ESC/EAS clinical guidelines recommend the use of high-intensity statin monotherapy before considering combination therapy (Mach et al., 2020). This combination therapy benefits patients deemed high-risk and intolerant to intense statin monotherapy. In addition, patients with limited LDLc response to statin therapy to achieve a targeted LDLc level could also benefit from such combination therapy. Recent studies have shown that PCSK9i could be of benefit as a combination therapy with a statin to manage residual LDLc risk (Gallego-Colon et al., 2020; Masana et al., 2020; Şener & Tokgözoğlu, 2022; Toth et al., 2017). However, ASCVD patients with high-intensity statin treatment might represent also residual inflammatory risk. These patients could benefit from an IL-1β antibody therapy with canakinumab or other anti-inflammatory therapy. The CANTOS trial revealed that IL-1β inhibition with canakinumab reduced atherosclerosis-linked inflammation and cardiovascular risk (Ridker et al., 2017). This study affirmed the atherosclerosis-inflammatory hypothesis and demonstrated that the reduction in inflammation linked to atherosclerosis would improve cardiovascular outcomes. Therefore, there is a strong justification for the targeting of inflammation in atherosclerosis as a secondary preventive strategy for CVDs. In addition to the lipid-lowering effect, statins exhibit a ‘pleiotropic’ effect by possessing anti-oxidative capacity and by suppressing inflammation to a certain extent. The anti-inflammatory properties of statins occur via the reduction in leukocyte adhesion and their migration into atherosclerotic plaque, and suppression of macrophage-expressing MMPs and T cell activation (Almeida & Budoff, 2019; Oesterle et al., 2017; Okyay, 2021). These effects are independent of the LDLc lowering capacity of statins. However, the anti-inflammatory effect of statins varies between the different types of statins (Diamantis et al., 2017; Koushki et al., 2021).

The targeting of inflammation to impede atherosclerosis progression is certainly promising and this approach deserves further exploration. Ideally, future clinical studies should accurately identify specific biological markers or pathways to guide the risk stratification of patients and the development and testing of novel immunomodulatory therapies. The CIRT (Cardiovascular Inflammation Reduction

Trial) study is another example, which demonstrated the biological complexity of atherosclerosis (Ridker et al., 2019). The study enrolled and randomized patients with previous MI or multivessel CAD to receive low-dose methotrexate (an immunosuppressant) 15 – 20 mg/week. Despite its general anti-inflammatory potential, methotrexate did not reduce plasma levels of biological markers (CRP, IL-1β or IL-6) or cardiovascular events when compared to a placebo (Ridker et al., 2019). In this study, patients were not identified and selected based on residual inflammatory risk, i.e. increased CRP, IL-1β or IL-6 levels. By contrast, the LoDoCo2 trial demonstrated that low-dose colchicine (anti-inflammatory alkaloid), in addition to standard medical therapy, is effective in reducing inflammation and the risk of cardiovascular events (Nidorf et al., 2020).

In general, the data from experimental studies have demonstrated promising observations in mitigating the development and progression of atherosclerosis using various anti-inflammatory therapies in mice such as inhibition of TNF or VCAM-1 (Brånén et al., 2004; Dong et al., 1998; Elhage et al., 1998; Nidorf et al., 2020; Sacks et al., 2018). Nevertheless, there is currently no anti-inflammatory intervention available for the clinical management of ASCVD. The previous clinical studies of atherosclerosis targeting different biological pathways have mostly failed to demonstrate concrete beneficial clinical endpoints (e.g. methotrexate; losmapimod, p38 MAPK inhibitor; varespladib, secretory phospholipase A2 inhibitor; darapladib, lipoprotein-associated phospholipase A2 inhibitor) (Jagavelu et al., 2007; Nicholls et al., 2014; O'Donoghue et al., 2014; Ridker et al., 2019; White et al., 2014). Such unfavorable outcomes could be attributable to multiple factors including lack of specificity, redundancy of the targeted pathway in human disease and poor participant selection. However, several other immune system modulators for the management of ASCVDs are under clinical trials (Apremilast, TNF/IL-6/CRP [NCT03082729]; Trehalose, Mϕ autophagy [NCT03700424]; Aldesleukin, IL-2/Treg [NCT04241601]; Tinzaparin, ICAM-1[NCT04741464]; Empagliflozin, T cell [NCT04907214]; Sarilumab, CRP/IL-6r [NCT04350216]) (Clinicaltrial.gov/accessed 02.2023).

2.4 The melanocortin system

Melanocortins include ACTH and α-, β- and γ-MSH. Melanocortins were initially identified over a century ago by Bennet and Atwell, who observed that the skin of hypophysectomized tadpoles was darkened by extracts from mammalian pituitary glands (Atwell, 1919). Centrally, the melanocortins are synthesized in the pituitary, hypothalamus and spinal cord (Wang et al., 2019; Yeo et al., 2021). The isolated frog skin experimentation on the pituitary gland extract eventually led to the isolation, sequencing and molecular characterization of ACTH and MSH peptides.

The purification and sequencing of α-MSH, β-MSH and ACTH revealed that α-MSH shares the amino acid sequence of $ACTH_{(1-13)}$. β-MSH, on the other hand, has a different sequence but it contained a heptapeptide core (Met-Glu-His-Phe-Arg-Trp-Gly) common to α-MSH and ACTH (**Fig. 3**), which is principal in inducing their melanogenic effects (Abdel-Malek, 2001). Of note, all melanocortin ligands share His-Phe-Arg-Trp conserved tetrapeptide pharmacophore sequence, which is considered "the MSH signature sequence" (Renquist et al., 2011). This common amino acid motif shared by the melanocortins is the minimum sequence needed for binding and activating receptors (Wang et al., 2019). While β-MSH is part of β-lipotropin/β-lipotropic hormone (β-LPH), the 13 amino acid sequence of α-MSH is contained within the N-terminal region of ACTH, which is a 39 amino acid peptide.

The melanocortin peptides are derived from a common larger precursor protein, proopiomelanocortin (POMC), which sequence was successfully cloned from its cDNA in the late seventies (Nakanishi et al., 1979). In addition to ACTH and β-LPH, several other biologically active fragments including γ-lipotropin and β-endorphin are also products of POMC enzymatic cleavage. At the N-terminus of POMC is γ-melanotropin or γ-melanocyte-stimulating hormone (γ-MSH) that shares similar homology with α- and β-MSH (Harno et al., 2018). Interestingly, γ-MSH evades the pigmentary effect common to its two relatives.

The melanocortin system has been connected to various biological activities including melanogenesis, cardiovascular regulation, energy homeostasis, analgesia, sexual function as well as modulation of inflammatory pathways (Wang et al., 2019). The anti-inflammatory and immunomodulatory actions of melanocortins have attracted a lot of interest lately. Melanocortins along with their cognate receptors (melanocortin receptors; MC1R to MC5R) could present a novel therapeutic option for the treatment of various inflammatory diseases (Fu et al., 2020; Maurya et al., 2022; Wang et al., 2019).

2.4.1 Pro-opiomelanocortin (POMC) and melanocortins

POMC is composed of 241 amino acids in humans and 209 in mice and rats. The human POMC gene was mapped on the short arm of chromosome 2 (Harno et al., 2018; Toda et al., 2017). Its gene sequence is located in a relatively uncluttered region between DNAs of uncertain functions, the DNA methyltransferase 3A (DNMT3A) gene and EFR3B (Clark, 2016). POMC is a product of a single gene that contains 3 exons separated by 2 introns (**Fig. 3**). Exon 2 (152bp) contains a sequence, including the initiator methionine and signal sequence, that is essential for the correct protein processing and subsequent secretion. Exon 3 is the largest (833bp) and contains the majority of the coding region (**Fig. 3**). Exon 3 encodes for the

biologically active peptides, MSHs (α-, β- and γ-MSH), ACTH, β-LPH and α-, β- and γ-endorphin. Exon 1 (87bp) however contains no translation product (Clark, 2016).

POMC is readily and chiefly expressed by the corticotrophs and melanotrophs of the pituitary gland. Its gene transcription in corticotrophs is cyclic adenosine monophosphate (cAMP)-dependent but cAMP/PKC (protein kinase C) dependent in melanotrophs. POMC is also expressed in other parts of the central nervous system (CNS) such as the hypothalamus (arcuate nucleus) and nucleus of the solitary tract as well as peripherally in the skin, liver, pancreas, placenta, gastrointestinal tract, kidney, thyroid and testis (Renquist et al., 2011).

POMC comprises 3 domains; an N-terminus, a highly conserved central $ACTH_{(1-39)}$ sequence and a C-terminus. The N-terminal region contains γ-MSH, while α-MSH is derived from the central $ACTH_{(1-39)}$ sequence. The C-terminal region carries β-LPH, which can be processed into β-endorphin (Harno et al., 2018). POMC is chemically inactive but undergoes modification in a tissue-specific post-translational process to yield smaller biologically active peptides. POMC is processed mainly by two pro-hormone convertases, subtilisin/kexin-like prohormone convertases 1 and 2 (PC1/3 and PC2). PC1/3 and PC2 cleave polypeptides at the sites of dibasic amino acid residues (Lys-Lys, Lys-Arg, Arg-Arg, Arg-Lys) (**Fig. 3**). These dibasic amino acid pairs demarcate all the POMC-derived peptides. PC1/3 cleaves POMC precursor protein into the larger and higher molecular weight peptides (ACTH, β-LPH and the large NH_2-terminal fragment), while PC2 generates the smaller peptides β-endorphin and α-, β-, and γ-MSH (Dib et al., 2017).

$ACTH_{(1-39)}$ is a product of PC1-driven cleavage of pro-ACTH in the anterior pituitary corticotrophs. PC2-driven cleavage of $ACTH_{(1-39)}$ results in α-MSH and $ACTH_{(1-13)}NH_2$. $ACTH_{(1-39)}$ is the only melanocortin peptide capable of stimulating all MCR subtypes (Yuan & Tao, 2022). The first 24 amino acid residue ($ACTH_{(1-24)}$) of full-length ACTH (39 aa residues) is reported to be the recognition domain and the 25-39 aa residues ($ACTH_{(25-39)}$) serve as the protection domain to the former ($ACTH_{(1-24)}$) against enzymatic degradation (Fridmanis et al., 2017). The $\alpha\text{-MSH}_{(1-13)}$ peptide contained in the N-terminal amino acids residue of $ACTH_{(1-39)}$ is highly conserved in mammals. Unlike α-MSH, β-MSH structurally differs from the former molecule in that it comprises 22 amino acid residues and lacks modification in the N-and C-terminals. γ-MSH (22-31 aa) on the other hand, is an N-terminal domain product of POMC and a dodecapeptide. The longer form, γ_3-MSH contains 23-residue N-glycosylated amino acids which can be cleaved at the dibasic amino acid pair cleavage site to γ_2-MSH and γ_1-MSH (N-terminal 12 amino acids of γ_3-MSH and N-terminal 11 amino acids of γ_3-MSH, respectively) with a carboxyamidated C-terminal (Ericson et al., 2017).

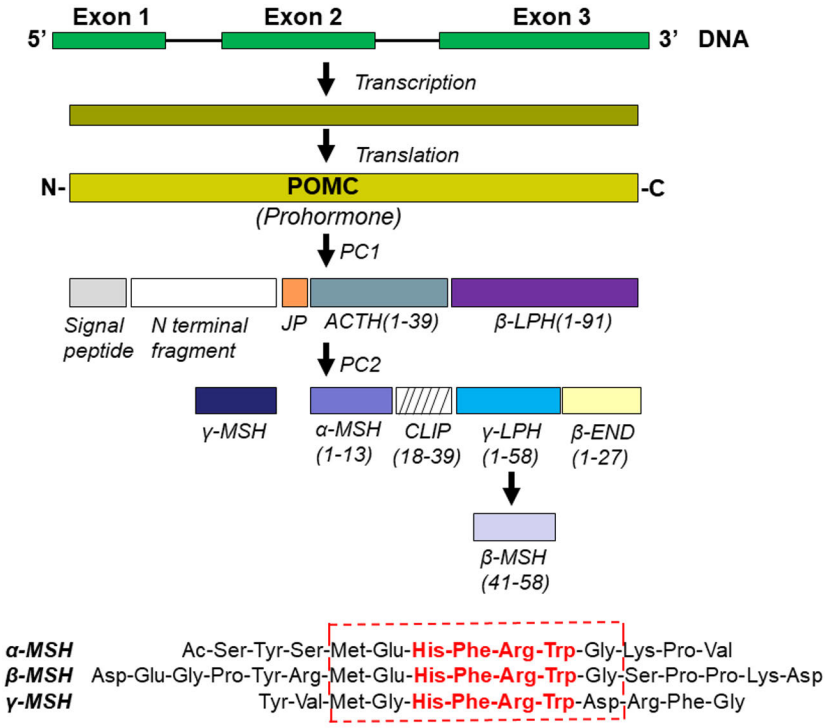

Figure 3. POMC proteolytic cleavage showing the dibasic amino acid processing sites into the melanocortin peptides.

2.4.2 Melanocortin receptors

Melanocortins exert their effects by interacting with MCRs. These receptors belong to the class A "rhodopsin-like family" of guanine nucleotide-binding protein-coupled receptors (GPCR). GPCRs have seven transmembrane domains spanning α-helices, which are linked by three intracellular and three extracellular loops connected to a short extracellular N-terminus and short intracellular C-terminus (Catania et al., 2004). The N-terminal domain carries N-glycosylation sites and the C-terminus contains two conserved cysteine residues that form disulfide bonds to stabilize the structure. Currently, five MCRs have been identified, named from

MC1R to MC5R, and each MCR is a product of a separate gene. These genes encoding the MCRs are conserved from fish to mammals (Cai & Hruby, 2016a; Kumar et al., 2011). Interestingly, all MCR genes have an intron-less structure with a few exceptions in some fish species (Kumar et al., 2011). MCR subtypes share sequence homologies ranging from 40% to 60%. MC4R shares 60% of amino acid identity with MC5R, while 38% of gene sequence similarities exist between MC2R and MC4R, about 45% between MC1R and MC3R and, 45% between MC2R and MC3R (Yang, 2011).

The MCRs are the smallest and most distinct G-protein coupled receptor family with each member positively coupled to G_s proteins, which activate adenylate cyclase resulting in intracellular cAMP accumulation. MCRs mediate their effects primarily via the cAMP-dependent signaling pathway, but other downstream effectors have been also identified including inositol 1,4,5 trisphosphate (IP_3) to increase intracellular Ca^{2+}, MAP kinases and Jak/STAT (Alfieri et al., 2018; Holloway et al., 2015). MCRs may also evoke G-protein-independent signaling that involves receptor phosphorylation by GPCR kinases and β-arrestin-driven signal transduction. These second messengers mediate the downstream effects of melanocortins.

MCRs are expressed in various tissues and they differ in their tissue distribution and exhibit different binding affinities to the melanocortin ligands (**Table 4**). MCRs are a unique form of GPCRs since they have also naturally occurring antagonists, namely agouti-related protein (AgRP) and agouti (or agouti-signaling protein, ASP, in the human genome). The Arg-Phe-Phe tripeptide sequence of ASP is vital for MC1R binding to induce its antagonistic effect. In rodents, agouti is only expressed in the skin, while the human homolog ASP is expressed in the skin, testes, adipose tissues, ovaries, heart, kidney and liver (Yuan & Tao, 2022). In the skin, ASP affects pigmentation and controls the amount of eumelanin synthesis in hair follicles by antagonizing α-MSH-mediated activation of MC1R (Nix et al., 2013; Walker & Gunn, 2010). A sustained antagonism of MC1R induces yellow coat color and promotes weight gain and linear growth in mice overexpressing agouti protein. The obese phenotype of these mice is caused by the antagonistic effect of agouti at MC4R (Abdel-Malek, 2009). Thus, agouti and ASP act as competitive antagonists of MC1R and MC4R and prevent α-MSH-induced stimulation of adenylate cyclase.

AgRP has high sequence similarity with ASP. However, these MCR antagonists possess different pharmacological properties. While ASP antagonizes MC1R, MC3R and MC4R, AgRP binds only to centrally expressed MC3R and MC4R but not MC1R. Therefore, transgenic mice overexpressing AgRP are similarly obese as agouti overexpressing mice but they do not display any change in coat color (Ollmann et al., 1997). AgRP is expressed centrally in the posterior hypothalamus, arcuate nucleus and paraventricular nucleus regions of the brain (Abdel-Malek,

2009). Both ASP and AgRP could play a role in inflammation mediation (Catania et al., 2004). AgRP was found to inhibit the anti-inflammatory modulation of MC3R activation in a mouse model of urate crystal peritonitis (Getting, 2006).

Table 4. Pharmacological properties of melanocortins at human MCR subtypes [Adapted & modified from (Yuan & Tao, 2022)]

Receptor	Binding affinity of endogenous ligand	Site of expression	Function
MC1R	α-MSH > β-MSH > γ3-MSH > ACTH > γ1-MSH > γ2-MSH	Melanocyte (skin), immune cells	Pigmentation, regulation of skin physiology,nociception, anti-inflammation
MC2R	ACTH	Adipocyte, adrenal cortex	Steroidogenesis, HPA stress response
MC3R	γ1-MSH > γ3-MSH > β-MSH > γ2-MSH > α-MSH > ACTH	Brain, digestive system, intestine, immune cells	Energy homeostasis, satiety, anti-inflammation
MC4R	β-MSH > α-MSH > ACTH > γ1-MSH > γ3-MSH > γ2-MSH	Brain	Energy Homeostasis satiety; obesity blood pressure, sexual function
MC5R	α-MSH > β-MSH > ACTH > γ1-MSH > γ2-MSH > γ3-MSH	Brain, liver, spleen, adipocytes, muscles, lungs, immune cells, heart	Exocrine secretion, lipolysis, thermo-regulation, immune system regulation

HPA (hypothalamic pituitary adrenal)

2.4.2.1 Melanocortin-1 receptor (MC1R)

MC1R was the first member of the MCR subtypes to be successfully cloned from mouse melanoma cell lines and human melanocytes in 1992 (Mountjoy et al., 1992). It is an intron-less gene located on chromosome 16q24.3 that encodes a 317 amino acid protein (Herraiz et al., 2021). MC1R expression was later found in various tissues including lutein cells of the corpus luteum, Leydig cells of the testis, keratinocytes, trophoblastic cells of the placenta and CNS (Rennalls et al., 2010). Its role in inflammation and immune modulation has been extensively investigated. These effects are ascribed to MC1R expression on monocytes, macrophages, neutrophils, fibroblast, endothelial cells, lymphocytes, mast cells, NK cells, a subset of cytotoxic T cells and dendritic cells (Brzoska et al., 2008). Monocytes express MCRs, particularly, MC1R. Furthermore, it was found that MC1R regulates the vascular endothelial function and cholesterol transport in macrophages (Rinne et al., 2015, 2017).

MC1R has the highest affinity for α-MSH, however, in humans, MC1R affinity for this ligand is almost equal to that of $ACTH_{(1-39)}$. α-MSH activates MCR subtypes

1,3,4 and 5 non-selectively at nanomolar and subnanomolar concentrations. A molecular structural scan revealed that the Met^4, Phe^7, Arg^8, and Trp^9 positions in melanocortin ligands are vital for binding and activating mouse MC1R and rat MC3R (Olivier, et al., 1994; Qarawi, et al., 1994). The activation of MC1R by α-MSH stimulates eumelanin synthesis in melanocytes leading to integumentary and follicular pigmentation. In contrast, loss-of-function mutations in *Mc1r* that uncouple the receptor from adenylate cyclase result in red/blond hair phenotype in humans (Herraiz et al., 2021). To evoke an adequate biological response, MC1R requires a full affinity of the melanocortin ligand.

2.4.2.2 Melanocortin-2 receptor (MC2R)

The human MC2R is a 297-amino-acid protein encoded by an intron-less gene on chromosome 18p11.2. It is the most selective MCR in terms of ligand binding since it recognizes only the $ACTH_{(1-39)}$ with no biological efficacy linked to other melanocortin peptides (Fridmanis et al., 2017). Therefore, it is also known as the ACTH receptor. MC2R is primarily expressed in the adrenal cortex where it regulates steroidogenesis. MC2R mRNA and protein have been also found in human skin and murine adipocytes. In white adipose tissue of rodents, MC2R mediates lipolysis when stimulated by its canonical ligand $ACTH_{(1-39)}$ (Møller et al., 2011). Contrastingly, human adipocytes do not express MC2R (Møller et al., 2015). Several missense mutations have been identified in the coding region of MC2R. These mutations are associated with hereditary unresponsiveness to ACTH, a rare autosomal recessive disorder known as familial glucocorticoid deficiency type 1 (Mohammed et al., 2022).

2.4.2.3 Melanocortin-3 receptor (MC3R)

MC3R was the third *Mcr* gene to be cloned and its gene is located on chromosome 20q13.2-q13.3. This gene also lacks non-coding regions (intron) in its nucleotide sequence. The human protein product of the *MC3R* gene contains 361 amino acids while in mice, its translation results in a 323 amino acid sequence. MC3R is expressed in various tissues of the periphery such as the placenta, kidney, duodenum, testis, pancreas, gut, heart, mammary gland, ovary, skeletal muscle and stomach, but it is also widely expressed within the CNS including the thalamus, hypothalamus, anterior amygdala, cortex and hippocampus (Demidowich et al., 2019). In contrast to MC1R and MC2R, MC3R protein expression is not present in melanocytes or the adrenal cortex (Ehtesham et al., 2019; Yuan & Tao, 2022).

MC3R differs from other MCRs, as it has no specificity for a particular melanocortin ligand. It interacts with $ACTH_{(1-39)}$ and α-, β- and γ-MSH with similar

binding affinity. γ-MSH shows a stronger affinity for MC3R, relative to other melanocortin MC3R and MC5R (Joseph et al., 2010). Amongst the five MCRs, γ-MSH has an affinity for MC3R in the nanomolar range suggesting that this peptide is a natural ligand for this receptor (Humphreys, 2004). In addition, MC3R responds to truncated $ACTH_{(4-10)}$ and $ACTH_{(1-10)}$ peptides as opposed to MC1R. This infers that the tetrapeptide core region (His-Phe-Arg-Trp) of melanocortins is enough to activate the MC3R subtype.

MC3R distribution in various tissues indicates a regulatory role in multiple functions including thermogenesis, control of feeding/obesity, cardiovascular regulation, sexual function and modulation of inflammatory responses (Cai & Hruby, 2016a; Patel et al., 2010). Deletion of *Mc3r* in mice results in altered energy metabolism decreased locomotive activity and salt-sensitive hypertension (Butler et al., 2000).

2.4.2.4 Melanocortin-4 receptor (MC4R)

The *Mc4r* gene is located on chromosome 18q22 and encodes a 332 amino acid-long protein. It is broadly expressed in the CNS with wide distribution in the hypothalamus, thalamus, cortex and brain stem. MC4R is similar to MC1R in its affinity for various melanocortin ligands. β-MSH has a stronger binding affinity to MC4R than α-MSH and ACTH. γ-MSH has the lowest affinity to this MCR subtype (Yuan & Tao, 2022). Moreover, α-MSH is 100-fold more potent in activating MC4R than γ-MSH.

MC4R is strongly implicated in the regulation of energy homeostasis as evidenced by the findings that loss-of-function mutations in the *Mc4r* gene result in hyperphagia, insulin resistance and obesity in mice and humans (Namjou et al., 2021). Tyr221Cys missense mutation in POMC gene transcript encoding non-functional β-MSH was identified in obese children with hyperphagia and increased linear growth, a phenotype also observed in individuals deficient in *Mc4r* (Lee et al., 2006). Conversely, activation of MC4R suppresses food intake and increases energy expenditure, thus protecting against weight gain. The pharmacological characterization of MC4R has also attracted interest within the pharmaceutical industry to develop MC4R agonists for the treatment of obesity. For example, setmelanotide, an MC4R agonist, has been recently approved for weight management in patients with obesity due to POMC, PCSK1 (i.e. PC1/3), or leptin receptor deficiency (Markham, 2021). MC4R also regulates sexual function, which has led to the development of bremelanotide (PT-141), an MC3R/MC4R agonist indicated for the treatment of hypoactive sexual desire disorder in premenopausal women (Safarinejad & Hosseini, 2008; Simon et al., 2019).

2.4.2.5 Melanocortin-5 receptor (MC5R)

Amongst the five MCRs, the *Mc5r* gene was the last to be cloned from chromosome location 18p11.2. The human and mouse MC5R protein contains 325 amino acids with the most sequence homology to MC4R and the least homology to MC2R. Similar to MC1R and MC4R, MC5R has the lowest binding affinity for γ-MSH but a stronger affinity for α-MSH followed by β-MSH and $ACTH_{(1-39)}$ (Yuan & Tao, 2022). It is detected at high concentrations in the exocrine glands such as sebaceous, Harderian and lacrimal glands (Ji et al., 2022). Therefore, MC5R is best known as a regulator of the synthesis and secretion of exocrine gland products. Furthermore, many other peripheral tissues such as the liver, ovary, thymus, mammary glands, bone marrow, fat cells, duodenum, skin, sebaceous gland, preputial gland, pancreas, prostate and the stomach also express MC5R (Xu et al., 2020). Akin to MC1R and MC3R subtypes, MC5R is potentially involved in the modulation of immune responses as it is also expressed in lymphocytes (Xu et al., 2020). Although MC5R is widely expressed in various tissues besides exocrine glands, its function in most of these tissues is poorly understood.

2.5 Synthetic melanocortin receptor ligands

The extensive distribution, complexity and characteristically high sequence homology of the MCRs have hindered the identification of selective and suitable synthetic ligands for these receptors. Developing potent and selective ligands for MCRs with favorable pharmacological profiles has been an arduous challenge. α-MSH, for instance, is rapidly degraded *in vivo* and exhibits a short functional half-life (D'Agostino & Diano, 2010; Diano, 2011).

The linearity of canonical melanocortin peptides allows the structure of these molecules to be susceptible to environmental influence. In addition, like other peptides, they undergo conformational mobility in solution. Therefore, synthetic MCR ligands have been developed to improve stability and pharmacokinetic profile. These characteristics can be, for instance, improved via cyclization that induces constraint on the peptide backbone and significantly limits the number of possible conformations, thus increasing selectivity (Cai & Hruby, 2016b). Cyclic analogs of α-MSH such as Melanotan-II (MTII: Ac-Nle-cyclo[Asp-His-D-Phe-Arg-Trp-Lys]-NH_2 display strong potency to various MCRs and improved serum stability with a half-life of 1.5 hours (Zhou & Cai, 2017). Consequently, MT-II is used as a template for further modifications and conjugations of melanocortin ligands to enhance their bioavailability and selectivity (Cai & Hruby, 2016b; Y. Zhou & Cai, 2017).

Numerous MCR ligands with higher potency and selectivity as well as improved duration of action have been developed and characterized (agonists; MS05, MS09,

HP-228, RO-27-3325, antagonists; SHU9119, PG901, PG911 HS014, HS024 and RO27-4680). More challenging to synthesize, however, is a selective agonist for MC3R. [D-TRP^{8}]-γ-MSH is a synthetic peptide with higher selectivity (EC_{50}= 0.33 nM) for the MC3R than MC4R (300-fold) and MC5R (250-fold) in comparison to the endogenous γ-MSH (EC_{50} = 5.9 nM) (Grieco et al., 2000). It is important to note that MC1R was not included in the study. [D-TRP^{8}]-γ-MSH appears to be the most potent ligand for MC3R with subnanomolar potency at this receptor.

There is an increasing interest to investigate the therapeutic potential of small molecules targeting the different MCR subtypes. The development of MC4R-targeting agonists for the treatment of obesity, for example, is of keen interest. Imcivree™, a first-in-class 'orphan drug', is an MC4R agonist (Setmelanotide) and was recently approved by FDA (Markham, 2021). It is the first drug approved for the treatment of obesity due to POMC, proprotein convertase subtilisin/kexin type 1 (PCSK1), or leptin receptor (LEPR) deficiency (Markham, 2021).

2.6 Regulation of inflammation by melanocortins

As alluded to in the previous sections, melanocortin peptides modulate inflammatory responses by interacting with their cognate receptors, particularly MC1R and MC3R (Montero-Melendez et al., 2022). α-MSH reduces acute inflammation by modulating the inflammatory responses of endothelial cells and a variety of leukocytes (Brzoska et al., 2008). It inhibits neutrophils and nitric oxide synthesis by macrophages and limits neutrophil migration as well as macrophage activities (Brzoska et al., 2008). Moreover, it has been reported that α-MSH peptide blocks the production of multiple pro-inflammatory cytokines including IL-1, IL-6 and TNF- α, while simultaneously stimulating the synthesis of anti-inflammatory molecules (Brzoska et al., 2008). Many of these mediators are implicated also in the pathophysiology of atherogenesis.

α-MSH has been reported to downregulate inflammatory mediators in various experimental disease models including arthritis, kidney ischemia, brain ischemia, bowel disease, brain inflammation, dermatitis, contact hypersensitivity, fever, endotoxin-induced liver inflammation and acute respiratory distress syndrome/ARDS (Wang et al., 2019). Furthermore, MSH peptides are proposed to be components of innate immunity due to their expression in the skin as well as in the mucosal barrier of the gastrointestinal tract. α-MSH and its truncated analog, C-terminal tripeptide KPV (α-$MSH_{(11-13)}$), inhibited *Staphylococcus aureus* and *Candida albicans* colony formation both *in vitro* and *in vivo* (Kannengiesser et al., 2008).

2.6.1 Molecular mode of anti-inflammatory action

Many of the anti-inflammatory effects of melanocortin are mediated by intracellular enhancement of cAMP level, which inhibits the synthesis of pro-inflammatory mediators. Additional signaling pathways mediating the anti-inflammatory actions of melanocortins have been reported including mitogen-activated protein kinases (MAPK) and IP_3-mediated increase in intracellular Ca^{2+} (Wang et al., 2019). The cAMP-PKA pathway inhibits the activation of NF-κB (**Fig. 4**), an essential transcription factor for more than 150 target genes including chemokines, cytokines, growth factors of the hematopoietic system, inducible nitric oxide synthase, major histocompatibility complexes, anti-apoptotic factors and various co-stimulatory factors (Liu et al., 2017). The activation of NF-κB is initiated by the degradation of the nuclear factor of kappa light polypeptide gene enhancer in B-cells inhibitor, alpha (IκBα) protein, a cytoplasmic inhibitor of NF-κB. α-MSH suppresses NF-κB nuclear translocation by inhibiting IκBα degradation and its nuclear translocation and DNA binding of NF-κB, which in turn, down-regulates transcription of pro-inflammatory cytokines (Dinparastisaleh & Mirsaeidi, 2021).

Further, the influence of melanocortins on the cAMP-PKA signaling pathway could affect downstream regulators and modulators in this pathway through various actions. PKA stimulation phosphorylates cAMP-responsive-element-binding protein (CREB), which prevents the binding of CREB-binding protein (CBP) co-factor with the p65 subunit of NF-κB. Activated PKA also inhibits the nuclear translocation of p65 and blocks the action of IκB kinase (IKK). Furthermore, PKA stimulation also blocks the activation of p38 MAP kinase and TATA-binding protein (TBP) by preventing the phosphorylation and activation of MAP kinase kinase kinase 1 (MEKK1), which in turn, deactivates c-JUN N-terminal kinase (JNK) activities (Gonzalez-Rey et al., 2007; Kaneva, 2011). The decrease in the intracellular amount of nuclear p65, CBP and phosphorylated TBP disrupts the formation of a trans-activating complex that is essential for the gene transcription of most cytokines and chemokines. Ultimately, melanocortins significantly disrupt the transcription machinery that is precisely assembled to the gene promoter of various inflammatory mediators (Gonzalez-Rey et al., 2007; Kaneva, 2011).

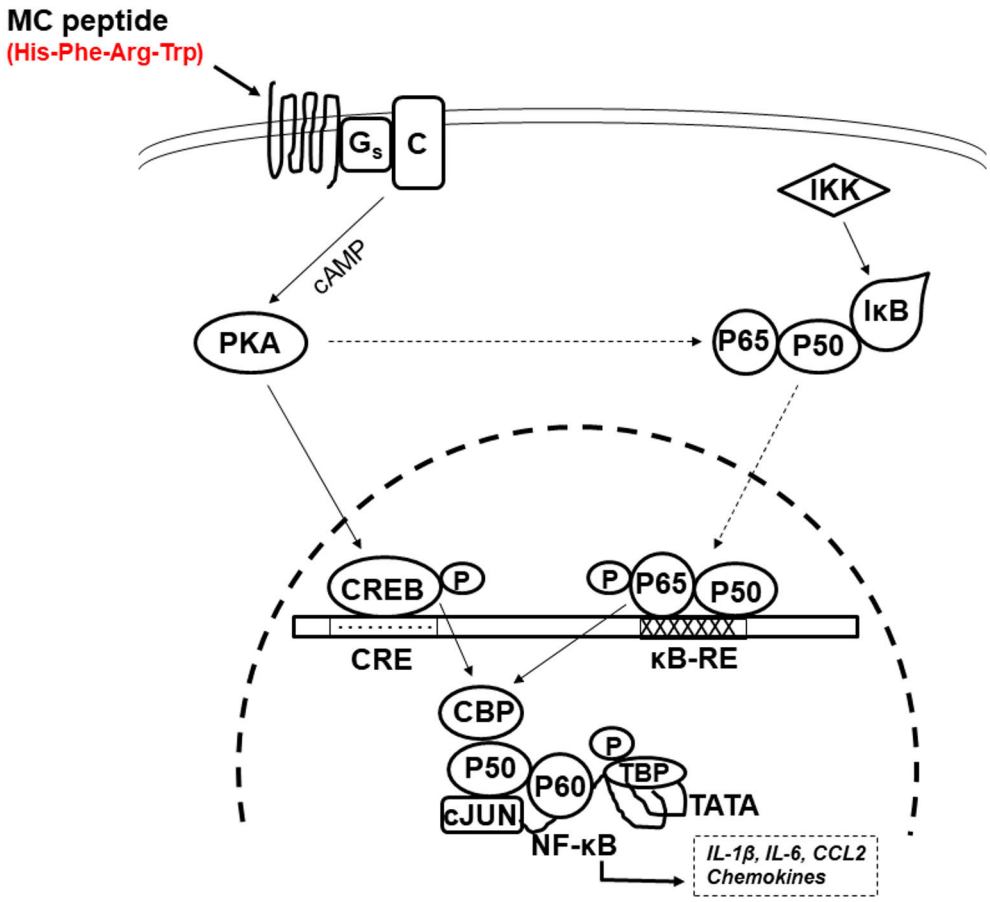

Figure 4. Melanocortin (MC) peptide modulation of NF-κB in mitigating inflammation. Melanocortin peptides activate MCRs to increase intracellular cAMP level, which, in turn, activates the enzyme protein kinase A (PKA). The activated PKA phosphorylates cAMP-responsive-element-binding protein (CREB) preventing downstream linkage of transcriptional co-activator CREB-binding protein (CBP) and p65 protein. PKA activation also induces the inhibition of IκB kinase (IKK), a contributor to the upstream NF-κB signal transduction cascade via the hindrance of p65 nuclear translocation. PKA activation also suppresses the activities of p38 mitogen-activated protein kinase and TATA-binding transcription factor (TBP) via mitogen-activated protein kinase kinase kinase 1 (MEKK1) inhibition to reduce c-JUN N-terminal kinase (JNK) activities, a pro-inflammatory gene regulator. Thus, NF-κB regulation of inflammatory mediator proteins such as pro-inflammatory cytokines and chemokines is hampered [Adapted and modified from (Gonzalez-Rey et al., 2007)].

2.7 Anti-inflammatory therapeutic potential of the melanocortin system

The melanocortin system acutely modulates the host inflammatory response. Together with various other inflammatory molecules, melanocortin peptides promote the protection and maintenance of homeostatic balance within the body. MCR subtype-1 and -3, when activated by natural or synthetic melanocortins, evoke potent and wide-ranging anti-inflammatory actions. Truncated peptide derivates of the C-terminal domain of α-MSH, such as α-$MSH_{(11-13)}$ and KdPT (a tripeptide derivative of the C-terminal end of α-MSH), which primarily activate MC1R are increasingly being investigated for their therapeutic potential in acne, inflammatory bowel disease and psoriasis (Mykicki et al., 2017). These ligands, like their parent molecule α-MSH, have been shown to modulate many signaling pathways connected to inflammation regulation such as NF-κB inhibition, IL-10 induction and TNF- α synthesis (Dinparastisaleh & Mirsaeidi, 2021). In *in vivo* studies, α-MSH has been shown to reduce systemic inflammation in various experimental models of inflammatory diseases such as colitis, rheumatoid arthritis and skin diseases (Wang et al., 2019). These studies demonstrate the potential therapeutic effects of these peptides through the activation of MC1R.

Similarly, [D-TRP^8]-γ-MSH mediates anti-inflammation by activating MC3R. In murine models of inflammatory diseases, the administration of this ligand attenuated pro-inflammatory mediators. For instance, [D-TRP^8]-γ-MSH reduces urate crystals-induced chemokine C-X-C motif chemokine ligand 1 (CXCL1) synthesis and inhibits the accumulation of polymorphonuclear cells in the peritoneal cavity (Getting et al., 2006). [D-TRP^8]-γ-MSH via MC3R activation promotes anti-inflammation by inhibiting NF-κB and by inducing the anti-inflammatory enzyme heme-oxygenase-1 (HO-1), thus protecting against various inflammatory diseases (Getting et al., 2008; Gómez-SanMiguel et al., 2016).

Natural and synthetic melanocortins are likely to display a better safety profile relative to many anti-inflammatory biologic drugs that are known for their paradoxical association with adverse effects such as bone marrow suppression, hypertension, dyslipidemia, gastrointestinal distress, kidney and liver injury (Boyman et al., 2014; Dorr et al., 2000; Singh et al., 2011; Ugwu et al., 1997). Owing to their antimicrobial activities (Mumtaz et al., 2020), melanocortin peptides might reduce the risk of infection, which is a common adverse effect associated with the prolonged usage of classical anti-inflammatory and immunosuppressive drugs. In addition to its anti-inflammatory potency, MC1R also mediates RCT. Thus, potential melanocortin pharmacotherapy for managing atherosclerosis would likely confer a double positive effect. Therefore, melanocortin ligands and their mimetics could be suitable drug candidates for the clinical management of immune-mediated inflammatory disorders.

3 Aims

This thesis aimed to investigate the contribution of melanocortin receptors MC1R and MC3R to the development of atherosclerosis and associated inflammatory processes via loss-of-function and pharmacological studies.

The specific objectives of this study were:

- To determine whether the global deficiency in MC1R signaling in *Apoe*$^{-/-}$ mice affects the development of atherosclerosis.

- To investigate the specific contribution of leukocyte-MC1R to the progression of atherosclerosis in *Apoe*$^{-/-}$ mice via bone marrow transplantation.

- To explore the therapeutic potential of MC3R in *Apoe*$^{-/-}$ atherosclerotic mice by selectively activating this receptor.

4 Materials and Methods

4.1 Animals and animal models

Double mutant *Apoe*$^{-/-}$ *Mc1r*$^{e/e}$ mice were generated from the crossing between the recessive yellow *Mc1r*$^{e/e}$ mice (Jackson Laboratory, strain# 000060, Bar Harbor, ME, USA) and *Apoe*$^{-/-}$ mice (Jackson Laboratory, strain# 002052), both of which were on C57Bl/6J background. Age- and sex-matched *Apoe*$^{-/-}$ single knockout mice served as controls. In Study I, both genotype groups consisted of 8–48 weeks old adult male mice. In Study II, bone marrow cells were isolated from female *Apoe*$^{-/-}$ or *Apoe*$^{-/-}$ *Mc1r*$^{e/e}$ mice and transferred into 8–10 weeks old *Apoe*$^{-/-}$ male recipient mice. For the drug intervention study (Study III), 8 weeks old female *Apoe*$^{-/-}$ mice were fed a high-fat diet/HFD (RD Western Diet, D12079B, Research Diets Inc, NJ, USA) for 12 weeks to enhance atherosclerosis before [D-Trp^{8}]-γ-MSH, an MC3R agonist was administered from week 8 of the HFD. Mice in Study I and Study II experiments were fed an HFD or standard rodent chow diet (SDS, Essex, UK) for 10 weeks *ad libitum*. The HFD contained 20% fat, 0.15% cholesterol and 35% carbohydrates. Mice had free access to regular tap water. Mice were group-housed and maintained at ~21ºC on a 12 h light/dark cycle in the Central Animal Laboratory at the University of Turku.

4.2 Ethical consideration

All animal experiments were approved by the Animal Experiment Board in Finland (License Number: ESAVI/6280/04.10.07/2016) and conducted as per the institutional and national guidelines for the care and use of laboratory animals. The number of animals used per group in each experiment was carefully planned and evaluated in compliance with the 3R (Replacement, Reduction and Refinement) principles of animal testing. Where possible, *in vivo* studies were replaced with *in vitro* experiments. Appropriate measures were taken to avoid stress and suffering for the animals. The animals were closely monitored throughout the experiments via regular inspection of food and water intake, weight gain and observing their physical condition.

4.3 *In vivo* experiments

4.3.1 Diet intake and body weight

To accelerate the development of atherosclerosis, mice were fed an HFD for 10-12 weeks or maintained on a normal chow diet. Experimental mice were group-housed (3-5 littermates/cage) on a 12-hour light/dark cycle. The food intake was recorded weekly and body weight development was monitored on a bi-weekly basis.

4.3.2 *In vivo* reverse cholesterol transport (RCT) assay

To study the efficiency of RCT *in vivo* (Study I), bone marrow-derived macrophages (BMDM) were labeled with ^{3}H-cholesterol (5 µCi/mL, PerkinElmer) and acetylated LDL (30 µg/mL, BioRad) in a complete medium for 48 hours. Cells were then suspended in PBS at a concentration of 10 million cells/mL. Approximately $4x10^{6}$ labeled BMDM cells were injected (i.p) into individually housed *Apoe*$^{-/-}$ and *Apoe*$^{-/-}$ *Mc1r*$^{e/e}$ mice. Animals were euthanized via CO_2 overdose and blood was withdrawn by cardiac puncture 48 hours following the injection of BMDM. The liver was excised and weighed and, feces from the bedding of each cage were collected, dried and weighed.

Fifty µL of plasma was directly mixed with 9 mL of LSC cocktail (Optiphase Hisafe, PerkinElmer) and measured in duplicate using a Wallac model 1410 liquid scintillation counter (Wallac, Turku, Finland). Fifty mg pieces of the excised liver samples were homogenized with 1 mL of SOLVABLE and processed with 0.2 mL of 30% H_2O_2 before heating for 30 min at 50-60 °C. Twelve mL of LSC cocktail was added to each sample and then ^{3}H radioactivity was measured. Similarly, 20 mg of dried fecal samples were processed, mixed with 16 mL of the LSC cocktail and measured for radioactivity. The RCT to plasma, liver and feces was estimated as a percentage of total injected radioactivity.

4.3.3 Bone marrow cells transplantation

To explore the contribution of leukocyte MC1R to the development of atherosclerosis (Study II), bone marrow (BM) cells were isolated from the femurs and tibiae of age-matched female *Apoe*$^{-/-}$ *Mc1r*$^{e/e}$ mice or *Apoe*$^{-/-}$ WT mice. The recipient *Apoe*$^{-/-}$ male mice were lethally irradiated with two doses of 5 Gy (Faxitron MultiRad 225 X-ray) at 3 hours apart. The recipient mice were reconstituted intravenously with $1x10^{7}$ BM cells 72 hours later from either *Apoe*$^{-/-}$ or *Apoe*$^{-/-}$ *Mc1r*$^{e/e}$ mice. After BM transplantation, mice received acidified and autoclaved water and were allowed to recover for 6 weeks. Animals were thereafter fed a standard chow diet or HFD for 10 weeks (**Fig. 5**). Mice were euthanized by CO_2

asphyxiation and whole blood was collected via cardiac puncture. The spleen, aorta, liver and bone marrow from the femur were isolated for further analysis.

The efficiency of BM reconstitution was determined from the genomic DNA (QIAamp DNA Blood Mini Kit, Qiagen, USA) obtained from the peripheral blood of recipient mice and quantified by real-time PCR (Applied Biosystems 7300 Real-Time PCR system) for the expression of the Y chromosome-specific gene *Zfy1* and a reference gene (*Bcl2*) (An & Kang, 2013). The engraftment of female donor cells in the recipient males was determined using a standard curve generated from samples with known percentages of male and female DNA. The donor cell engraftment in the peripheral blood ranged from 95 % to 99 % (**Fig 13A**).

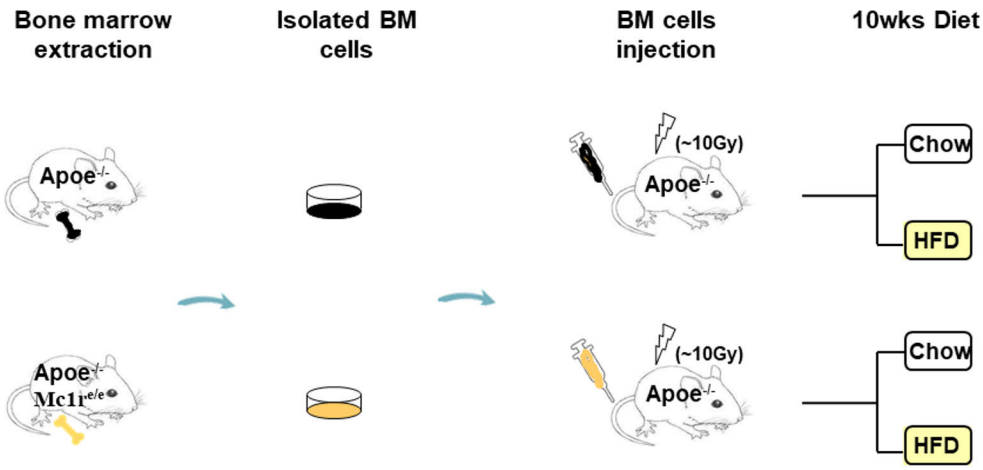

Figure 5. Schematic illustration of BM cell transplantation into irradiated *Apoe*$^{-/-}$ mice (An & Kang, 2013).

4.3.4 *In vivo* homing assay

To examine *in vivo* leukocyte cell migration in *Apoe*$^{-/-}$ mice (Study II), spleen or bone marrow cells from *Apoe*$^{-/-}$ and *Apoe*$^{-/-}$ *Mc1r*$^{e/e}$ male mice were harvested, washed and filtered through a 70-µm cell strainer. These cells were then stained with eFluor™ or carboxyfluorescein succinimidyl ester/CFSE at 37°C for 15 min. Approximately 1x10^{7} million splenocytes or bone marrow cells were intravenously injected into the tail vein of each recipient *Apoe*$^{-/-}$ male mouse. Mice were sacrificed 24 hours later and spleen, blood, and para-aortic lymph nodes were harvested for staining with antibodies against CD45, CD4, CD8, TCR-β and CD11b or CD45, CD115, CD11b, Ly6C and Ly6G (**Table 5**). Flow cytometry (LSR Fortessa, BD Biosciences) analysis of samples was carried out and the results are expressed as a percentage of injected CD45^{+} cells.

4.3.5 Drug intervention studies

To investigate the anti-inflammatory and therapeutic potential of MC3R activation in atheroprogression (Study III), female *Apoe*$^{-/-}$ mice were randomly assigned to receive daily intraperitoneal injections of either vehicle (phosphate-buffered saline/PBS) or [D-Trp^{8}]-γ-MSH (γ-MSH; 15 μg/mouse/day) in the last 4 weeks of HFD feeding (**Fig. 6**). Earlier anti-inflammatory studies in mice using [D-Trp^{8}]-γ-MSH administered a fixed dose of 10μg/mouse. In a crystal-induced inflammation study, mice demonstrated dose-responsiveness for the drug peaking around 10μg/mouse (Getting et al., 2006). However, a dose of 15μg/mouse/day was administered in this study to account for the higher body weight of *Apoe*$^{-/-}$ mice, which had been on HFD for 8 weeks before the drug intervention commenced. [D-Trp^{8}]-γ-MSH ([H-Tyr-Val-MetGly-His-Phe-Arg-DTrp-Asp-Arg-Phe-Gly-OH], a potent MC3R agonist, was generously gifted to our laboratory by Minying Cai & Victor J. Hruby (Department of Chemistry and Biochemistry, University of Arizona, Tucson, AZ, USA. [D-Trp^{8}]-γ-MSH was dissolved in PBS and stored at -20^{o}C before use. [D-Trp^{8}]-γ-MSH has a 300- and 250-fold higher selectivity for MC3R compared to MC4R and MC5R, respectively (Grieco et al., 2000). The weight and food consumption of each mouse was monitored every week. Mice were sacrificed via CO_2 asphyxiation at the end of week 12.

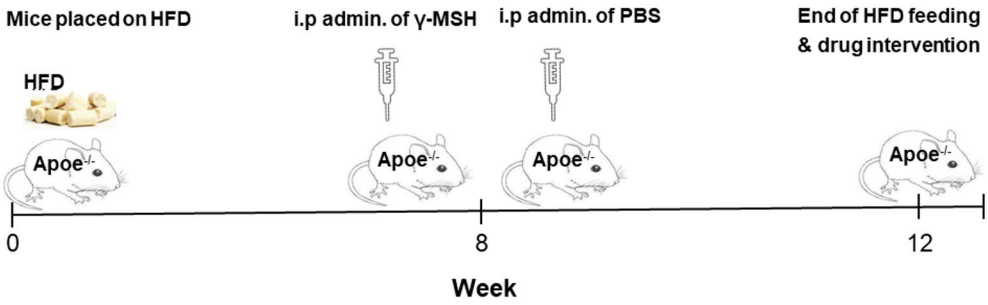

Figure 6. Schematic illustration of MC3R intervention study (Study III) in atherosclerotic mice.

4.3.6 Tissue collection

In all three studies, terminal blood (0.5 – 1.0 mL) was obtained via cardiac puncture into EDTA-coated collection tubes. Fifty μL of blood was used for flow cytometry analyses of blood cells and the surplus blood was centrifuged at 4000 rpm for 10 min. The resultant plasma was carefully collected, snap-frozen in liquid nitrogen and stored at -70^{o}C. The spleen, liver, gonadal white adipose tissue and retroperitoneal white adipose tissue were weighed. The descending aorta was carefully isolated for further investigation. The spleen samples were dissected and the middle cross-sectioned sample was used for RNA extraction and/or immunohistochemical

staining whilst the remainder was processed for flow cytometry analysis. Liver samples were obtained from the larger left lateral lobe for tissue-specific analyses. Tissue samples reserved for RNA extraction (aorta, spleen, liver, bone marrow and WAT) were snap-frozen and stored at -70°C until further processing. Samples intended for histological analyses were fixed in 10% formalin for 24 hours and then stored in 70% ethanol or snap-frozen in liquid nitrogen before cryosectioning a few hours later. For $CD4^+$ T cell isolation in Study II, spleens from *Apoe*$^{-/-}$ and *Apoe*$^{-/-}$ *Mc1r*$^{e/e}$ mice were excised and processed into single-cell suspensions. Splenic $CD4^+$ T cells were then enriched by positive selection (Miltenyi Biotec) and the resulting cell fraction was subjected to total RNA or protein extraction.

4.4 *Ex vivo* and *in vitro* assays

4.4.1 Cell culture and drug treatments

To investigate the direct effect of [D-Trp^8]-γ-MSH on the endothelium (Study III), primary endothelial cells were isolated from freshly excised mouse thoracic aortae. The isolated thoracic aorta was flushed with ice-cold PBS to remove blood before the removal of attached small lateral vessels and adipose tissues with micro-dissection forceps. Pieces of aortae were cut open before placing them in gelatin (0.2%)-coated wells. The endothelial cell surface was placed facing downward. Sterile needles were used to gently remove the aortic segments from the matrix without disturbing the growing endothelial cells (Rinne et al., 2015). Cells were cultured in a mix of DMEM-F12 and RPMI (Lonza, Basel, Switzerland) at a 1:1 ratio supplemented with endothelial cell growth supplement (R&D Systems, Minneapolis, MN, USA), 10% fetal bovine serum (FBS) and 100 U/100 µg/mL penicillin-streptomycin (Gibco Life Technologies, NY, USA) on Geltrex-coated (Gibco) plates. When the cell confluency reached about 80%, [D-Trp^8]-γ-MSH was applied for 1, 3, 6 and 24 hours at a concentration range between 0.01–10 µM and cells were thereafter collected in Qiazol (Qiagen) for RNA extraction and qPCR analyses.

To analyze the direct effect of [D-Trp^8]-γ-MSH on macrophages (Study III), isolated and differentiated bone marrow-derived macrophage cells from *Apoe*$^{-/-}$ mice were exposed to the same concentrations of the drug and duration as the primary endothelial cells. The BMDM cells were isolated from the femurs and tibiae of *Apoe*$^{-/-}$ mice by flushing out the bone marrow cells and suspended in IMDM medium (Gibco) supplemented with penicillin/streptomycin, 10% FBS and 20 ng/mL M-CSF (PeproTech, NJ, USA). The medium was replaced on day 4 and cells were allowed to differentiate for a total of 6–7 days. Thereafter, cells were seeded into 24-well plates (100 000 cells/well) (CELLSTAR, Helsinki, Finland), treated with [D-Trp^8]-γ-MSH for 1–24 hours and harvested for RNA extraction.

4.4.2 Flow cytometry analysis

To quantify total leukocyte and leukocyte subsets in all three Studies, flow cytometry analysis in the aorta, whole blood, bone marrow (femur) and spleen was employed. Aortic samples were digested with a cocktail of enzymes (Collagenase I, 450 U/mL; Collagenase XI, 250 U/mL; DNase I, 120 U/mL Hyaluronidase, 120 U/mL; Sigma Aldrich) for 60 min at 37°C and then filtered through a 50-µm cell strainer (BD Biosciences). Single-cell suspensions of aortic lysate, blood, splenic cells and bone marrow cells were stained for 30 min at 4°C with fluorochrome-conjugated antibodies (**Table 5**).

Table 5. List of fluorochrome-conjugated antibodies applied in the flow cytometry experiments of Study I–III.

Study I	Study II	Study III
CD11b (clone M1/70) BioLegend	**CD45.2** (clone 30-F11) BD Biosciences	**CD11b** (clone M1/70) BioLegend
CD11c (clone N418) **BioLegend**	**CD11b** (clone M1/70) BioLegend	**CD11c** (clone N418) BioLegend
CD18 (clone M18/2) **eBioscience**	**CD115** (clone AFS98) BioLegend	**CD31/PECAM-1** (clone MEC13.3) BD Biosciences
CD31/PECAM-1 (clone MEC13.3) BD Biosciences	**Ly6C** (clone AL-21) BD Biosciences	**CD45.2** (clone 30-F11) BD Biosciences
CD45.2 (clone 30-F11) **BD Biosciences**	**Ly6G** (clone 1A8) BD Biosciences	**CD54/ICAM-1** (clone 3E2) BD Biosciences
CD49d/VLA4 (clone R1-2) eBioscience	**CD19** (clone 6D5) BioLegend	**CD106/VCAM-1** (clone MVCAM.A) BD Biosciences
CD54/ICAM-1 (clone 3E2) **BD Biosciences**	**CD4** (GK1.5) BioLegend	**CD115** (clone AFS98) BioLegend
CD62L (clone MEL-14) BD Biosciences	**CD8a** (clone 53-6.7) BioLegend	**Ly6C** (clone AL-21) BD Biosciences
CD62P (clone RMP-1) BioLegend	**NK1.1** (clone PK136) BioLegend	**Ly6G** (clone 1A8) BD Biosciences
CD106/VCAM-1 (clone MVCAM.A) BD Biosciences	**TCR-β** (clone H57-597) BioLegend	
CD115 (clone AFS98) **BioLegend**		
CD162/PSGL-1 (clone2PH1) BD Biosciences		
F4/80 (clone BM8) **BioLegend**		
Ly6C (clone AL-21) **BD Biosciences**		
Ly6G (clone 1A8) BD Biosciences		

To stain intracellular antigens (Study II), splenocytes were harvested and incubated in RPMI 1640 medium supplemented with 10% FBS, 100 U/100 µg/mL penicillin-streptomycin (Gibco Life Technologies, NY, USA) cell stimulation and protein transport inhibitor cocktail (eBioscience) for 18 hours. Cells were then washed with PBS, stained for surface antigens (CD45, CD11b, TCR-β and CD4), fixed, permeabilized (eBioscience) and then stained with antibodies against FoxP3 (clone JJK-16s, eBioscience) and IFN-γ (clone XMG1.2, Biolegend).

For hematopoietic stem cells analysis, bone marrow suspensions were stained with antibodies (BioLegend) against lineage markers: a cocktail of Ter119, CD3, CD11b, B220 (BioLegend) and GR1 (BioLegend); Sca-1 (clone D7/ BioLegend); c-Kit (clone 2B8/ BioLegend); CD150 (clone TC15-12F12.2/BioLegend) and CD48 (clone HM48-1/BioLegend).

Fixable viability dye (Zombie Aqua, Biolegend) was applied at room temperature for 15 min to differentiate dead cells from viable cells before leukocyte staining. Data were acquired on an LSR Fortessa (BD Biosciences) and the results were analyzed with FlowJo software (FlowJo, LLC, Ashland, USA).

4.4.3 Chemotaxis assay

To investigate the migration of isolated $CD4^+$ T cells toward CCR5 ligands (CCL3, CCL4 and CCL5), splenocytes were harvested and processed into a single-cell suspension. A CD4 positive selection kit (Invitrogen) was used to isolate $CD4^+$ cells, which were after isolation suspended in RPMI1640 medium supplemented with 0.5% fatty acid-free BSA (Study II). Chemotaxis assay was performed using 6.5 mm Transwell® polycarbonate membrane cell culture inserts (5.0-µm pore size, Corning, NY, USA). Murine recombinant CCL3, CCL4, or CCL5 (100 ng/mL, PeproTech, London, UK)-containing migration medium (RPMI-1640 + 0.5% fatty acid-free BSA) was placed in the bottom of the well and 100 µL ($1x10^6$ cells) of cell suspension was seeded in the top chamber. Following 3 hours of incubation at 37°C in a 5% CO_2 atmosphere, the top chamber was removed and migrated cells were stained for CD45, CD4, CD8, TCR-β, CD115, Ly6C and Ly6G. Flow cytometry technique was applied to count the positively stained cells. The number of migrated cells was expressed as a percentage of $CD45^+$ cells that were seeded in the top chamber.

4.4.4 CCR5 internalization and recycling assay

To probe the internalization and recycling of CCR5, splenocytes were harvested from *Apoe*$^{-/-}$ and *Apoe*$^{-/-}$ *Mc1r*$^{e/e}$ mice and suspended in RPMI1640 medium (supplemented with 0.5% fatty acid-free BSA) at a density of 1 x 10^6 cells/mL. The

cells were incubated at 37°C for 60 min. The cells were left untreated or stimulated with recombinant murine CCL5 (400 ng/mL, 60 min, PeproTech) to induce CCR5 internalization. To examine CCR5 recycling, CCL5-stimulated cells were washed three times with RPMI1640 medium, resuspended in RPMI1640 medium containing 0.5% fatty acid-free BSA and incubated for 60 minutes at 37°C. Cells were harvested, stained for CD45, TCR-β, CD4, CD8, and CCR5 (clone HM-CCR5, Biolegend) and analyzed for the expression of cell surface CCR5 with flow cytometry.

4.4.5 Lipid analysis

The lipid content in the liver (Study I) was determined from a transverse piece of the left lobe embedded in O.C.T compound (Tissue-Tek®, Sakura Finetek USA Inc, Torrance, CA, USA) for cryosectioning. Liver sections were thereafter stained with Oil-Red-O or hematoxylin and eosin (H&E). A separate piece (100 mg) from the left liver lobe was homogenized (TissueLyser) in 500 µL of PBS with 0.1% NP-40 and then centrifuged to remove the insoluble material. The cholesterol concentration in the liver homogenates was quantified using a CHOD-PAP reagent (Roche, Basel, Switzerland).

4.4.5.1 Plasma lipid and cytokine/chemokine assays

Plasma total cholesterol and triglyceride concentrations were determined with commercial colorimetric assays (CHOD-PAP and GPO-PAP, mti Diagnostics, Idstein, Germany). Plasma cholesterol concentrations in the HDL and LDL/VLDL fractions were determined after processing the fractions using LDL/VLDL precipitation buffer (Abcam, Cambridge, United Kingdom). In addition, plasma pro-inflammatory cytokines and chemokines in all three studies were determined using ProcartaPlex™ Multiplex Immunoassays (Chemokine 20-Plex Mouse Panel 1 and High Sensitivity 5-Plex Mouse Panel, eBioscience). Furthermore, the plasma immunoglobulin levels (Study II) were quantified with Mouse Antibody Isotyping Panel (Thermo Fisher Scientific).

4.4.5.2 Bile acids and neutral sterol assay

In Study I, total bile acids were extracted from the feces and gall bladder bile. Feces were collected over 48 hours from individually housed mice and samples were dried for 24 hours at 50 °C, weighed and pulverized. Bile acid pools in the gall bladder were collected from the same mice after euthanasia via CO_2 asphyxiation before processing. Total bile acids were extracted and analyzed through a gas-liquid

chromatography system equipped with a nonpolar Ultra 1 capillary column for bile acids and an Ultra 2 column for neutral sterols (Agilent 6890N Network GC System, Agilent Technologies, Santa Clara, CA, USA). The standards (Sigma-Aldrich) were run to identify individual bile acids (chenodeoxycholic acid, cholic acid, β-muricholic acid, epideoxycholic acid, deoxycholic acid, ursodeoxycholic acid, lithocholic acid and isolithocholic acid), and neutral sterols (cholesterol and coprostanol).

4.4.6 Histology and Immunohistochemistry

For histological evaluation of tissue morphology and expression of target proteins, aortic root, spleen and liver samples were embedded in paraffin after fixing in 10% formalin for 24 hours and then cut into 4 μm-thick serial sections. Atherosclerotic plaque area, necrotic core size and plaque collagen content were determined at the level of the aortic sinus in H&E and Masson's trichrome-stained sections. Aortic sections were also immunostained with Mac-2 (1:400, clone M3/38 Cedarlane Labs, Burlington, ON, Canada), iNOS (1:100, polyclonal, Abcam, Cambridge, United Kingdom), α-SMA (1:200, clone 1A4, Sigma-Aldrich, St. Louis, MO, USA), MC3R (1:200, polyclonal, Abcam) and CD206 (1:500, polyclonal, Abcam) antibodies followed by detection with a horseradish peroxidase-conjugated secondary antibody and diaminobenzidine (ABC kit, Vector Labs, Burlingame, USA) to determine macrophage, smooth muscle cell-positive areas and MC3R expression, respectively.

En face staining was applied to quantify the aortic lesion burden (Study I). Aortae from the iliac bifurcation to the aortic root were excised and the adventitia was removed. Samples were fixed in 10 % neutral-buffered formalin overnight, opened longitudinally and stained with Sudan IV (Sigma-Aldrich) to quantify the atherosclerotic lesion area. For quantitative analysis, images were captured using a Zeiss Stemi 2000-C stereomicroscope and the atherosclerotic plaque area per total intimal area was determined using image analysis software (ImageJ, NIH, Bethesda, MD, USA).

For immunofluorescence staining, tissue sections were stained with antibodies against VCAM-1 (1:200, clone EPR5047, Abcam), iNOS (1:100, polyclonal, Abcam), Mac-2 (1:400, M3/38, Cedarlane), MC3R (polyclonal, 1:100, Abcam) and CD11b (1:50, clone M1/70, Biolegend) followed by detection with fluorochrome-conjugated secondary antibodies (anti-rabbit Alexa Fluor 647 and anti-rat Alexa Fluor 488, Jackson ImmunoResearch, West Grove, USA). Cryosectioned (6μm) spleen samples (Study II) were stained with antibodies against MC1R (1:50, polyclonal, Alomone Labs, Israel) and CD4 (1:50, clone RM4-5, Biotechne). Sections were counterstained with hematoxylin (CarlRoth) or DAPI (Fluoroshield mounting medium, Abcam) and scanned in Pannoramic 250 or Pannoramic Midi

digital slide scanner (3DHISTECH Kft, Budapest, Hungary). Images were processed with Pannoramic/Caseviewer (3DHISTECH, Hungary) and ImageJ software (NIH, Bethesda, MD, USA).

4.4.7 mRNA isolation, cDNA synthesis and RT-PCR analysis

Total RNA was extracted from cell culture and tissue samples (aorta, liver, bone marrow and spleen) with a Direct-zol RNA Miniprep kit (Zymo Research, USA). RNA concentration was quantified (NanoDrop Spectrophotometer, ThermoFisher Scientific, MA, USA) and 500–1000 ng of total RNA was reverse-transcribed (PrimeScript RT reagent kit, Takara Clontech) into cDNA. Before RNA extraction, tissue samples were first homogenized using Qiagen TissueLyser LT Bead Mill (QIAGEN, Venlo, Netherlands). SYBR Green protocols (Kapa Biosystems, MA, USA) were employed for quantitative real-time PCR (RT-PCR) and samples were run in duplicates on an Applied Biosystems 7300 Real-Time PCR system. Target gene expression was normalized to the geometric mean of *Rps29* (*s29*) and *Actb* (*β-actin*) house-keeping genes using the comparative ΔCt method ($2^{-\Delta\Delta Ct}$) and results are presented as relative transcript levels.

4.4.8 Western blot analysis

In Study II, cell culture ($CD4^+$ sorted cells) and tissue (aorta and spleen) samples were lysed and homogenized (Qiagen TissueLyser LT Bead Mill, QIAGEN, Venlo, Netherlands) in radioimmunoprecipitation assay (RIPA) buffer. The protein concentration of the samples was quantified with a copper-based BCA protein assay (ThermoFisher Scientific, MA, USA). Aliquots (10-30 µg protein) of total protein were mixed with Lammli buffer at a 1:5 ratio, separated by SDS-PAGE (6–10%) and transferred onto a nitrocellulose membrane. Non-specific binding to membranes was blocked with 5% nonfat dry milk in TBST (tri-buffer saline with 1% Tween) buffer. Blots were probed with antibodies against CCR5 (Novus Biologicals, Biotechne Ltd, UK), MC1R (Alomone Labs, Israel), or β-actin (Sigma-Aldrich Co.) overnight at 4ºC. Horseradish peroxidase-conjugated anti-IgG (Cell Signaling Tech, Frankfurt, DE) secondary antibodies detection were applied and membranes were developed using an enhanced chemiluminescence system (ECL detection reagent: Pierce ECL Western (Thermo Scientific, USA). The target protein expression was normalized against the β-actin protein expression to correct for loading. Protein bands were analyzed with ImageJ (ImageJ, Fiji, NIH, MD, USA).

4.5 Data analysis

All data are expressed as mean ± standard error of the mean (SEM) and analyzed with GraphPad Prism versions 6.0, 7.0 and 8.0 (La Jolla, CA, USA). Differences between the genotype groups and experimental conditions were assessed with unpaired Student's *t-test* or with one- or two-way analysis of variance (ANOVA) followed by Bonferroni *post hoc* tests. An unpaired student *t-test* with Welch's correction was used to analyze data that revealed unequal variances with the F test. Gaussian distribution of data sets was assessed with the D'Agostino and Pearson omnibus for the normality test of the data. For data that were not normally distributed or had $n < 8$ per group, non-parametric Mann-Whitney *U* test or Kruskal-Wallis test was applied. Possible outliers in the data sets were identified via the regression and outlier removal (ROUT) method at a Q-level of 1%. Results were considered statistically significant for two-tailed $p < 0.05$.

5 Results

5.1 The effects of global *Mc1r* deficiency on the development of atherosclerosis

5.1.1 Plaque phenotype in *Apoe*$^{-/-}$*Mc1r*$^{e/e}$ mice

The role of MC1R in the development of atherosclerosis was investigated by generating *Apoe*$^{-/-}$ *Mc1r*$^{e/e}$ mice. The *Apoe*$^{-/-}$ *Mc1r*$^{e/e}$ and *Apoe*$^{-/-}$ control mice were fed HFD for 12 weeks before examining atherosclerotic plaque size and composition in these mice. Atherosclerotic plaque analysis showed a marked increase in the aortic sinus plaque size (**Fig. 7A&B**). The total lesion area in the aorta of the *Apoe*$^{-/-}$ *Mc1r*$^{e/e}$ mice that are deficient in global functional MC1R increased by approximately 50% ($p = 0.02$). Plaques in the aortic sinus of these mice revealed a significant increase in the necrotic core area within the plaque (**Fig. 7C**). The lesion macrophage population was also increased in *Apoe*$^{-/-}$ *Mc1r*$^{e/e}$ mice, but the ratio of M1- to M2-type macrophage markers was not different between the genotypes ($p > 0.05$). Nonetheless, aortic sinus plaques from *Mc1r* deficient mice exhibited a vulnerable plaque phenotype characterized by reduced expression of α-SMA (**Fig. 7D&E**) and collagen (**Fig. 7F**). In contrast to HFD conditions, *Apoe*$^{-/-}$ *Mc1r*$^{e/e}$ mice on standard chow diet did not differ from control *Apoe*$^{-/-}$ in terms of plaque size ($p = 0.39$). However, in concordance with the phenotype observed in HFD-fed mice, the acellular necrotic core area was significantly increased in chow-fed *Apoe*$^{-/-}$ *Mc1r*$^{e/e}$ mice ($p < 0.01$).

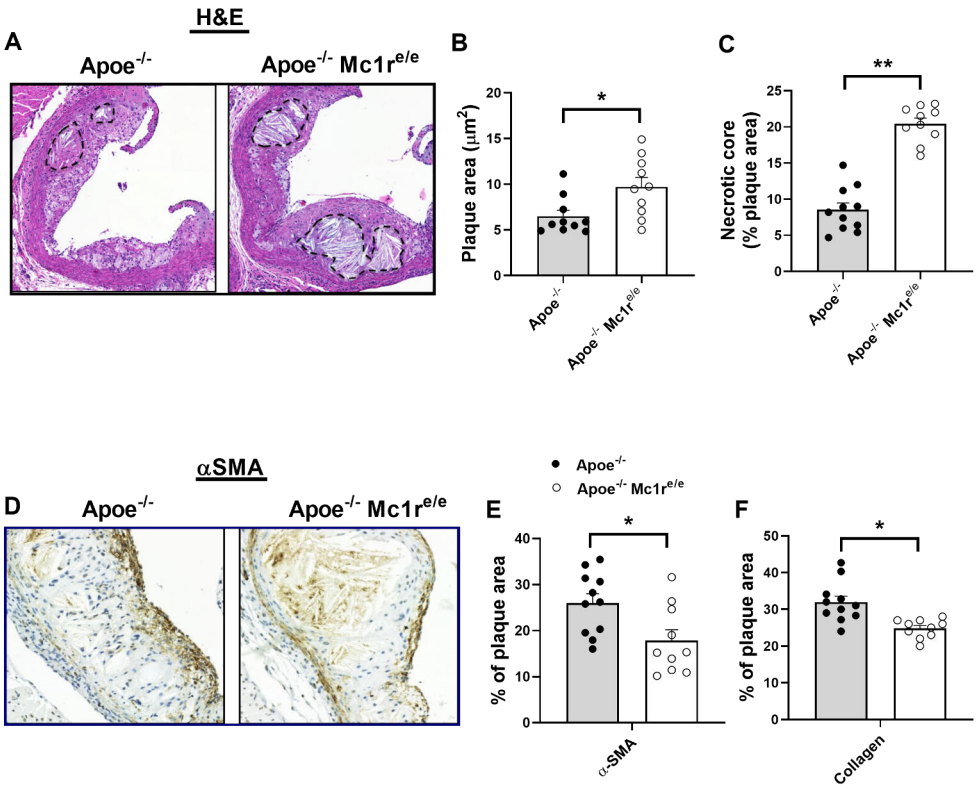

Figure 7. Global deficiency in melanocortin-1 receptor exacerbates atherosclerosis development in Apoe$^{-/-}$ mice. (Modified from original communication I). (**A**) Representative images of hematoxylin and eosin (H&E) staining of the aortic sinus of *Apoe*$^{-/-}$ and *Apoe*$^{-/-}$ *Mc1r*$^{e/e}$ fed a high-fat diet (HFD) for 12 wks. (**B**) Quantification of plaque area in aortic sinuses of *Apoe*$^{-/-}$ and *Apoe*$^{-/-}$ *Mc1r*$^{e/e}$ mice. (**C**) Quantification of acellular necrotic core areas relative to the total plaque area. (**D**) Representative images of α-SMA (α-smooth muscle actin)-immunostained aortic sinuses. (**E**) Quantification of α-SMA–positive area relative to the total plaque area. (**F**) Quantification of plaque collagen content relative to the total plaque area. n = 8–10 mice/group, *p<0.05 and **p<0.01 vs *Apoe*$^{-/-}$ mice, values are mean±SEM (Student's *t*-test for unpaired samples). Each dot represents individual mouse.

5.1.2 The effects of global *Mc1r* deficiency on hypercholesterolemia, hepatic lipid profile and bile acid metabolism

To investigate the impact of global deficiency in *Mc1r* on plasma cholesterol levels at the outset of atherosclerosis, *Apoe*$^{-/-}$ *Mc1r*$^{e/e}$ and *Apoe*$^{-/-}$ were fed a chow or HFD for 4 weeks. It was found that 4 weeks of HFD resulted in a significant elevation in total cholesterol levels in *Apoe*$^{-/-}$ *Mc1r*$^{e/e}$ mice (**Fig. 8A**). This was largely attributable to an increase in LDL and VLDL cholesterol (**Fig. 8B**), while HDL concentration was comparable between the genotypes (p = 0.93). Furthermore, the liver weight of

HFD-fed *Apoe*$^{-/-}$ *Mc1r*$^{e/e}$ mice was increased (**Fig. 8C**), which was accompanied by increased hepatic cholesterol content (**Fig. 8D**) and lipid accumulation as evidenced by H&E and Oil-Red-O staining (**Fig. 8E**).

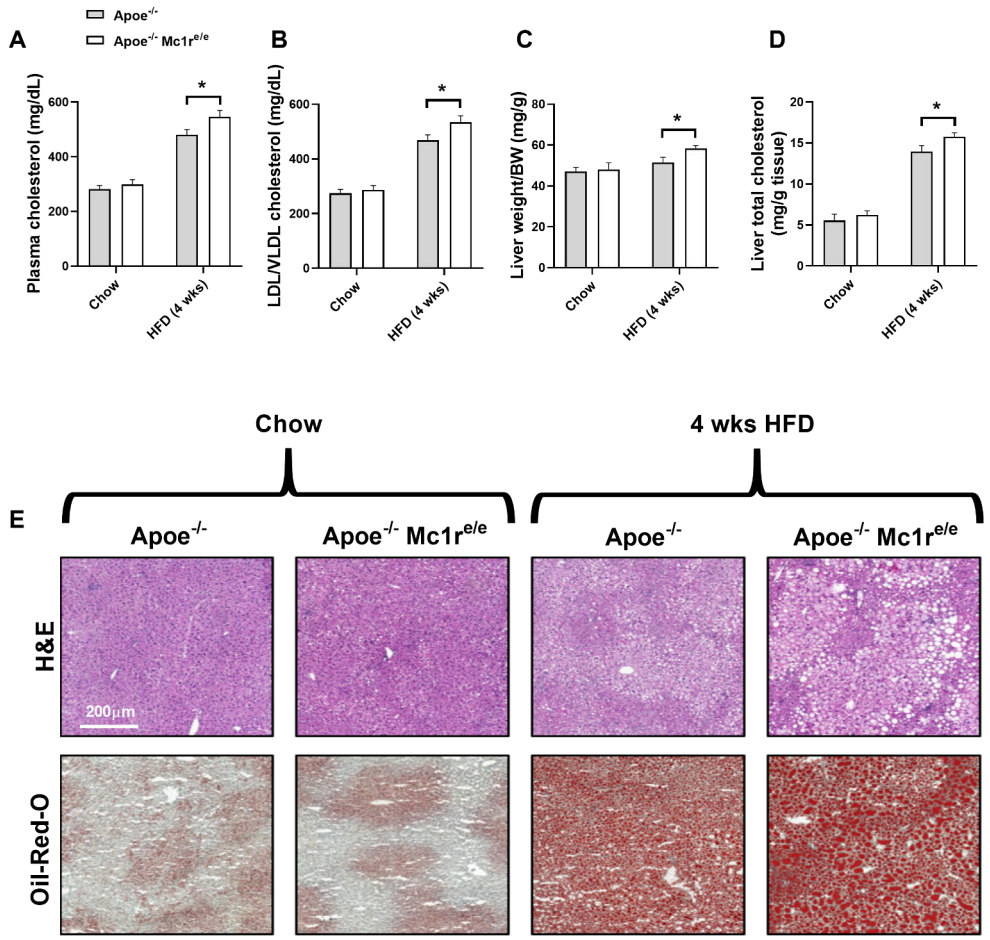

Figure 8. *Mc1r* deficient mice exhibit increased plasma cholesterol level and hepatic lipid accumulation after 4 weeks of high-fat diet (HFD). (Modified from original communication I). (**A**) Total cholesterol and (**B**) LDL (low-density lipoprotein)/VLDL (very-low-density lipoprotein) cholesterol levels in the plasma of *Apoe*$^{-/-}$ and *Apoe*$^{-/-}$ *Mc1r*$^{e/e}$ mice fed a normal chow diet or an HFD for 4 wks. (**C**) Liver:body weight ratio in *Apoe*$^{-/-}$ and *Apoe*$^{-/-}$ *Mc1r*$^{e/e}$ mice. (**D**) Quantification of liver total cholesterol in *Apoe*$^{-/-}$ and *Apoe*$^{-/-}$ *Mc1r*$^{e/e}$ mice. (**E**) Representative hematoxylin and eosin (H&E)-stained and Oil-Red-O–stained liver sections. n=8–10 mice/group. *p<0.05 vs *Apoe*$^{-/-}$ mice. Values are mean±SEM (two-way ANOVA for diet and genotype effects). BW indicates body weight; HFD, high fat diet.

Furthermore, the mechanism influencing the increased cholesterol level and accumulation of lipids in the liver was investigated by quantifying the expression of

genes involved in the regulation of cholesterol synthesis and transport in the liver. Hepatic mRNA expression levels of cholesterol synthesis (7-dehydrocholesterol reductase; *Dhcr7*, 3-Hydroxy-3-Methylglutaryl-CoA Reductase; *Hmgcr*) and transporter (*Abca1*, *Ldlr* and *Scarb1*) genes and their transcriptional regulators (Liver X receptor alpha; *Lxra,* Sterol regulatory element-binding protein 2; *Srebp2*) were comparable between *Apoe*$^{-/-}$ and *Apoe*$^{-/-}$ *Mc1r*$^{e/e}$ mice ($p > 0.05$). However, the mRNA expression levels of *Abcg5* and *Abcg8*, which mediate the excretion of neutral sterols into the bile, were increased in *Apoe*$^{-/-}$ *Mc1r*$^{e/e}$ mice on chow diet (**Appendix Fig. 1**). HFD upregulated *Abcg5* and *Abcg8*, but *Apoe*$^{-/-}$ *Mc1r*$^{e/e}$ mice were deficient of this compensation and showed markedly less upregulated *Abcg5* and *Abg8* expression after HFD feeding.

To clarify whether the reduction of *Abcg5* and *Abcg8* gene expression has functional significance in terms of cholesterol transport efficiency, an *in vivo* RCT assay was employed using tritium-labeled cholesterol. No significant changes were observed in RCT to plasma, liver or feces of *Apoe*$^{-/-}$ *Mc1r*$^{e/e}$ mice ($p = 0.15$, 0.29 and 0.57, respectively), indicating that the reduced mRNA up-regulation of *Abcg5* and *Abcg8* in the liver has no apparent functional consequence.

To further investigate other potential factors driving the hypercholesterolemia phenotype, the size and composition of gall bladder and fecal bile acid pools were measured using gas-liquid chromatography. Bile acids are the end products of cholesterol catabolism in the liver. The total bile acids in the gall bladder bile were reduced in *Apoe*$^{-/-}$ *Mc1r*$^{e/e}$ mice compared to control mice (**Fig. 9A**), but not in the feces of these mice (**Appendix Fig. 2**). In addition, *Apoe*$^{-/-}$ *Mc1r*$^{e/e}$ mice demonstrated reduced cholic acid (primary bile acid) level in the bile (**Fig. 9B)** and increased secondary bile acid (deoxycholic and lithocholic acids) levels in the feces (**Appendix Fig. 2**). Next, crucial enzymes and regulators involved in bile acids synthesis and conjugation were quantified but no changes were observed between the genotypes in this regard (data not shown). Similarly, no changes were observed in the mRNA expression level of the transporters mediating bile acid uptake into hepatocytes and their excretion into bile (data not shown).

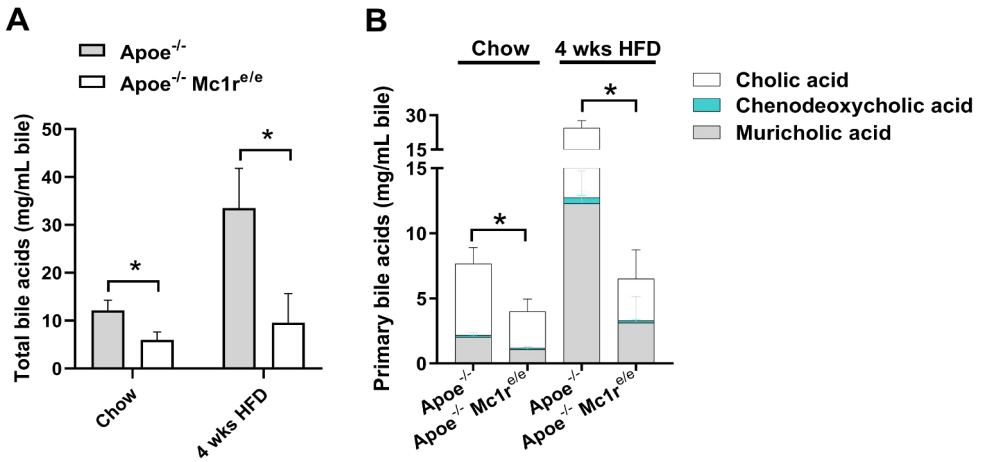

Figure 9. The lack of functional MC1R reduces the amount of biliary bile acids in Apoe$^{-/-}$ mice. (Modified from original communication I). (**A**) Concentration of total bile acids and (**B**) primary bile acids in the gall bladder bile of *Apoe*$^{-/-}$ and *Apoe*$^{-/-}$ *Mc1r*$^{e/e}$ mice fed a standard chow diet or a high-fat diet (HFD) for 4 weeks. Primary bile acids consist of cholic acid (CA), chenodeoxycholic acid (CDCA), and muricholic acid (MCA). n=4–6 mice/group. *p<0.05 vs *Apoe*$^{-/-}$ mice. Values are mean±SEM (two-way ANOVA for diet and genotype effects).

5.2 The role of MC1R in mediating leukocyte accumulation and properties in atherosclerosis

5.2.1 Leukocyte profiles and monocyte characteristics in global *Mc1r* deficient mice

To study leukocyte behavior in *Mc1r* deficient mice, total leukocytes and leukocyte subsets were quantified by flow cytometry in the blood, spleen and aorta of chow- and HFD-fed mice. The numbers of circulating total leukocytes, lymphocytes, monocytes and neutrophils were comparable between the genotypes in both diet groups (**Appendix Fig. 3**). However, chow-fed *Apoe*$^{-/-}$ *Mc1r*$^{e/e}$ mice showed a significant reduction of Ly6C^{low} monocyte quantity in the blood (**Fig. 10A**), while Ly6C^{high} monocyte count was unaffected ($p > 0.05$). On the other hand, the number of Ly6C^{high} monocytes was increased in the bone marrow of HFD-fed *Apoe*$^{-/-}$ *Mc1r*$^{e/e}$ mice (**Fig. 10B**).

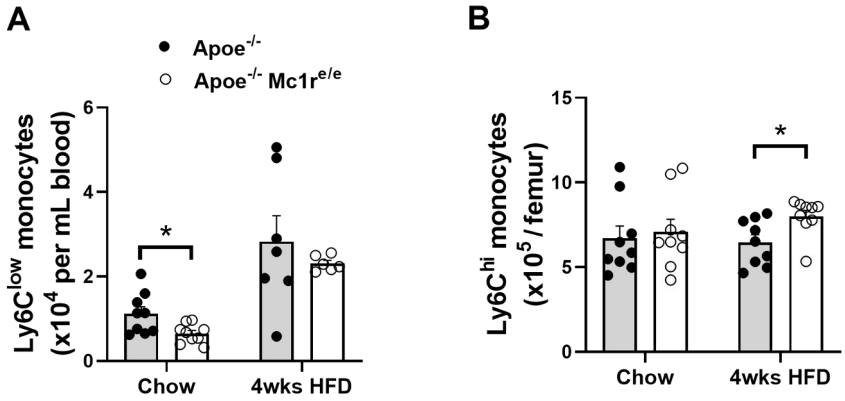

Figure 10. Quantification of tissue monocyte counts in *Apoe*$^{-/-}$ *Mc1r*$^{e/e}$ mice. (Modified from original communication I). (**A**) Quantification of Ly6C^{low} monocytes (CD45^{+}, CD11b^{+}, CD115^{+}, Ly6C^{low}) in the blood and (**B**) Ly6C^{high} monocytes (CD45^{+}, CD11b^{+}, CD115^{+}, Ly6C^{high}) in the bone marrow of *Apoe*$^{-/-}$ and *Apoe*$^{-/-}$ *Mc1r*$^{e/e}$ mice fed a standard chow diet or high-fat diet (HFD) for 4 weeks. n=6 – 10 mice/group. *p<0.05 vs *Apoe*$^{-/-}$ mice. Values are mean±SEM (two-way ANOVA for diet and genotype effects). Each dot represents individual mouse.

Flow cytometric analyses further revealed that chow-fed *Apoe*$^{-/-}$ *Mc1r*$^{e/e}$ mice had significantly lower Ly6C^{high} monocyte as well as neutrophil counts in the spleen (**Fig. 11A&B**). When these mice were challenged with 4 weeks of HFD, the quantities of splenic monocytes and neutrophils were balanced between the genotypes. Since *Mc1r* deficiency did not affect the propensity of cell death among monocytes and neutrophils or local cell differentiation into macrophages or dendritic cells (data not shown), it implied that monocytes are perhaps being mobilized out of the spleen to inflammatory tissues. Figure **11C** shows the loss of CD11b^{+} (myeloid lineage) cells from the subcapsular red pulp, the principal site of rapidly recruitable monocytes, in the spleen of *Apoe*$^{-/-}$ *Mc1r*$^{e/e}$ mice (Swirski et al., 2009). Correspondingly, the aorta of these mice was noted to accumulate an increased number of leukocytes in the chow-fed state, a phenotype that dissipated following 4 weeks of HFD (**Fig. 11E**). Hence, the onset of atherosclerosis in *Apoe*$^{-/-}$ mice lacking functional *Mc1r* appeared to be marked by an increased aortic leukocyte accumulation arising potentially from splenic Ly6C^{high} monocyte recruitment. This phenotype was associated with increased plasma levels of pro-inflammatory cytokines and chemokines including CCL2 that promote monocyte infiltration into the aorta (**Fig. 11D**).

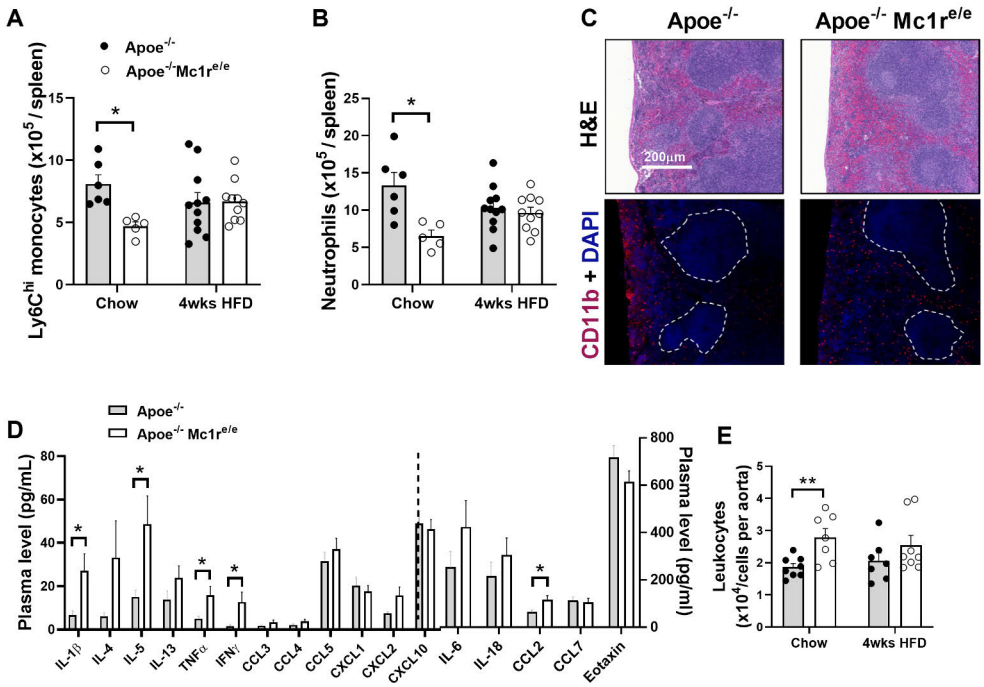

Figure 11. Characterization of tissue leukocyte profiles in *Apoe*$^{-/-}$ *Mc1r*$^{e/e}$ mice. (Modified from original communication I). **(A)** Quantification of Ly6C^{high} (CD45^{+}, CD11b^{+}, CD115^{+}, Ly6C^{high}) and **(B)** neutrophil (CD45^{+}, CD11b^{+}, Ly6G^{+}) in the spleen of *Apoe*$^{-/-}$ and *Apoe*$^{-/-}$ *Mc1r*$^{e/e}$ mice fed a standard chow diet or high-fat diet (HFD) for 4 weeks. (**C**) Representative hematoxylin and eosin (H&E)–stained andCD11b-stained spleen sections from chow-fed *Apoe*$^{-/-}$ and *Apoe*$^{-/-}$ *Mc1r*$^{e/e}$ mice. Broken lines indicate the areas of white pulps. (**D**) Plasma cytokine levels in chow-fed *Apoe*$^{-/-}$ *Mc1r*$^{e/e}$ mice (n=12-13/group; Student's *t*-test). (**E**) Total leukocyte (CD45^{+}) count in the aortic lysates from *Apoe*$^{-/-}$ and *Apoe*$^{-/-}$ *Mc1r*$^{e/e}$ mice on 4 weeks chow or HFD. n=6–10 mice/group. *p<0.05 and **p<0.01 vs *Apoe*$^{-/-}$ mice. Values are mean±SEM (two-way ANOVA for diet and genotype effects; Student's *t*-test/unpaired for cytokines expression in plasma). Each dot represents individual mouse.

Flow cytometry of aortic endothelial cells was employed to explore the mechanism driving increased monocyte infiltration to the aorta of *Apoe*$^{-/-}$ *Mc1r*$^{e/e}$ mice. No difference was observed between the genotypes in the expression level of VCAM-1, ICAM-1, PECAM-1 and P-selectin in the aortic endothelial cells (**Appendix Fig. 4**). Supporting this finding, quantitative RT-PCR analysis of aortic lysates showed comparable expression levels of these adhesion molecules between the genotypes (**Appendix Fig. 4**). Since the endothelial inflammation, which aids adhesion, rolling and migration of Ly6C^{high} monocytes to the aorta, appeared to be unaffected by *Mc1r* deficiency, the characteristics of Ly6C^{high} and Ly6C^{low} monocytes was next examined using flow cytometry. Interestingly, Ly6C^{high} monocytes deficient in *Mc1r* showed significantly increased expression of CD62L

and PSGL-1 (**Fig. 12A&B**). Additionally, the incubation of monocytes with soluble VCAM-1 fragment following CCL2 stimulation demonstrated that Ly6C^{high} monocytes lacking functional *Mc1r* exhibited increased binding activity for VCAM-1 (**Fig. 12C&D**).

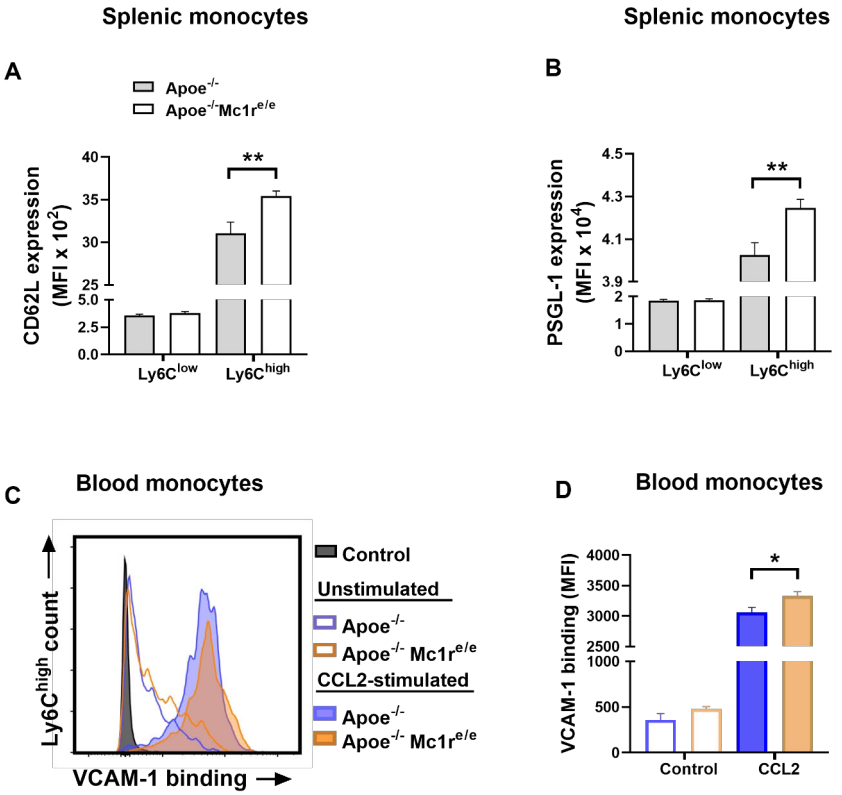

Figure 12. Monocytes deficient in MC1R demonstrate increased expression of adhesion molecules and enhanced binding activity to VCAM-1 (vascular cell adhesion molecule 1). (Modified from original communication I). (**A**) Mean fluorescence intensity (MFI) of CD62L and (**B**) PSGL-1 (P-selectin glycoprotein ligand 1) in the Ly6C^{low}- and Ly6C^{high}-gated splenic monocytes from *Apoe*$^{-/-}$ and *Apoe*$^{-/-}$ *Mc1r*$^{e/e}$ mice (n=6–8 mice/group). (**C**) Representative histogram of binding of blood Ly6C^{high} monocytes to soluble VCAM-1-Fc under unstimulated and CCL2 (chemokine (C-C motif) ligand 2)-stimulated (5 µg/mL, 5 min) conditions. Control sample was incubated with secondary antibody that was not preconjugated to soluble VCAM-1-Fc. (**D**) Quantification of VCAM-1-Fc binding in Ly6C^{high}-gated monocytes from *Apoe*$^{-/-}$ and *Apoe*$^{-/-}$ *Mc1r*$^{e/e}$ mice, n=4–6 mice/group. *p<0.05 and **p<0.01 vs *Apoe*$^{-/-}$ mice. Values are mean±SEM (two-way ANOVA for monocyte subtype and genotype effects).

5.2.2 The influence of hematopoietic *Mc1r* deficiency on tissue leukocyte counts

To investigate the contribution of leukocyte MC1R to atherosclerosis, bone marrow cells isolated from *Apoe*$^{-/-}$ or *Apoe*$^{-/-}$ *Mc1r*$^{e/e}$ were transplanted into lethally irradiated *Apoe*$^{-/-}$ recipient mice followed by 10 weeks of chow or HFD after the radiation recovery period. The donor cells successfully repopulated the bone marrow of the *Apoe*$^{-/-}$ recipient mice, since the engraftment rate in the peripheral blood ranged from 95 – 99 % at the end of the experiment (**Fig. 13A**). In addition, LSK cells (Lineage^{-} Sca-1^{+} c-Kit^{+}), which drive bone marrow cell regeneration after irradiation, were comparably expressed between the *Apoe*$^{-/-}$ and *Apoe*$^{-/-}$ *Mc1r*$^{e/e}$ genotypes of the recipient mice. This comparable level of chimerism between the genotypes indicates that hematopoietic *Mc1r* deficiency did not influence the efficiency of bone marrow cell reconstitution following irradiation and transplantation (**Appendix Fig. 5**). Immunophenotyping of leukocytes in the blood, spleen and bone marrow via flow cytometry revealed a substantial increase in systemic total leukocyte counts in *Apoe*$^{-/-}$ *Mc1r*$^{e/e}$ bone marrow recipient mice in both diet groups (**Fig. 13B**). This effect could be ascribed to the significant elevation in lymphocyte counts in these mice (**Fig. 13C**). *Apoe*$^{-/-}$ *Mc1r*$^{e/e}$ chimeric mice also showed an increase in circulating Ly6C^{high} monocyte and neutrophil counts (**Fig. 13D&E**). Further gating of lymphocytes in the blood of *Apoe*$^{-/-}$ *Mc1r*$^{e/e}$ chimeric mice indicated a significant increase in B and CD4^{+} T cell counts (**Fig. 13F**). Consistent with the elevated B cell count, plasma antibody concentrations across the different isotypes IgG1, IgG2a, IgG2b, IgA and IgM were markedly raised in *Apoe*$^{-/-}$ *Mc1r*$^{e/e}$ chimeric mice, particularly in the HFD state (**Appendix Fig. 5**).

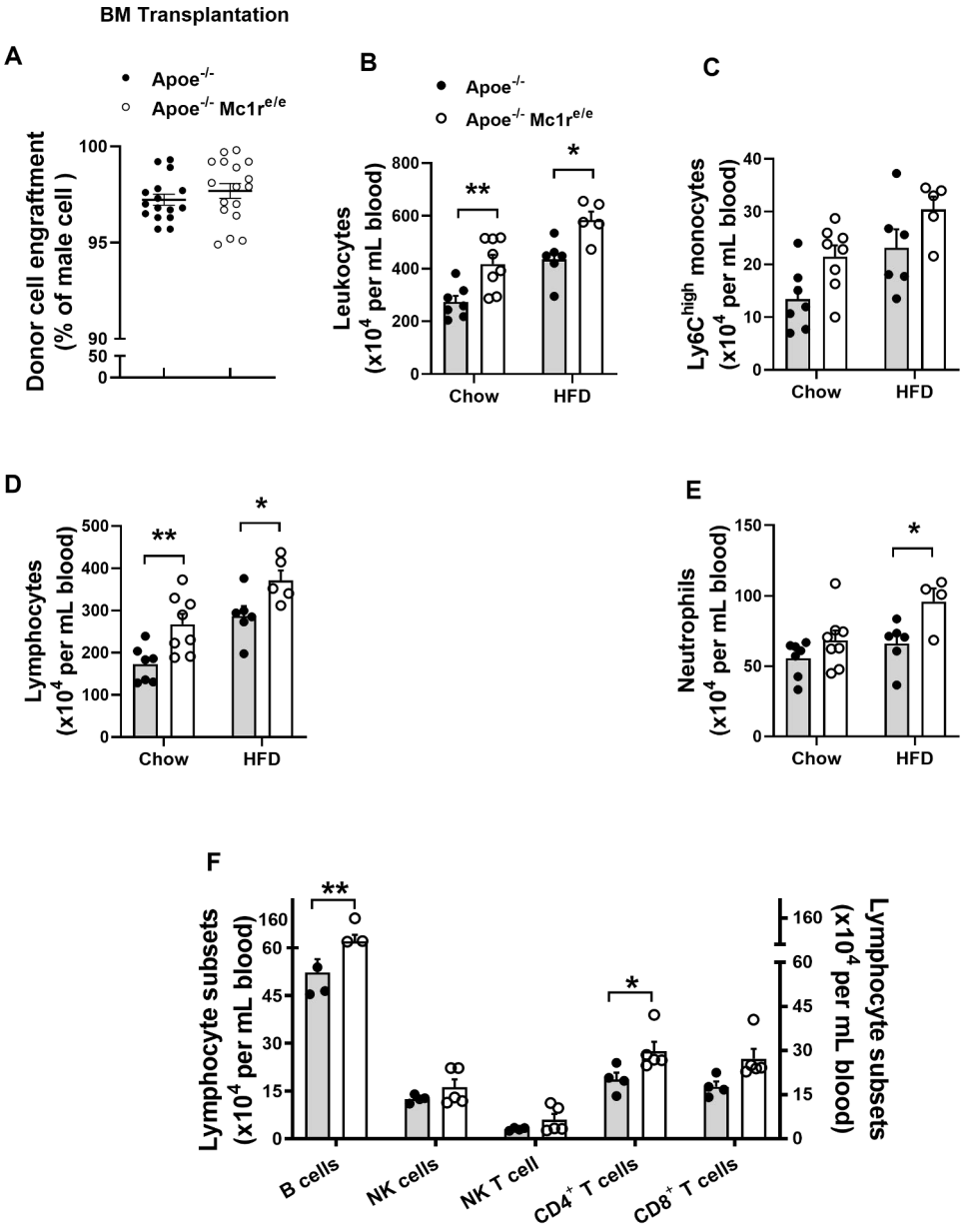

Figure 13. Bone marrow (BM) *Mc1r* deficiency induced leukocytosis in *Apoe*$^{-/-}$ mice. (Modified from original communication II). (**A**) Quantification of donor *Apoe*$^{-/-}$ or *Apoe*$^{-/-}$ *Mc1r*$^{e/e}$ bone marrow cell engraftment in the peripheral blood of *Apoe*$^{-/-}$ recipient mice at the end of the experiment. (**B–E**) Quantification of total leukocyte (CD45^{+}), lymphocyte (CD45^{+}, CD11b^{-}), Ly6C^{high} monocyte (CD45^{+}, CD11b^{+}, CD115^{+}, Ly6C^{high}) and neutrophil (CD45^{+}, CD11b^{+}, CD115^{-} Ly6G^{+}) counts in the peripheral blood of *Apoe*$^{-/-}$ and *Apoe*$^{-/-}$ *Mc1r*$^{e/e}$ BM transplanted mice fed a chow or high-fatdiet (HFD) for 10 weeks. (**F**) Flow cytometry analysis of lymphocyte subsets in the blood of HFD-fed *Apoe*$^{-/-}$ and *Apoe*$^{-/-}$ *Mc1r*$^{e/e}$ chimeric mice. *p<0.05 and **p<0.01 versus *Apoe*$^{-/-}$ mice. Data are mean ± SEM (two-way ANOVA for diet and genotype effects). Each dot represents individual mouse.

Flow cytometry was further employed to quantify total leukocytes, leukocyte subsets, hematopoietic stem cells and progenitor cells in the bone marrow. HFD provoked the expansion of total leukocytes, Ly6C^{high} monocytes and neutrophils in the bone marrow of *Apoe*$^{-/-}$ *Mc1r*$^{e/e}$ chimeric mice (**Fig. 14A-C**). Furthermore, the number of long-term hematopoietic stem cells (HSC) capable of repopulating the hematopoietic system was notably increased in the bone marrow of HFD-fed *Apoe*$^{-/-}$ *Mc1r*$^{e/e}$ chimeric mice (**Fig. 14D**). On the other hand, lymphocyte count was only increased in *Apoe*$^{-/-}$ *Mc1r*$^{e/e}$ chimeric mice that were fed a chow diet (**Fig. 14E**). This increase was mainly derived from increased CD4^{+} and CD8^{+} T cell counts (**Fig. 14F**).

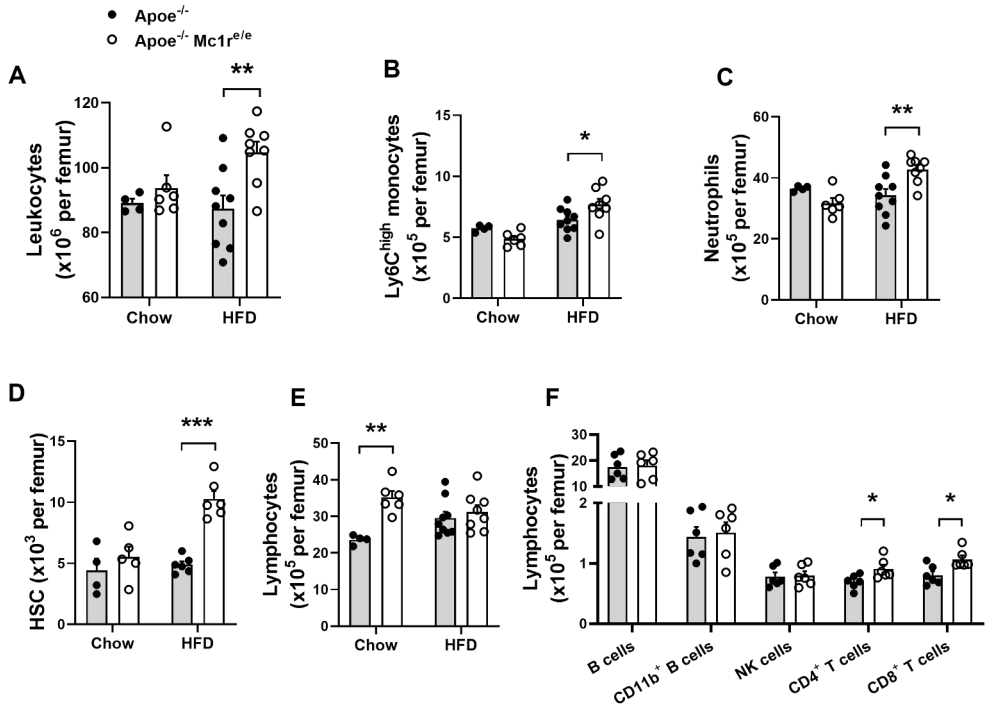

Figure 14. Hematopoietic *Mc1r* deficiency enhanced leukocyte and hematopoietic stem cell populations in the bone marrow of *Apoe*$^{-/-}$ recipient mice. (Modified from original communication II). (**A–E**) Quantification of total leukocytes (CD45^{+}), Ly6C^{high} monocytes (CD45^{+}, CD11b^{+}, CD115^{+} and Ly6C^{high}), neutrophils (CD45^{+}, CD11b^{+}, Ly6G^{+}), HSC (Lin1^{-}, Sca-1^{+}, Kit^{+}; and CD150^{+}, CD48^{-}) and lymphocytes (CD45^{+}, CD11b^{-}) by flow cytometry in the bone marrow of *Apoe*$^{-/-}$ and *Apoe*$^{-/-}$ *Mc1r*$^{e/e}$ chimeric mice on standard chow diet or HFD (high fat diet). (**F**) Quantification of lymphocyte subsets in chow-fed *Apoe*$^{-/-}$ and *Apoe*$^{-/-}$ *Mc1r*$^{e/e}$ chimeric mice. Data are mean ± SEM, *p<0.05, **p<0.01 and ***p<0.001 versus *Apoe*$^{-/-}$ mice (two-way ANOVA for diet and genotype effects). Each dot represents individual mouse. Lin-, indicates lineage-negative; Sca-1, stem-cell antigen-1; c-Kit, proto-oncogene receptor tyrosin kinase; HSC, hematopoietic stem cell.

5.2.3 The role of MC1R in CD4$^+$ T cells

The spleen is an important secondary lymphoid organ crucial to the movement of inflammatory leukocytes into atherosclerotic plaque. Similarly to the phenotype observed in the blood, total leukocyte, as well as lymphocyte counts were markedly increased in the spleen of *Apoe*$^{-/-}$ *Mc1r*$^{e/e}$ chimeric mice (**Fig. 15A&B**). The splenic Ly6C^{high} monocyte and neutrophil count on the other hand did not differ between the genotypes ($p > 0.05$). Further analysis of the lymphocyte subsets showed an increase in splenic B cell and CD4$^+$ T cell populations in *Apoe*$^{-/-}$ *Mc1r*$^{e/e}$ BM transplanted mice (**Fig. 15C&D**). As CD4$^+$ T cell count was consistently increased in the blood, bone marrow and spleen of these mice, RT-PCR analysis was used to quantify mRNA expression levels of different markers of CD4$^+$ T cell subtypes in the spleen. *Apoe*$^{-/-}$ *Mc1r*$^{e/e}$ chimeric mice showed an increased expression level of interferon-γ (*Ifng*) and *T-bet* transcription factor, which regulates the polarization of CD4$^+$ T into the Th1 phenotype (**Fig. 15F**). This finding was corroborated by flow cytometry analysis, which showed an increased count of IFN-γ expressing CD4$^+$ T cells in the spleen of *Apoe*$^{-/-}$ *Mc1r*$^{e/e}$ chimeric mice (**Fig. 15D&E**), suggesting that Th1 effector cells seem to be driving the CD4$^+$ T cell expansion. Furthermore, the plasma concentration of IL-2 and IL-4 was increased and plasma IL-6 and IFN-γ levels tended to be elevated ($p = 0.06$) in HFD-fed *Apoe*$^{-/-}$ *Mc1r*$^{e/e}$ chimeric mice (**Fig. 15G**).

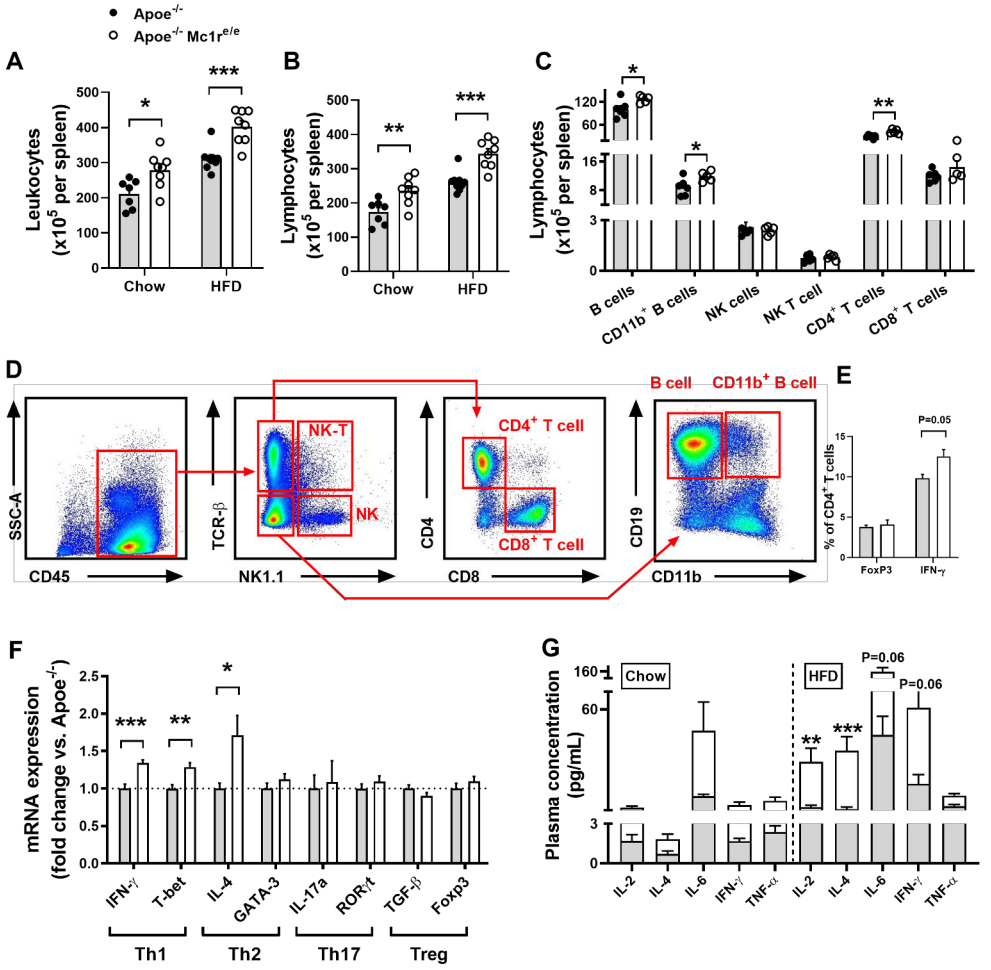

Figure 15. *Mc1r* deficient BM reconstitution increased leukocyte and lymphocyte counts in the spleen of *Apoe*$^{-/-}$ mice. (Modified from original communication II). **(A)** Quantification of total leukocytes (CD45$^+$) and **(B)** lymphocytes (CD45$^+$, CD11b$^-$) in the spleen of *Apoe*$^{-/-}$ recipient mice. (**C**) Quantification of splenic lymphocyte subsets in HFD-fed recipient mice. (**D**) Representative dot plots for the gating of B cells (CD45$^+$, TCRβ$^-$, CD19$^+$, CD11b$^-$), CD11b$^+$ B cells (CD45$^+$, TCRβ$^-$, CD19$^+$, CD11b$^+$), CD4$^+$ T cells (CD45$^+$, TCRβ$^+$, CD4$^+$), CD8$^+$ T cells (CD45$^+$, TCRβ$^+$, CD8$^+$), NK T cells (CD45$^+$, TCRβ$^+$, NK1.1$^+$) and NK cells (CD45$^+$, TCRβ$^-$, NK1.1$^+$) in the spleen of *Apoe*$^{-/-}$ BM transplanted mouse. (**E**) Quantification of IFN-γ$^+$ and Foxp3$^+$ CD4$^+$ T cells (CD45$^+$, TCRβ$^+$, CD4$^+$) in the spleen of *Apoe*$^{-/-}$ and *Apoe*$^{-/-}$ *Mc1r*$^{e/e}$ BM transplanted mice. n=4 mice per genotype. (**F**) Quantitative real-time PCR (qPCR) analysis of effector CD4$^+$ T cell markers in the spleen of *Apoe*$^{-/-}$ and *Apoe*$^{-/-}$ *Mc1r*$^{e/e}$ BM transplanted mice. n=8-9 mice per genotype. (**G**) Pro-inflammatory cytokine concentrations in the plasma of chow- and HFD-fed *Apoe*$^{-/-}$ and *Apoe*$^{-/-}$ *Mc1r*$^{e/e}$ BM transplanted mice. *p<0.05, **p<0.01 and ***p<0.001 versus control *Apoe*$^{-/-}$ mice. Data are mean ± SEM (two-way ANOVA for diet and genotype effects; Student *t*-test/unpaired for cytokine expression level). Each dot represents individual mouse.

Despite enhanced leukocytosis in *Apoe*$^{-/-}$ *Mc1r*$^{e/e}$ BM transplanted mice, histological analysis of aortic root lesions revealed no effect of *Mc1r* deficiency on plaque size in chow- or HFD-fed mice (**Fig. 16A&B**). Further characterization of the lesions of HFD-fed mice showed no significant genotype difference in terms of plaque macrophage, SMC, collagen content or necrotic core size (**Fig. 16C-G**). In addition, no differences were noted in flow cytometry analyzed aortic lysate in total leukocytes, lymphocytes, neutrophils or Ly6C^{high} monocytes accumulation between the genotypes (**Appendix Fig. 6**).

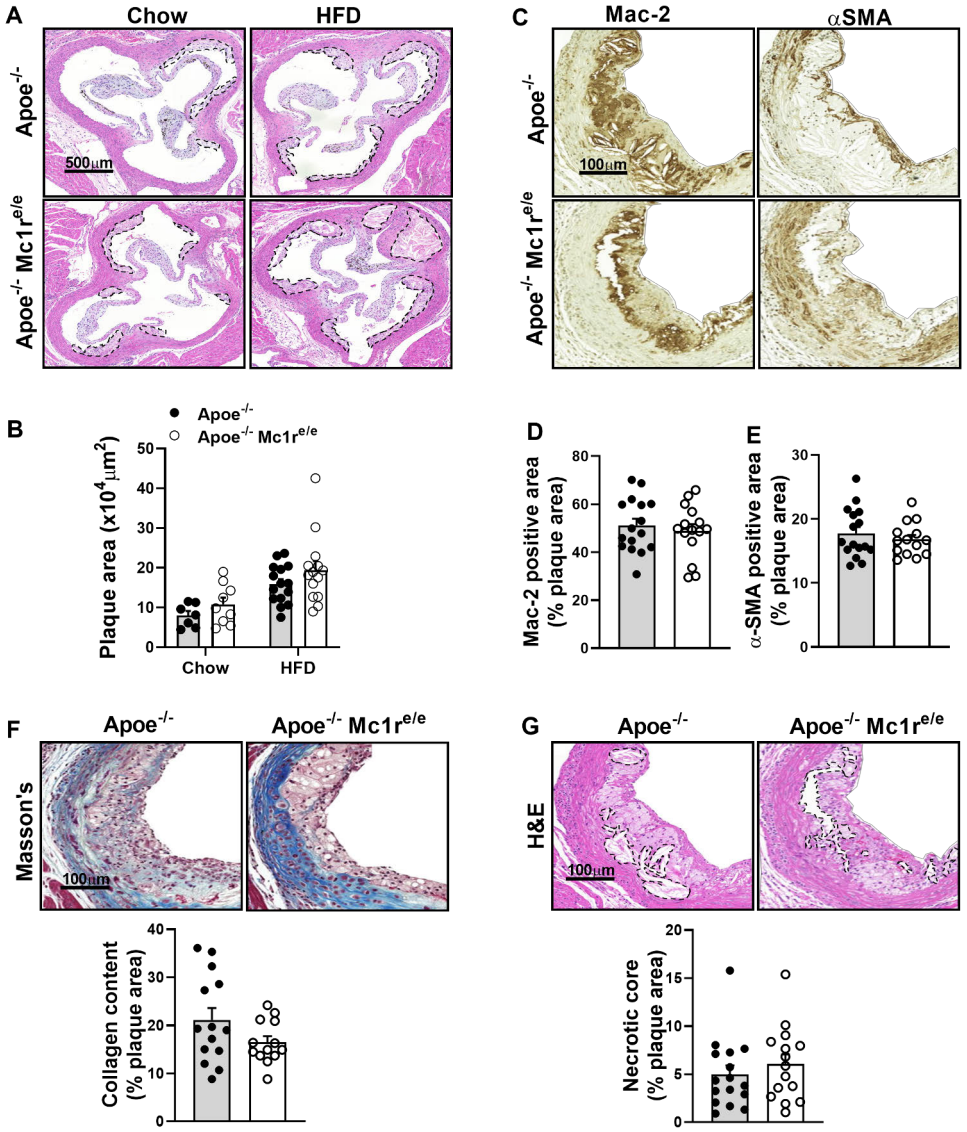

Figure 16. Hematopoietic *Mc1r* deficiency does not affect plaque phenotype in *Apoe*$^{-/-}$ mice. (Modified from original communication II). **(A)** Representative images of hematoxylin and eosin (H&E) staining of the aortic sinus of chow- and HFD-fed *Apoe*$^{-/-}$ and *Apoe*$^{-/-}$ *Mc1r*$^{e/e}$ BM engrafted mice. (**B**) Quantification of plaque area in aortic sinuses. (**C**) Representative images of Mac-2 (galectin-3), α-SMA (α-smooth muscle actin) and (**D-E**) quantification of Mac-2 and α-SMA-psotive areas as percentage of total plaque area in the aortic sinus. (**F**) Representative images of Masson trichrome staining and the quantification of plaque collagen content in the aortic sinus as percentage of total plaque area. (**G**) Representative images of necrotic core areas, indicated with broken lines in H&E-stained images, and quantification of acellular core area as percentage of total plaque area in the aortic sinuses. Data are mean ± SEM (two-way ANOVA for diet and genotype effects; Student *t*-test/unpaired for genotype effect in aortic composition). Each dot represents individual mouse.

The discrepancy between the enhanced leukocytosis and lack of effect on plaque size and composition in *Apoe*$^{-/-}$ *Mc1r*$^{e/e}$ BM transplanted mice warranted the examination of leukocyte migratory characteristics in these mice. For this purpose, an *in vivo* homing assay was conducted using isolated CD45^{+} cells from the spleen of male *Apoe*$^{-/-}$ or *Apoe*$^{-/-}$ *Mc1r*$^{e/e}$ mice that were fluorescently labeled and injected into *Apoe*$^{-/-}$ recipient male mice. Flow cytometry detection and quantification of labeled CD45^{+} cells following 24 hours of the injection revealed a significant reduction of *Mc1r* deficient CD4^{+} and CD8^{+} T cells in the blood and para-aortic lymph nodes (paLNs) (**Fig. 17A&B**). The CD4^{+} and CD8^{+} T cells from *Apoe*$^{-/-}$ *Mc1r*$^{e/e}$ cells were rather migrating to the spleen instead (**Fig. 17C**). No genotype difference was observed in the number of T cells expressing markers for both CD4^{+} and CD8^{+} T (double-positive/DP T cells) that represented an internal control. A similar *in vivo* assay experiment was performed using myeloid cells from the bone marrow of *Apoe*$^{-/-}$ or *Apoe*$^{-/-}$ *Mc1r*$^{e/e}$ mice. It was found that Ly6C^{high} and Ly6C^{low} monocytes from *Apoe*$^{-/-}$ *Mc1r*$^{e/e}$ mice readily migrate into the spleen, while still maintaining high counts in the blood (**Appendix Fig. 7**). Collectively, CD4^{+} T cells, CD8^{+} T cells and monocytes deficient in *Mc1r* preferentially migrated into the spleen of *Apoe*$^{-/-}$ mice.

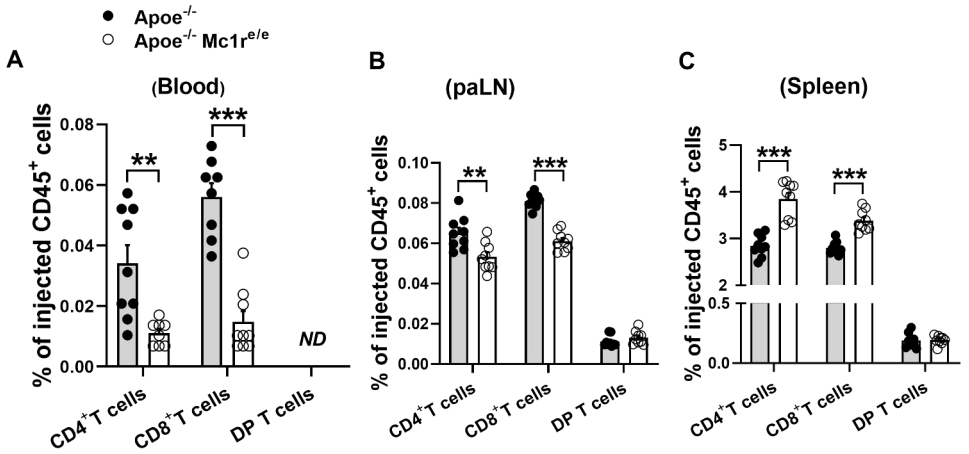

Figure 17. *Mc1r* deficiency significantly alters homing behavior of CD4^{+} and CD8^{+} T cells. (Modified from original communication II). (**A–C**) Quantification of CD4^{+} T cells (CD45^{+}, TCRβ^{+}, CD4^{+}), CD8^{+} T cells (CD45^{+}, TCRβ^{+}, CD8^{+}) and double positive (DP) T cells (CD45^{+}, TCRβ^{+}, CD4^{+}, CD8^{+}) by flow cytometry in the blood, para-aortic lymph nodes (paLNs) and spleen as percentage of injected CD45^{+} cells. Data are mean ± SEM (Student *t*-test/unpaired for genotype effects), **p<0.01 and ***p<0.001 versus control *Apoe*$^{-/-}$ mice. Each dot represents individual mouse.

To search for the underlying cause for the observed differences in the homing behavior, RT-PCR analysis was conducted on CD4^{+} T cells isolated from the spleen of *Apoe*$^{-/-}$ and *Apoe*$^{-/-}$ *Mc1r*$^{e/e}$ mice to analyze the mRNA expression level of chemokine

receptors and adhesion molecules regulating lymphocyte migration. Of the various screened genes, *Ccr5* mRNA was solely upregulated in *Apoe*$^{-/-}$ *Mc1r*$^{e/e}$ CD4^{+} T cells (**Fig. 18A**). In addition, the CCR5 protein level was increased in isolated *Mc1r*-deficient CD4^{+} T cells (**Fig. 18B**). This observation contradicts the function of CCR5 in recruiting T cell to atherosclerotic plaques (Griffith et al., 2014; Turner & Farber, 2014) and the finding of preferential homing of *Mc1r*-deficient T cells into the spleen. In contrast, flow cytometry analysis revealed that the surface expression of CCR5 was markedly reduced in CD4^{+} T cells of the *Apoe*$^{-/-}$ *Mc1r*$^{e/e}$ genotype, but not in CD8^{+} T cells (**Fig. 18C**).

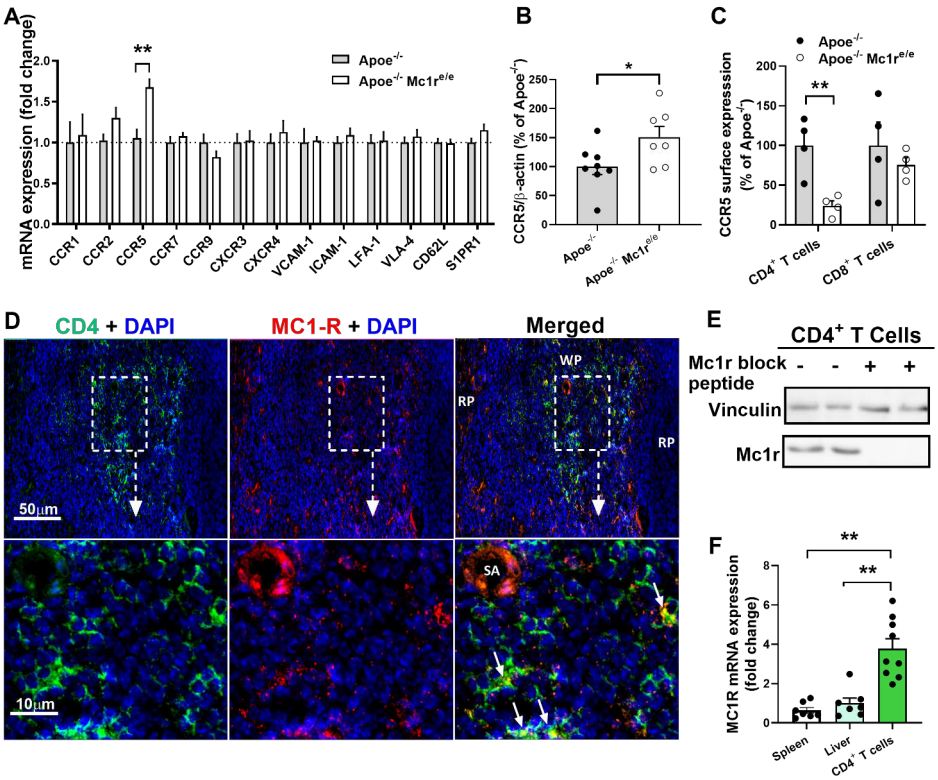

Figure 18. Splenic CD4^{+} T cells express MC1R that selectively modulates CCR5 expression. (Modified from original communication II). (**A**) Quantitative real-time PCR (qPCR) analysis of chemokine receptor and adhesion molecule expression in isolated CD4^{+} T cells from *Apoe*$^{-/-}$ and *Apoe*$^{-/-}$ *Mc1r*$^{e/e}$ mice. (**B**) Representative Western blots and quantification of CCR5 and β-actin (loading control) in isolated CD4^{+} T cells lysates from *Apoe*$^{-/-}$ *and Apoe*$^{-/-}$ *Mc1r*$^{e/e}$ mice. (**C**) Quantification of CCR5 surface expression by flow cytometry in CD4^{+} and CD8^{+} T cells from the spleen of *Apoe*$^{-/-}$ and *Apoe*$^{-/-}$ *Mc1r*$^{e/e}$ mice. (**D**) Immunofluorescence staining of MC1R and CD4 in the mouse spleen. White arrows indicate co-localization of MC1R and CD4. RP indicates red pulp; WP, white pulp; SA, splenic artery (**E**) Western blot analysis of MC1R protein expression in isolated CD4^{+} T cell samples from the spleen. The expression of vinculin is shown as loading control. Lanes on the right were incubated with anti-Mc1r antibody solution that was premixed with a molar excess of a blocking Mc1r peptide. (**F**) Quantitative real-time PCR (qPCR) analysis of *Mc1r* expression in the mouse spleen, liver and isolated splenic CD4^{+} T cells. Data are mean ± SEM (Student's *t*-test for unpaired samples). *p<0.05 and **p<0.01 versus control *Apoe*$^{-/-}$ mice. Each dot represents individual mouse.

Next, it was investigated whether MC1R is expressed by CD4$^+$ T cells, which might influence or contribute to the observed leukocytosis and altered homing behavior of cells derived from *Apoe*$^{-/-}$ *Mc1r*$^{e/e}$ mice. Previous reports have highlighted the presence of MC1R in mouse and human CD8$^+$ cells and its mRNA expression in human CD4$^+$ T cells (Andersen et al., 2005; Loser et al., 2010). Immunofluorescence analysis revealed that MC1R is expressed by CD4$^+$ T cells in a mouse spleen (**Fig. 18D**). Consistently, MC1R protein expression on sorted CD4$^+$ T cells was validated by Western blotting (**Fig. 18E**) and RT-PCR screening revealed higher expression of *Mc1r* mRNA in isolated CD4$^+$ T cell samples compared to the whole spleen or liver (**Fig. 18F**).

Next, the functional impact of reduced CCR5 surface expression was investigated via chemotaxis assay using isolated splenic cells from *Apoe*$^{-/-}$ and *Apoe*$^{-/-}$ *Mc1r*$^{e/e}$ mice. The migration of these cells towards the CCR5 ligands CCL3, CCL4 and CCL5 was examined. Of note, migration of *Apoe*$^{-/-}$ *Mc1r*$^{e/e}$ CD4$^+$ T cells towards CCL4 and CCL5 was considerably reduced (**Fig. 19A**). The potential defect in CCR5 intracellular trafficking in *Mc1r* deficient cells was explored by stimulating isolated splenic CD4$^+$ T cells with CCL5 followed by the ligand withdrawal to induce recycling of the receptor to the cell membrane. CCR5 internalization and the accompanied recycling were impaired in *Apoe*$^{-/-}$ *Mc1r*$^{e/e}$ CD4$^+$ T cells (**Fig. 19B**), which possibly influences their migratory behavior.

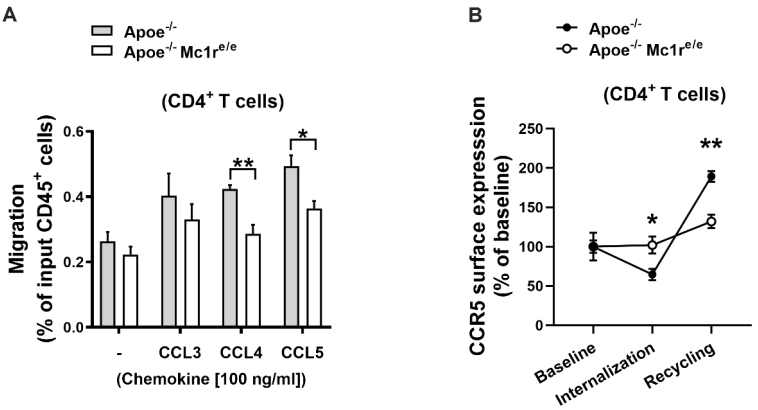

Figure 19. CD4$^+$ T cells deficient in MC1R demonstrated impaired CCR5-dependent migration and defective CCR5 receptor recycling. (Modified from original communication II). **(A)** Transwell migration assay in the splenocytes of *Apoe*$^{-/-}$ and *Apoe*$^{-/-}$ *Mc1r*$^{e/e}$ mice. Cells were allowed to migrate for 3 hours towards CCL3, CCL4 and CCL5 chemokines. CD4$^+$ T cell migration towards these chemokines was quantified by flow cytometry as percentage of input CD45$^+$ cells. n=4 mice per genotype. (**B**) Quantification of CCR5 surface expression on CD4$^+$ T cells that were isolated from *Apoe*$^{-/-}$ or *Apoe*$^{-/-}$ *Mc1r*$^{e/e}$ mice. CCR5 surface expression was quantified during baseline, after CCL5-induced internalization and after withdrawal of CCL5. n=4 mice per genotype. Data are mean ± SEM (Student's *t*-test for unpaired samples). *p<0.05 and **p<0.01 versus *Apoe*$^{-/-}$ mice.

5.3 Targeting of MC3R by [D-Trp^8]-γ-MSH in atherosclerotic mice

5.3.1 Anti-inflammatory modulation of MC3R activation in *Apoe*$^{-/-}$ mice

In study III, the therapeutic potential of MC3R activation and its associated anti-inflammatory modulation was evaluated in atherosclerotic *Apoe*$^{-/-}$ mice. First, immunofluorescence staining of MC3R was carried out on the aortic root of HFD-fed *Apoe*$^{-/-}$ mice. In the aortic root lesions, MC3R was identified to be mainly co-localized with the macrophage marker Mac-2 and to some extent also with the endothelial cell marker CD31 (**Fig. 20A & B**). Next, HFD-fed *Apoe*$^{-/-}$ mice were treated with the MC3R potent agonist [D-Trp^8]-γ-MSH (15µg/mouse/day, i.p, 4 weeks) to investigate the effects of MC3R activation on inflammation and atheroprogression. Quantification of plasma cytokine and chemokine concentrations showed that [D-Trp^8]-γ-MSH significantly reduced the level of pro-inflammatory cytokines CCL2, CCL4 and CCL5 (**Fig. 20C**), which are established chemoattractants for leukocytes in atherosclerosis. Furthermore, flow cytometry of blood samples revealed that the drug treatment decreased the total leukocyte count as well as the number of lymphocytes and neutrophils, but not the Ly6C^{high} monocyte count (**Fig. 20B**). A similar phenotype was also appearing in the spleen, where total leukocyte and lymphocyte counts were reduced in [D-Trp^8]-γ-MSH-treated mice (**Fig. 20D**). However, drug treatment did not affect myelopoiesis as no difference was observed in leukocyte counts in the flow cytometry analysis of the bone marrow (**Fig. 20E**).

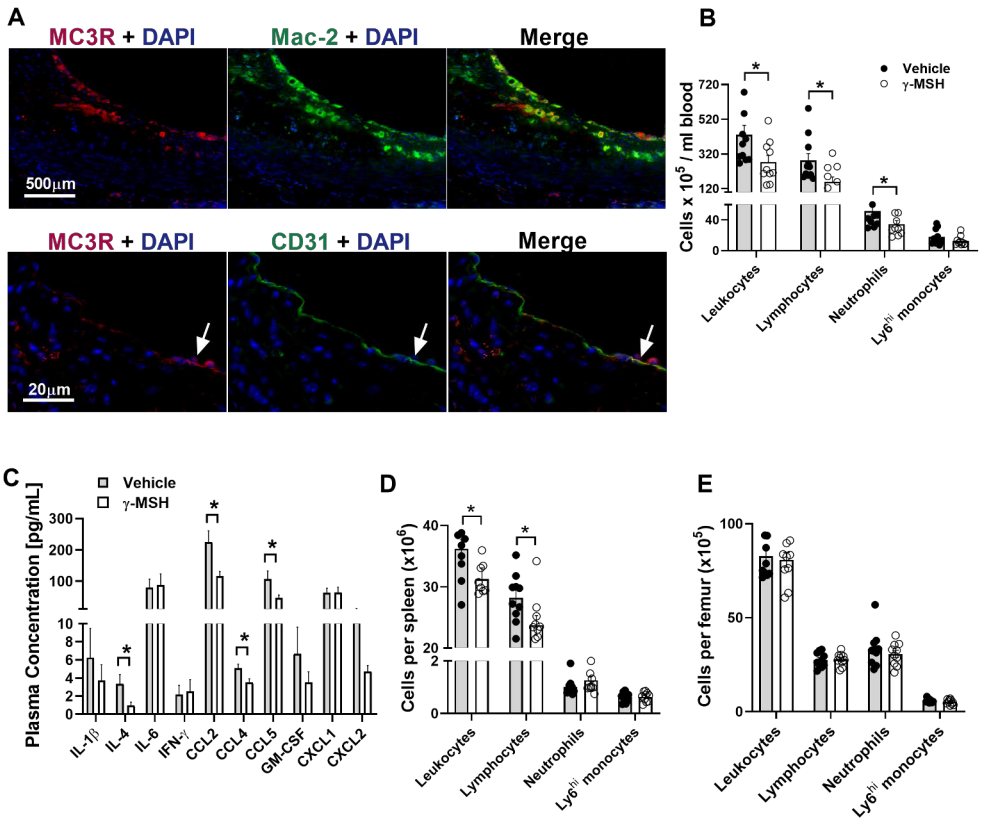

Figure 20. [D-Trp8]-γ-MSH decreased plasma cytokine levels and circulating leukocyte counts in *Apoe*$^{-/-}$ mice. (Modified from original communication III). (**A**) Melanocortin-3 receptor (MC3R) protein expression on murine atherosclerotic plaque. Top panel; MC3R (red) and Mac-2 (green) immunofluorescence staining and, bottom panel; MC3-R (red) and CD31 (green) immunofluorescence staining in the aortic root section of *Apoe*$^{-/-}$ mouse fed 12 weeks of HFD. (**B**) Quantification of total leukocyte and lymphocyte counts (cells per mL of blood) in the blood of *Apoe*$^{-/-}$ mouse. (**C**) The effect of [D-Trp8]-γ-MSH on plasma pro-inflammatory cytokine levels in *Apoe*$^{-/-}$ mice. Quantification of splenic (**D**) and bone marrow (**E**) total leukocytes (CD45$^+$), lymphocytes (CD45$^+$, CD11b$^-$), neutrophils (CD45$^+$, CD11b$^+$, CD115$^-$, Ly6G$^+$) and LyC6^{high} monocytes (CD45$^+$, CD11b$^+$, CD115$^+$, Ly6G$^-$, Ly6C^{high}) in vehicle- and [D-Trp8]-γ-MSH-treated *Apoe*$^{-/-}$ mice. Data are mean ± SEM (Student's *t*-test for unpaired samples), n = 11 (vehicle) and 10 ([D-Trp8]-γ-MSH). *p<0.05 Vs vehicle. Each dot represents individual mouse. γ-MSH = [D-Trp8]-γ-MSH.

5.3.2 The effects of [D-Trp^8]-γ-MSH on plaque size and composition

To examine the plaque size and to characterize the lesion composition in the aortic root, histological (H&E and Masson's Trichrome) and immunohistochemical (α-SMA and Mac-2) staining were employed. Daily treatment with [D-Trp^8]-γ-MSH did not affect plaque size or necrotic core area in the aortic root (**Fig. 21A&B**). Plaque collagen content and α-SMA positive area between the vehicle and treatment group

were unchanged (p = 0.77 and 0.37, respectively). The macrophage content was also comparable between the treatment groups (p = 0.20). Consistent with these findings, RT-PCR analysis of aortic lysates showed no significant difference in the mRNA expression level of collagen *Col1a2*, *Col3a1*, *Col4a1*, *Acta2* (α-SMA*)* or *Mmp9* following [D-Trp^8]-γ-MSH treatment (**Fig. 21C**). To investigate the effect of [D-Trp^8]-γ-MSH on aortic leukocyte accumulation, lysates of the whole aorta were analyzed with flow cytometry for leukocyte counts, which showed that the drug treatment markedly reduced the aortic accumulation of total leukocytes, lymphocytes and myeloid cells (**Fig. 21D**). Taken together, despite the suppression of systemic inflammation and aortic leukocyte accumulation, [D-Trp^8]-γ-MSH treatment did not translate to mitigation of atherosclerosis progression in HFD-fed *Apoe*$^{-/-}$ mice.

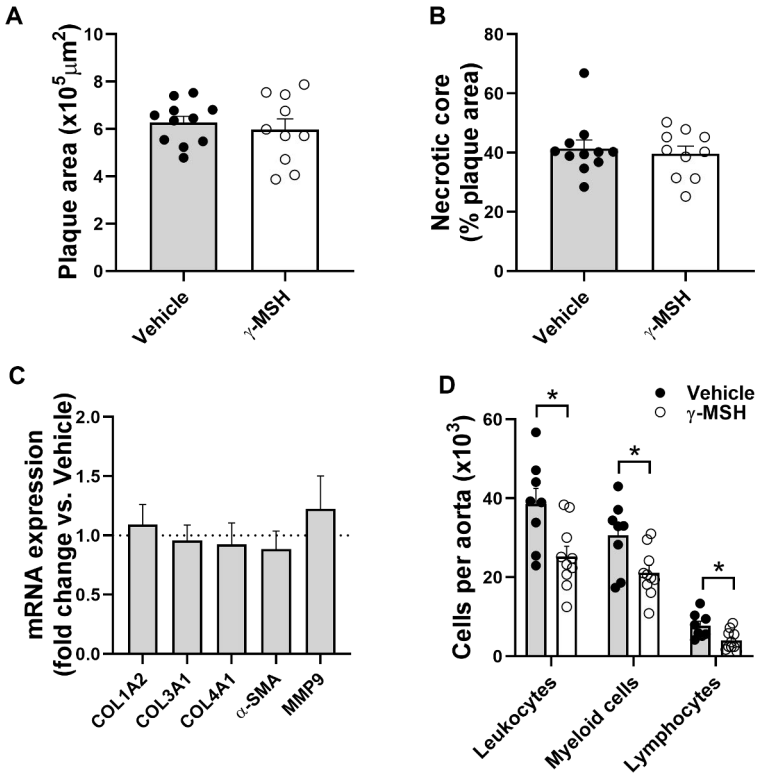

Figure 21. [D-Trp8]-γ-MSH treatment reduced leukocyte counts in the aorta of *Apoe*$^{-/-}$ mice but did not impact plaque size or composition. (Modified from original communication III). (**A-B**) Aortic root plaque size and necrotic core area (expressed as percentage of total plaque area) of vehicle- and [D-Trp8]-γ-MSH-treated mice. (**C**) Quantitative real-time PCR analysis of aortic plaque stability markers in vehicle- and [D-Trp8]-γ-MSH administered mice. n=11 (vehicle) and 10 (γ-MSH). (**D**) Quantification of total leukocytes (CD45$^+$), myeloid cells (CD45$^+$, CD11b$^+$) and lymphocytes (CD45$^+$, CD11b$^-$) in aortic lysates of descending aortae of vehicle- and [D-Trp8]-γ-MSH-treated *Apoe*$^{-/-}$ mice. Data are mean ± S.E.M. (Student's *t*-test for unpaired samples), *p<0.05 Vs vehicle. Each dot represents individual mouse. γ-MSH = [D-Trp8]-γ-MSH.

5.3.3 Divergent effects of MC3R activation on endothelial cells and macrophages

Crucial to leukocyte accumulation in atherosclerotic lesions are the endothelial adhesion molecules that facilitate the infiltration of leukocytes into inflamed lesions. Aortic lysates from vehicle- and [D-Trp^8]-γ-MSH-treated mice were therefore subjected to flow cytometry analysis and gated for CD31$^+$ endothelial cells to quantify the expression of VCAM-1 and ICAM-1 in these cells. The drug treatment did not however affect the expression of VCAM-1 or ICAM-1 in the aortic endothelial cells (**Fig. 22A**). In addition, RT-PCR analyses on aortic lysates revealed no difference in the mRNA expression level of *Vcam1* or *Icam1* following [D-Trp^8]-γ-MSH treatment (**Fig. 22B**). The mRNA expression levels of platelet endothelial cell adhesion molecule (*Pecam1*), lymphocyte function-associated antigen 1 (*Lfa1*) and P-selectin (*Cd62p*) were also unchanged in the aorta of [D-Trp^8]-γ-MSH-treated mice (**Fig. 22B**). To further evaluate the direct effect of γ-MSH on the endothelium, primary endothelial cells from mouse aortae were treated with 0.01–10 μM concentrations of [D-Trp^8]-γ-MSH for 1–24 hours. No significant difference was observed in the mRNA transcript levels of *Vcam1* and *Icam1* ($p = 0.13$ and 0.19, respectively). However, [D-Trp^8]-γ-MSH up-regulated *Ccl5* expression in a concentration-dependent manner following 3-hour exposure (**Fig. 22C**).

Interestingly, RT-PCR analyses of the aortic lysates revealed that [D-Trp^8]-γ-MSH intervention upregulated the expression of the M2-type macrophage markers chitinase-like 3 (*Ym1*: $p = 0.08$), C-type mannose receptor 1 (*Cd206*: $p = 0.06$) and interleukin-1 receptor antagonist (*Il1ra*: $p = 0.06$) (**Fig. 22E**). Furthermore, the drug treatment tended to down-regulate the classical M1-type macrophage markers *Ccl5* ($p = 0.28$), *Ccr1* ($p = 0.06$) and *Tnfa* ($p = 0.12$) (**Fig. 22E**). To further study the direct effects of [D-Trp^8]-γ-MSH on macrophages, bone marrow cells (BMDM) were isolated from *Apoe*$^{-/-}$ mice and differentiated into macrophages before treatment with [D-Trp^8]-γ-MSH (0.01–10μM; exposure time: 1–24 hours). In agreement with the RT-PCR findings in the aorta, the M1-type macrophage markers *Il1b and Ccl5* were downregulated in BMDMs after 3 hours of exposure to [D-Trp^8]-γ-MSH (**Fig. 22F&G**). However, the M2-type macrophage markers were not strongly affected by [D-Trp^8]-γ-MSH in BMDMs (**Appendix Fig. 8**), except for *Ym1*, which was upregulated after 24 hours of drug treatment (**Fig. 22D**).

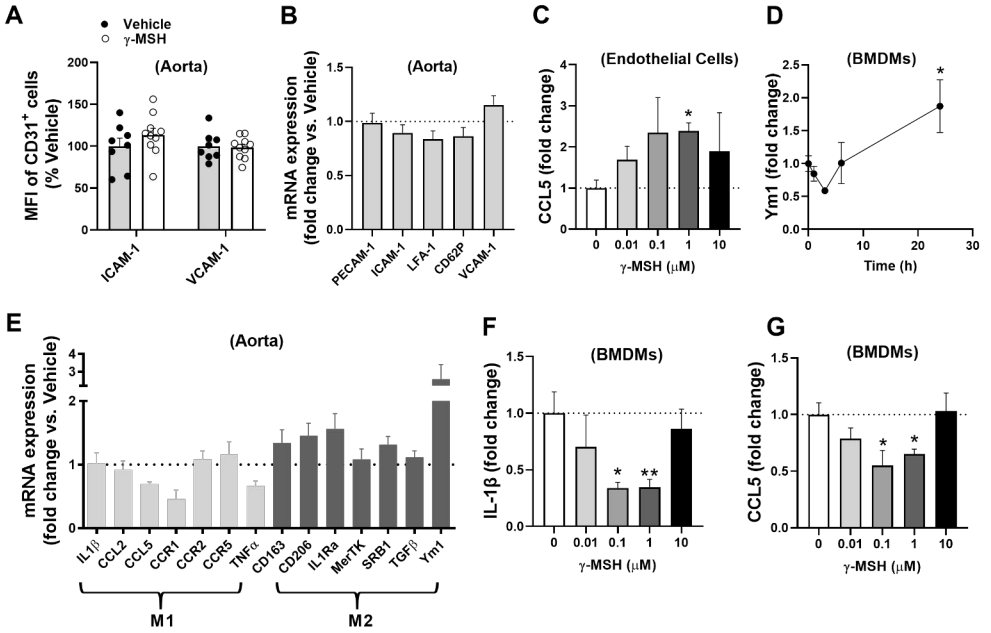

Figure 22. [D-Trp8]-γ-MSH induced opposing effects in cultured endothelial cells and macrophages. (Modified from original communication III). (**A**) VCAM-1 and ICAM-1 mean fluorescence intensity (MFI, expressed as percentage of vehicle) in gated $CD31^+$ cells in the aorta of vehicle- and [D-Trp8]-γ-MSH treated *Apoe*$^{-/-}$ mice. (**B**) Quantitative real-time PCR analysis for cell adhesion molecules in the aorta of vehicle- and [D-Trp8]-γ-MSH treated *Apoe*$^{-/-}$ mice. (**C**) Quantitative real-time PCR analysis of *Ccl5* mRNA expression in aortic endothelial cells treated with increasing concentrations of [D-Trp8]-γ-MSH for 3 h. n = 3-5 per group. (**D**) Quantitative real-time PCR analysis of chitinase-like 3 (*Ym1*) mRNA expression in mouse bone marrow-derived macrophages treated with 1 μM [D-Trp8]-γ-MSH for 1-24 h or left untreated (control, 0 h time point). n = 3-6 per group. (**E**) Quantitative real-time PCR analysis of M1-and M2-type macrophage markers in the aorta of vehicle- and [D-Trp8]-γ-MSH treated mice. n = 11 (vehicle) and 10 (γ-MSH). (**F**) and (**G**) Quantitative real-time PCR analysis of *Il1b* and *Ccl5* mRNA expression in bone marrow-derived macrophages that were treated with increasing concentrations of [DTrp8]-γ-MSH for 3 h. Data are mean ± SEM (Student's t-test for unpaired samples), n = 3-6 per group *p<0.05 and **p<0.01 versus control. Each dot represents individual mouse. BMDMs indicates bone marrow-derived macrophages. γ-MSH = [D-Trp8]-γ-MSH.

6 Discussion

6.1 Comparison of global and bone marrow transplantation models of *Mc1r* deficiency

6.1.1 Assessment of leukocyte behavior and inflammation phenotype

One of the objectives of this thesis was to evaluate the effect of dysfunctional MC1R on inflammatory processes in atherosclerosis. Study I examined the biological consequences of *Mc1r* deficiency using *Apoe*$^{-/-}$ mice carrying globally mutated *Mc1r* gene. After feeding a fat- and cholesterol-rich HFD, *Apoe*$^{-/-}$ *Mc1r*$^{e/e}$ mice showed enhanced atherosclerosis that was associated with hypercholesterolemia and enhanced hepatic lipid accumulation. Considering that hypercholesterolemia induces monocytosis, in particular, an increase in Ly6C^{high} monocytes (Swirski et al., 2007), it was unexpected that HFD-fed *Apoe*$^{-/-}$ *Mc1r*$^{e/e}$ mice did not show any significant change in circulating leukocyte or monocyte counts compared to HFD-fed *Apoe*$^{-/-}$ mice. However, HFD feeding triggered a significant increase in the number of bone marrow Ly6C^{high} monocytes in *Apoe*$^{-/-}$ *Mc1r*$^{e/e}$ mice in comparison with HFD-fed *Apoe*$^{-/-}$ mice, an effect that is likely attributable to the elevation of plasma cholesterol in these mice. Under chow-fed conditions, *Mc1r* deficient mice demonstrated a significant increase in aortic accumulation of total leukocytes, Ly6C^{high} monocytes and macrophages. Meanwhile, the Ly6C^{high} monocyte population in the spleen was markedly reduced in *Apoe*$^{-/-}$ *Mc1r*$^{e/e}$ mice, suggesting that splenic Ly6C^{high} monocytes were exiting the spleen to accumulate in the aorta in these mice. Collectively, the effects of *Mc1r* deficiency on tissue monocyte counts appeared to be more pronounced in chow-fed mice when dietary cholesterol is not triggering excessive arterial leukocyte accumulation or monocytosis. Given that early atherosclerosis is marked by the influx of monocytes and their differentiation into macrophages, while advanced lesions rely on local macrophage proliferation (Robbins et al., 2013; Swirski et al., 2006, 2007), it is plausible that impaired MC1R signaling accelerates monocyte recruitment and plaque macrophage expansion only in the early phases of atherosclerosis.

The increase in atherosclerosis burden and aortic leukocyte population in *Apoe*$^{-/-}$ *Mc1r*$^{e/e}$ mice established a link between MC1R and atherosclerosis inflammation in experimental settings. However, it was crucial to ascertain the specific role of leukocyte MC1R in the observed phenotype. Study II utilized the bone marrow transplantation approach to analyze the contribution of hematopoietic cells carrying dysfunctional *Mc1r* to atherosclerosis-linked inflammation and plaque development in *Apoe*$^{-/-}$ mice. Firstly, the level of chimerism between the genotypes was comparable and no statistical difference was observed in the bone marrow LSK^{+} cell count between the genotypes, suggesting that the reconstitution was efficient and did not falsely skew the results. Leukocyte-specific *Mc1r* deficiency induced significant expansion of circulating and splenic total leukocytes and lymphocytes that was further aggravated by HFD feeding. This phenotype was contradictory to the leukocyte profiles observed in mice with global *Mc1r* deficiency. In Study I, increased amounts of leukocytes, particularly Ly6C^{high} monocytes, were attracted to the inflamed aorta, which may have contributed to the increased plaque size and vulnerable plaque composition in *Apoe*$^{-/-}$ *Mc1r*$^{e/e}$ mice. In contrast, *Apoe*$^{-/-}$ *Mc1r*$^{e/e}$ chimeric mice showed a significantly increased number of total leukocytes in the circulation and spleen, but not in the aorta. Taking into account the wide expression of MC1R in various tissues, it is plausible that the presence of dysfunctional *Mc1r* in non-leukocyte cells is modulating the accumulation of leukocytes in the aorta of the global knockout model. The endothelial lining of the aorta, for example, also expresses the MC1R subtype and its deficiency is associated with enhanced inflammation in these cells (Rinne et al., 2015). Accordingly, dysfunctional *Mc1r* in aortic endothelial cells may have contributed to the increased local inflammation in the aorta, thereby stimulating leukocyte accumulation within the plaque. An effort to substantiate the role of endothelial cells in the observed phenotype (Study I) did not however reveal a significant difference in the endothelial expression of various adhesion molecules between the genotypes. Admittedly, only a few adhesion molecules were selected and analyzed and thus, it is possible that *Mc1r* deficiency in endothelial cells has evoked a pro-inflammatory phenotype that was not revealed in this study. Moreover, global *Mc1r* deficiency induced disturbances in cholesterol and bile acid metabolism that resulted in increased cholesterol levels in the plasma and liver, which may have provoked arterial cholesterol accumulation and subsequent increase in arterial inflammation and leukocyte recruitment to the aorta. Therefore, it appears that the enhanced arterial leukocyte accumulation and inflammation in Study I is not the direct effect of *Mc1r* deficiency on leukocytes, thus the contrasting phenotype in leukocyte behavior between the two models is likely driven by non-leukocyte cells such as endothelial cells.

Intriguingly, chimeric *Apoe*$^{-/-}$ *Mc1r*$^{e/e}$ mice exhibited significant upregulation of total leukocytes and lymphocytes, particularly CD4^{+} T cells, in the blood and spleen

regardless of the diet type. This phenotype was, however, absent in the global *Mc1r* deficiency model, thus suggesting a possible methodological influence by the bone marrow transplantation approach on tissue leukocyte expression. On the other hand, life-long *Mc1r* deficiency may have led to compensatory changes that have counteracted the immediate effect of *Mc1r* deficiency on lymphocyte count (as observed in Study II).

Finally, because the bone marrow transplantation model of *Mc1r* deficiency demonstrated a lack of significant leukocyte expansion within the aorta of *Apoe*$^{-/-}$ *Mc1r*$^{e/e}$ chimeric mice despite increased leukocyte counts in the circulation and the spleen, an *in vivo* homing assay was central in investigating this discrepancy in leukocyte accumulation. The homing assay revealed that Ly6C^{high} monocytes, CD4^{+} T cells, and CD8^{+} T cells from *Mc1r* deficient mice were rather moving into the spleen instead of residing in the circulation or accumulating in paLNs, suggesting that these cells have a lower tendency to invade the adventitial tissues of the aorta or the atherosclerotic plaque itself. Another key finding in Study II was the expression of *Mc1r* mRNA and its protein product in mouse CD4^{+} T cells. Interestingly, *Mc1r* deficiency impaired the migratory behavior of CD4^{+} T cells *via* a CCR5-dependent mechanism. Since CCR5 modulates the migration of monocytes and T cells to the lesion (Braunersreuther et al., 2007; van Wanrooij et al., 2005), impaired CCR5-dependent migration of *Mc1r* deficient leukocytes might also explain the lack of exaggerated leukocyte accumulation in the aorta and thereby, also influence the observed plaque phenotype in Study II. In conclusion, MC1R protein expression on leukocytes, particularly on CD4^{+} T cells, influences the functionality of these cells, thus affecting their migration to atherosclerotic plaques and ultimately the development of atherosclerosis.

6.1.2 Evaluation of plaque phenotype

The global deficiency of *Mc1r* (Study I) in HFD-fed *Apoe*$^{-/-}$ mice enhanced plaque formation with increased lesional macrophage content and necrotic core size but reduced SMC content and collagen, which are considered hallmarks of a vulnerable plaque. These mice also exhibited reduced expression of *Abca1* and *Abcg1* in the aorta, which might accelerate atherosclerosis and influence the formation of vulnerable plaques (Westerterp et al., 2014; Yvan-Charvet et al., 2007). It has been shown that the deletion of ABCA1 and ABCG1 transporter proteins in macrophages promotes plaque inflammation and aggravates atherosclerosis in mice (Westerterp et al., 2013). Conversely, the activation of MC1R in macrophages upregulated ABCA1 and ABCG1 expression, thereby enhancing macrophage reverse cholesterol transportation (Rinne et al., 2017). Interestingly, on chow-fed *Apoe*$^{-/-}$ mice, when plasma cholesterol level was comparable between the genotypes, the acellular

necrotic core area of the plaque was markedly increased in *Mc1r* deficient mice despite the lack of difference in plaque size. In agreement with these findings, treatment of *Apoe*$^{-/-}$ mice with a selective MC1R agonist promoted plaque stability as evidenced by increased plaque collagen content and α-SMA expression (Rinne et al., 2017). Consequently, the downregulation of *Abca1* and *Abcg1* in *Mc1r* deficient mice might interfere with macrophage cholesterol handling, thus exacerbating atherosclerosis-linked inflammation and the formation of vulnerable plaques. Therefore, functional MC1R appears to be an essential modulator of atherosclerotic plaque integrity.

In contrast, in study II, the introduction of leukocyte MC1R-deficient bone marrow cells into recipient *Apoe*$^{-/-}$ mice induced upregulation of circulating, splenic and bone marrow leukocyte counts but it did not increase the accumulation of leukocytes in the aorta or accelerate atherosclerosis. Thus, the plaque characteristics in terms of size and composition were inconsistent between the global (Study I) and leukocyte-specific (Study II) *Mc1r* deficiency models. It could be argued that elevated plasma cholesterol levels owing to disturbed cholesterol and bile acid metabolism may have accelerated atherosclerosis in the global *Mc1r* deficiency model. On the other hand, a vulnerable plaque phenotype was also observed in chow-fed *Apoe*$^{-/-}$ *Mc1r*$^{e/e}$ mice when there was no difference in plasma cholesterol level between the genotypes. This raises the question of whether MC1R is also expressed by non-leukocyte cells within the atherosclerotic plaque such as the endothelial cells, SMCs or fibroblasts. It is plausible that nonfunctional MC1R in non-leukocyte cells is mediating the observed plaque characteristics in the global *Mc1r* deficiency model. Supporting this notion, MC1R protein has been reported to be present also in SMCs and fibroblasts (Alfieri et al., 2018; Stanisz et al., 2011). SMCs, in particular, play a crucial role in vascular remodeling and cardiovascular diseases. They exhibit high plasticity and are capable of existing in different phenotypic states such as contractile and synthetic (Rattik et al., 2015; Saporiti et al., 2019). Migration of SMCs into the intima from the tunica media and subsequent release of various extracellular fibrous matrix proteins such as collagen, elastin and proteoglycans mediate atherosclerotic plaque stability. The activation of MC1R with α-MSH has been shown to modulate the migratory behavior of cultured human aortic SMCs (Alfieri et al., 2018). Potentially, this MC1R signaling on SMCs could also be driving the observed change in plaque stability (i.e. reduced SMC and collagen content) in *Apoe*$^{-/-}$ *Mc1r*$^{e/e}$ mice and explain the difference in aortic plaque phenotype between the global and leukocyte-specific *Mc1r* deficiency models employed in Study I and Study II.

6.2 Pharmacological effects of systemic administration of [D-Trp^8]-γ–MSH on inflammation and atherosclerosis in *Apoe*$^{-/-}$ mice

The anti-inflammatory potential of melanocortin is also linked to the MC3R subtype. Previous studies have established the role of MC3R in mediating anti-inflammatory responses and providing protection against various inflammatory diseases (Demidowich et al., 2019; Ehtesham et al., 2019; Wang et al., 2021). The anti-inflammatory effects mediated by this receptor are largely due to its expression in diverse leukocyte subsets (Dinparastisaleh & Mirsaeidi, 2021; Wang et al., 2019, 2021). In particular, MC3R is expressed in macrophages, which are predominant effector cells in atherosclerosis, and regulates their function under inflammatory conditions (Wang et al., 2019, 2021). In Study III, MC3R expression was also identified on macrophages residing in atherosclerotic plaque of *Apoe*$^{-/-}$ mice. To dissect the anti-inflammatory potential of MC3R signaling in atherosclerosis, atherosclerotic *Apoe*$^{-/-}$ mice were treated with the MC3R agonist [D-Trp^8]-γ-MSH. It was found that [D-Trp^8]-γ-MSH administration suppressed systemic and local inflammation, which resulted also in lower circulating and aortic leukocyte counts. Furthermore, the expression of inflammatory cytokines and leukocyte adhesion molecules were downregulated in the spleen and liver of [D-Trp8]-γ-MSH-treated mice, suggesting tissue-specific anti-inflammatory benefit of [D-Trp8]-γ-MSH-MC3R interaction.

[D-Trp8]-γ-MSH, however, fell short in reducing plaque size or favorably altering plaque composition in *Apoe*$^{-/-}$ mice. Despite the lack of effect on plaque size or composition, the drug administration upregulated M2-type macrophage markers and downregulated pro-inflammatory M1-type macrophage markers in the aorta. Consistently, [D-Trp8]-γ-MSH treatment of bone marrow-derived macrophages *in vitro* elevated the expression of M2-type markers expression and reduced the expression of M1-type markers. To the best of our knowledge, this was the first study to explore the therapeutic potential of targeting MC3R with [D-Trp8]-γ-MSH in experimental atherosclerosis. As such, it is challenging to correlate the findings from Study III to previous studies. However, *Ldlr*$^{-/-}$ mice with transgenic overexpression of α- and γ-MSH demonstrated a significant reduction in HFD-induced pro-inflammatory cytokines and plaque size, as well as induced protection against endothelial dysfunction (Nuutinen et al., 2018). In this transgenic model, γ-MSH was overexpressed together with α-MSH in various tissues, which does not allow concluding the exact contribution of γ-MSH-MC3R-axis to the observed phenotype. Furthermore, the lipid profile between *Ldlr*$^{-/-}$ and *Apoe*$^{-/-}$ mice is different, which may influence also the atherosclerosis phenotype between α- and γ-MSH overexpressing *Ldlr*$^{-/-}$ mice and [D-Trp8]-γ-MSH-treated *Apoe*$^{-/-}$ mice. Hypercholesterolemia in *Ldlr*$^{-/-}$

mice is driven by the deficiency of *Ldlr* in hepatocytes and it is significantly aggravated by feeding the mice a cholesterol-rich diet. However, hypercholesterolemia in *Apoe*$^{-/-}$ mice is more robust and it is also manifested when these mice are fed a standard chow diet. Hypercholesterolemia and associated atherosclerosis in *Apoe*$^{-/-}$ mice are provoked by the absence of *Apoe* in hepatocytes and also by its deficiency in other cell types including macrophages (Hartvigsen et al., 2007; Véniant et al., 2001; Véniant et al., 2008). Therefore, these differences between *Ldlr*$^{-/-}$ and *Apoe*$^{-/-}$ mice may partly explain the difference in plaque phenotype between the transgenic overexpression model and the intervention study (Study III).

In intervention studies, the pharmacokinetic properties of a drug compound are essential for its efficacy. In Study III, [D-Trp8]-γ-MSH reduced local and systemic inflammation in atherosclerotic mice, but the effect did not extend to plaque size or composition. A potential limitation in this study could be associated with the dosage frequency of [D-Trp^{8}]-γ-MSH. Although [D-Trp^{8}]-γ-MSH is efficacious in stimulating MC3R, it is rather short-acting (Zhou et al., 2017) and thus invites the question of appropriate dosing regimens for *in vivo* studies. In previous anti-inflammatory studies in mice (Holloway et al., 2015; Leoni et al., 2008), [D-Trp^{8}]-γ-MSH has been administered with a fixed dose of 10 µg/mouse. An earlier *in vivo* study demonstrated a dose-responsiveness for [D-Trp^{8}]-γ-MSH that peaked around this dose level in crystal-induced inflammation (Getting et al., 2006). In Study III, a slightly higher dose of 15µg of [D-Trp^{8}]-γ-MSH per mouse was administered to account for the higher body weight of *Apoe*$^{-/-}$ mice that had been already on HFD before the start of the drug intervention. Nevertheless, an increase in dosing frequency to twice/trice daily or greater than 4 weeks of treatment duration might have increased the chance to observe a reduction in plaque size. Additionally, [D-Trp8]-γ-MSH peptide has a strong affinity for MC3R, but it also binds and activates other MCRs (Joseph et al., 2010). A selective agonist that exclusively activates this receptor could improve the observed outcome and potentially attenuate plaque progression.

Finally, considering the important roles of CCL5 and its receptor CCR5 in leukocyte migration and atherosclerosis (Braunersreuther et al., 2007, 2008; Koenen et al., 2009; Krohn et al., 2007), the increase in endothelial cell expression of CCL5 following [D-Trp8]-γ-MSH treatment could partly explain the lack of effect on aortic plaque size in Study III.

6.3 Therapeutic prospects and future directions

In atherosclerosis, various factors influence the disease progression. Dyslipidemia and inflammatory responses tightly regulate the atherosclerotic plaque development as well as the composition of the lesion (Jebari-Benslaiman et al., 2022; Kim et al., 2020; Libby, 2021). The suppression of the inflammatory elements driving the

disease pathogenesis could potentially attenuate disease progression. In recent years, targeting atherosclerosis-linked inflammation has garnered interest as a therapeutic strategy to manage ASCVD. The outcome of the CANTOS trial, for instance, gives more credence to new therapeutic options to target inflammation as a therapeutic option for CVD reduction in clinical settings (Paul M Ridker et al., 2017). This encourages for further studies on the anti-inflammatory strategies that could be safe and applicable for managing atherosclerosis.

Small-chain peptide drugs such as the melanocortin peptides present one of the most promising molecules for managing various inflammatory conditions (Gonzalez-Rey et al., 2007; Gonzalez-Rey et al., 2006; Gonzalez-Rey et al., 2006; Montero-Melendez et al., 2011; Patel et al., 2011; Rennalls et al., 2010). As alluded to in earlier chapters of this thesis, melanocortins possess favorable anti-inflammatory properties. In particular, MC1R appears to regulate inflammation driving atherosclerosis in experimental settings. The ubiquitous dysfunction of this receptor accelerates disease progression, while the leukocyte-specific deficiency of this receptor increases the accumulation of leukocytes in various tissues. However, taking into account the preferential homing of *Mc1r* deficient leukocytes to the spleen and not to the aorta (Study II), MC1R agonist treatment in atherosclerosis could potentially lead to an undesired effect in terms of leukocyte migration into the aorta. However, treatment of atherosclerotic *Ldlr*$^{-/-}$mice with Melanotan II, an α-MSH analog, did not cause enhanced leukocyte accumulation in the aorta, but rather improved aortic endothelial function (Rinne et al., 2013, 2014). This suggests that endothelial MC1R activation could suppress the inflammation of the endothelium and consequent leukocyte adherence, and thus counterbalance the possible undesired effect of leukocyte MC1R activation. Furthermore, the pharmacological stimulation of MC1R in atherosclerotic mice could increase plaque macrophage cholesterol efflux, thereby reducing the cholesterol load of foam cells and facilitating the resolution of inflammation within the atherosclerotic plaque (Rinne et al., 2017). Hence, pharmacological stimulation of MC1R could be of therapeutic benefit in the management of ASCVD.

The specific targeting of the MC3R subtype (Study III), which also mediates the anti-inflammatory response of the melanocortins, attenuated local and systemic inflammation in experimental atherosclerosis. Collectively, the findings from this thesis work demonstrated the anti-inflammatory potential of both the MC1R and MC3R in atherosclerosis and the role of MC1R role in regulating plaque size and composition. Therefore, a melanocortin peptide bearing agonistic activity and selectivity for the MC1R and MC3R would likely exert multiple synergistic benefits to attenuate inflammation and disease progression in atherosclerosis.

Lastly, the melanocortin peptides present an important advantage as anti-inflammatory agents by moderately suppressing the immune system but not at the

expense of the protective function of the system against infections. Furthermore, melanocortin ligands are relatively short and hydrophilic peptide-chain molecules that can gain quick access to the inflammatory site and interact with MC1R and MC3R with high specificity to regulate and reduce atherosclerosis-linked inflammation (**Fig. 23**). Due to the favorable physicochemical properties, melanocortin ligands are intrinsically innoxious, do not usually induce antigenicity and could have rapid renal and hepatic clearance. The data from this thesis revealed that MC1R and MC3R could improve the inflammation regulating atherosclerosis and therefore, the melanocortin system offers a plausible and promising target to manage ASCVD.

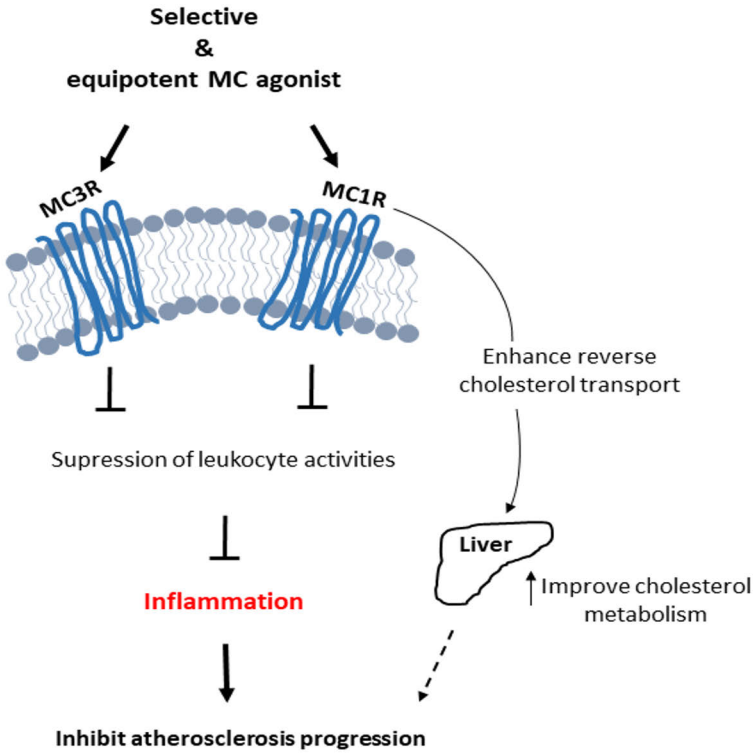

Figure 23. The stimulation of MC1R and MC3R potentially presents a therapeutic option for the management of atherosclerosis.

7 Summary/Conclusions

The main findings and conclusions of this thesis work were as follows:

1. Global deficiency of MC1R signaling in *Apoe*$^{-/-}$ *Mc1r*$^{e/e}$ mice accelerated atherosclerosis by disturbing cholesterol and bile acid metabolism. This genotype promoted aortic monocyte accumulation thereby exacerbating the disease progression.
2. Leukocyte-specific *Mc1r* deficiency in *Apoe*$^{-/-}$ chimeric mice significantly increased total leukocyte counts in the circulation through the expansion of T cells. The migration of leukocyte-*Mc1r*$^{e/e}$ was impaired due to defective CCR5 recycling, seemingly, affecting their accumulation in the aorta of *Apoe*$^{-/-}$ chimeric mice.
3. The *in vivo* activation of MC3R by [D-Trp8]-γ-MSH dampened systemic and local inflammation in HFD-fed *Apoe*$^{-/-}$ mice with a consequential reduction of leukocyte counts in the blood and aorta. [D-Trp8]-γ-MSH did not however reduce plaque size or favorably modulate plaque composition in *Apoe*$^{-/-}$ mice.

The data from these studies highlight the crucial roles of MC1R and MC3R in modulating lipid metabolism, inflammatory responses and leukocyte behavior in the context of experimental atherosclerosis. Selective targeting of MC1R and/or MC3R could hold promise as a therapeutic strategy in the management of atherosclerosis, but further investigations are warranted to evaluate the potential of more potent agonists and refined dosing regimens in this regard.

Acknowledgements

My utmost gratitude is directed to the creator (Allah) of the universe and its constituent. The omnipotent fabricator of all living and insentient entities, the begetter of the smallest component of matter up to the largest multiverses imaginable. He who is singular and indivisible, the eternal refuge, He begets not nor is He begotten, nor is there to Him any equivalent. Praise to He who author knowledge and wisdom, the programmer of the beginning ("Big Bang"; Qur'an 21 vs 30) and the sole omniscient of the Big Rip, the Big Slurp, the Big Crunch & the Big Freeze (Qur'an 81 vs 1-2; 82 vs 1-2; 21 vs 104; 7 vs 187). I proclaim His worthiness to be worshiped and affirm His final messenger (Muhammad) as the seal of all the prophets.

This thesis was conducted at the Department of Integrative Physiology and Pharmacology, Institute of Biomedicine, University of Turku. I am humbly honored to have been allowed to study in this great citadel of knowledge (University of Turku) under the authority of the previous and current faculty/department heads including the amazing Professor Markku Koulu, the current vice dean Prof. Eerika Savontaus and prof. Sari Mäkelä. Particularly, the drug research and development (DRDP) unit of the university has been 'home' to my educational progression. My warm appreciation to the entire overseer of the DRDP program (Prof. Ullamari Pesonen & co.) and the two awesome coordinators (Eeva^2 - Eeva Rainio and Eeva Valve) administering the MSc & Ph.D. student affairs, respectively. I commend your ever-ready-to-help attitude toward the students. Deservingly, I also wish to express my indebtedness to the DRDP graduate school, Turun Yliopistosäätiö and the Finnish Foundation for Cardiovascular Research as the principal financial contributors in form of working grants during the course of my Ph.D. studies. I acknowledge your relentless patronage to help subsist me through the progression of this thesis work.

To my supervisor, Adj. Prof. Petteri Rinne, who has been a remarkable guide in steering my Ph.D. career journey from the beginning, I say to you, a big, fatty, MC4R-deficient and morbidly obese THANK YOU. With your stewardship, I was able to gain valuable knowledge and essential support needed to effectuate successful biomedical research projects. Under your supervision, I have grown in

my quest for a deep sapience in life sciences, stupendously. I admire your relentlessness for excellence in biomedical/pharmacological investigations and for setting a higher standard during this process. For that, I will always appreciate the guidance and the passion for scientific aptitude you provoked in me during this thesis project.

I was fortunate to be secondarily supervised during the course of my Ph.D. studies by the frontierlady of melanocortin metabolic research in Finland, prof. Eriika Savontaus. You have been an inspiration to me. I recognized your immeasurable input towards my Ph.D. adventure via helpful and supportive piece of advice in my projects as well as career-building tips. In addition, I am grateful to you and Ilkka Heinonen for being part of my follow-up committee team. It has been a pleasure to have such great minds overseeing the progress of my thesis work.

Prof. Jaana Rysä and Dr. Trinidad Montero-Melendez, the official examiner of this thesis manuscript, I want to extend my gratitude to you guys for accepting to help review this dissertation. Your valuable comments and suggestions were vastly helpful in enhancing the manuscript.

To my teammates at the melanocortin-cardiovascular colony, Keshav Thapa and Anni Suominen, thank you for your moral and unwavering team support. I acknowledge your help in stamping the memory of the melanocortin system to my subconsciousness. It is like ‘eating’, ‘drinking’, and ‘burping’ of the MC ligands/receptors during the last few years in the laboratory with you guys. For that, you get an Eppendorf-full of melanocortin-concentrated salute from me.

The observations presented in this thesis were predicated on the results obtained mainly from our laboratory with help from some collaborators. Thusly, I would like to recognize the contribution of the entire co-authors feature in the three articles that form the base to which this thesis work was developed: Velasco-Delgado Mauricio, Nuutinen Salla, Viitala M, Hollmén M, Rami M, Steffens S. Thapa K, Kaipio Katja, Cai M, Hruby Victor J, Tadayon Sina, and Suominen Anni. I would also like to thank Sanna Batsman, Hanna Haukkala, Elina Kahra, and Satu Mäkelä for their astounding technical support. Helena Gylling and Leena Kaipainen are duly acknowledged for their scientific assistance with gas-liquid chromatography analysis as well as Obada Alzghool and Markus Peurla for frozen histological tissue processing and technical assistance in imaging.

The MedC6 Farmis family (past and present) has made this journey a memorable one for me. You all; Sanna Soini, Minttu Mattila, Liisa Ailanen, Milka hauta-aho, Mikko Uusi-Oukari, Markku Koulu, Ali Benkherouf, Olli pentikkäinen & co., Kim Eerola, Johanna Jukkala, Virpi Aaltonen, Hanna Haukkala, etc made Medisiina C (floor-6) and excellent scientific hub and a conducive workplace for me through the years. I am grateful to have met with you all. A special Kiitos to the late Lauri Vuorilehto, a gentleman who never failed to smile. Thank you for the regular check-

up on the progression of my Ph.D. projects and for always encouraging me to keep pushing forward, as well as giving tips on maximizing Milli-Q water usage effectively. May your soul rest in peace!

I am grateful to my D=R=D=P dimer brothers, Ali Benkherouf (De Real G) and Obada Alzghool who have been my unshakable network of support here in Turku. Y'all have been central to my progression in both my educational and personal life. I will not forget the bliss, laughter, and the "sikin sokin" of life we went through, together! The experiences we shared during DDD & DRDP adventures, like some type of polymerized peptides crawling through a jagged electrophoresis gel are forever engraved in my heart. By the way, shout out to the University of Turku DRDP graduate school family. I will also like to extend similar gratitude to the rest of the aromatic-bonded Habibis (my Arab connection) – Tarek Omran (T-Stein), Khalil Shahramian (K-wizard) and Sherif Sami. It is never a dull moment with these happy-go-bunnies bros, you always bring out the 'J' in joy to my face. I love you all solely for the sake of Allah (swt). To my other connections i.e. Turku connection - Sami Penttilä, Kristian Hakala, Evgeniy Matsiychuk, Akeem Abbas (Eng.), Ari Lehmusvuori (Hidex Oy); Helsinki connection - Alexei Dzyuba and Aliu Muhammed; Nigeria connection - Hassan Lawal (Snr Eng.) and the Lawal battalion (Faria, Faiza, Famida, Firdaus, Abd Salam & Fahima); Nottingham connection - James Ondimu, Ismail Omisola, Caroline Wyatt, Zu, and Giovanni Scotti, I say ginormous cheers to you guys for being there for me in various capacities. I appreciate you all for the perpetual encouragement.

Lastly, special gratitude goes to my parents, particularly, my exceptional mom. Thank you for nurturing me well to trail the right path in life. I deeply appreciate the unconditional love and care I receive from you. You are my inspiration. Thanks for the constant motivation, prayer and unlimited motherly support throughout my life. You are simply the BEST! To you are my utmost love, admiration, and respect. I am gratitude indebted also to my siblings - Islamiyah, Azeez, Saheed, and Kafeelat. Thanks a lot for your patience and endless support even when life drives me to afar destinations from you. I cherish y'all unequivocally, my indispensable bunch of Kadiris. Finally, a meritorious gramercy to my distinguished wife, Maija, and the kids (Hamza & Tijan) for tolerating my time away from home during the course of this thesis project. You ease the hard days at work for me with your soothing smiles. I count myself lucky to have you guys in my life.

Turku, April 2023
James Jamal Kadiri

References

A, B. M. (1916). The results of extirpation of the anterior lobe of the hypophysis and of the thyroid of rana pipiens larvae. *Science (New York, N.Y.)*, *44*(1143), 755–758. https://doi.org/10.1126/science.44.1143.755

Abdel-Malek, Z A. (2001). Melanocortin receptors: their functions and regulation by physiological agonists and antagonists. *Cellular and Molecular Life Sciences : CMLS*, *58*(3), 434–441. https://doi.org/10.1007/PL00000868

Abdel-Malek, Zalfa A. (2009). Agouti signal protein: crossing the "yellow" signal and arriving to pathways that affect tumorgenesis. In *Pigment cell & melanoma research* (Vol. 22, Issue 3, pp. 253–254). https://doi.org/10.1111/j.1755-148X.2009.00564.x

Ait-Oufella, H., Salomon, B. L., Potteaux, S., Robertson, A.-K. L., Gourdy, P., Zoll, J., Merval, R., Esposito, B., Cohen, J. L., Fisson, S., Flavell, R. A., Hansson, G. K., Klatzmann, D., Tedgui, A., & Mallat, Z. (2006). Natural regulatory T cells control the development of atherosclerosis in mice. *Nature Medicine*, *12*(2), 178–180. https://doi.org/10.1038/nm1343

Alfieri, V., Saporiti, F., Ferrari, F., Piacentini, L., Chiesa, M., & Colombo, G. I. (2018). MC1R regulates P38 MAPK pathway to reduce human aortic smooth muscle cell migration. *Atherosclerosis*, *275*, e127–e128. https://doi.org/10.1016/j.atherosclerosis.2018.06.368

Almeida, S. O., & Budoff, M. (2019). Effect of statins on atherosclerotic plaque. *Trends in Cardiovascular Medicine*, *29*(8), 451–455. https://doi.org/10.1016/j.tcm.2019.01.001

An, N., & Kang, Y. (2013). Using quantitative real-time PCR to determine donor cell engraftment in a competitive murine bone marrow transplantation model. *Journal of Visualized Experiments : JoVE*, *73*, e50193. https://doi.org/10.3791/50193

Andersen, G. N., Hagglund, M., Nagaeva, O., Frangsmyr, L., Petrovska, R., Mincheva-Nilsson, L., & Wikberg, J. E. S. (2005). Quantitative measurement of the levels of melanocortin receptor subtype 1, 2, 3 and 5 and pro-opio-melanocortin peptide gene expression in subsets of human peripheral blood leucocytes. *Scandinavian Journal of Immunology*, *61*(3), 279–284. https://doi.org/10.1111/j.1365-3083.2005.01565.x

Askari, N., Lipps, C., Voss, S., Staubach, N., Grün, D., Klingenberg, R., von Jeinsen, B., Wolter, J. S., Kriechbaum, S., Dörr, O., Nef, H., Liebetrau, C., Hamm, C. W., & Keller, T. (2021). Circulating Monocyte Subsets Are Associated With Extent of Myocardial Injury but Not With Type of Myocardial Infarction. *Frontiers in Cardiovascular Medicine*, *8*, 741890. https://doi.org/10.3389/fcvm.2021.741890

Atwell, W. J. (1919). On the nature of the pigmentation changes following hypophysectomy in the frog larva. *Science (New York, N.Y.)*, *49*(1254), 48–50. https://doi.org/10.1126/science.49.1254.48

Auffray, C., Fogg, D., Garfa, M., Elain, G., Join-Lambert, O., Kayal, S., Sarnacki, S., Cumano, A., Lauvau, G., & Geissmann, F. (2007). Monitoring of blood vessels and tissues by a population of monocytes with patrolling behavior. *Science (New York, N.Y.)*, *317*(5838), 666–670. https://doi.org/10.1126/science.1142883

Bäck, M., Yurdagul, A. J., Tabas, I., Öörni, K., & Kovanen, P. T. (2019). Inflammation and its resolution in atherosclerosis: mediators and therapeutic opportunities. *Nature Reviews. Cardiology*, *16*(7), 389–406. https://doi.org/10.1038/s41569-019-0169-2

Badimon, L., Padró, T., & Vilahur, G. (2012). Atherosclerosis, platelets and thrombosis in acute ischaemic heart disease. *European Heart Journal. Acute Cardiovascular Care*, *1*(1), 60–74. https://doi.org/10.1177/2048872612441582

Badimon, L., Peña, E., Arderiu, G., Padró, T., Slevin, M., Vilahur, G., & Chiva-Blanch, G. (2018). C-Reactive Protein in Atherothrombosis and Angiogenesis. *Frontiers in Immunology*, *9*, 430. https://doi.org/10.3389/fimmu.2018.00430

Bellosta, S., Mahley, R. W., Sanan, D. A., Murata, J., Newland, D. L., Taylor, J. M., & Pitas, R. E. (1995). Macrophage-specific expression of human apolipoprotein E reduces atherosclerosis in hypercholesterolemic apolipoprotein E-null mice. *The Journal of Clinical Investigation*, *96*(5), 2170–2179. https://doi.org/10.1172/JCI118271

Biessen, E. A. L., & Wouters, K. (2017). Macrophage complexity in human atherosclerosis: opportunities for treatment? *Current Opinion in Lipidology*, *28*(5), 419–426. https://doi.org/10.1097/MOL.0000000000000447

Boisvert, W. A., Spangenberg, J., & Curtiss, L. K. (1995). Treatment of severe hypercholesterolemia in apolipoprotein E-deficient mice by bone marrow transplantation. *The Journal of Clinical Investigation*, *96*(2), 1118–1124. https://doi.org/10.1172/JCI118098

Borén, J., Chapman, M. J., Krauss, R. M., Packard, C. J., Bentzon, J. F., Binder, C. J., Daemen, M. J., Demer, L. L., Hegele, R. A., Nicholls, S. J., Nordestgaard, B. G., Watts, G. F., Bruckert, E., Fazio, S., Ference, B. A., Graham, I., Horton, J. D., Landmesser, U., Laufs, U., … Ginsberg, H. N. (2020). Low-density lipoproteins cause atherosclerotic cardiovascular disease: pathophysiological, genetic, and therapeutic insights: a consensus statement from the European Atherosclerosis Society Consensus Panel. *European Heart Journal*, *41*(24), 2313–2330. https://doi.org/10.1093/eurheartj/ehz962

Boyman, O., Comte, D., & Spertini, F. (2014). Adverse reactions to biologic agents and their medical management. *Nature Reviews. Rheumatology*, *10*(10), 612–627. https://doi.org/10.1038/nrrheum.2014.123

Brånén, L., Hovgaard, L., Nitulescu, M., Bengtsson, E., Nilsson, J., & Jovinge, S. (2004). Inhibition of tumor necrosis factor-alpha reduces atherosclerosis in apolipoprotein E knockout mice. *Arteriosclerosis, Thrombosis, and Vascular Biology*, *24*(11), 2137–2142. https://doi.org/10.1161/01.ATV.0000143933.20616.1b

Braunersreuther, V., Steffens, S., Arnaud, C., Pelli, G., Burger, F., Proudfoot, A., & Mach, F. (2008). A novel RANTES antagonist prevents progression of established atherosclerotic lesions in mice. *Arteriosclerosis, Thrombosis, and Vascular Biology*, *28*(6), 1090–1096. https://doi.org/10.1161/ATVBAHA.108.165423

Braunersreuther, V., Zernecke, A., Arnaud, C., Liehn, E. A., Steffens, S., Shagdarsuren, E., Bidzhekov, K., Burger, F., Pelli, G., Luckow, B., Mach, F., & Weber, C. (2007). Ccr5 but not Ccr1 deficiency reduces development of diet-induced atherosclerosis in mice. *Arteriosclerosis, Thrombosis, and Vascular Biology*, *27*(2), 373–379. https://doi.org/10.1161/01.ATV.0000253886.44609.ae

British Heart Foundation. (2022). *Global Heart & Circulatory Diseases Factsheet*.

Brzoska, T., Luger, T. A., Maaser, C., Abels, C., & Bohm, M. (2008). Alpha-melanocyte-stimulating hormone and related tripeptides: biochemistry, antiinflammatory and protective effects in vitro and in vivo, and future perspectives for the treatment of immune-mediated inflammatory diseases. *Endocrine Reviews*, *29*(5), 581–602. https://doi.org/10.1210/er.2007-0027

Butler, A. A., Kesterson, R. A., Khong, K., Cullen, M. J., Pelleymounter, M. A., Dekoning, J., Baetscher, M., & Cone, R. D. (2000). A unique metabolic syndrome causes obesity in the melanocortin-3 receptor-deficient mouse. *Endocrinology*, *141*(9), 3518–3521. https://doi.org/10.1210/endo.141.9.7791

Cai, M., & Hruby, V. J. (2016a). The Melanocortin Receptor System: A Target for Multiple Degenerative Diseases. *Current Protein & Peptide Science*, *17*(5), 488–496.

Cai, M., & Hruby, V. J. (2016b). Design of cyclized selective melanotropins. *Biopolymers*, *106*(6), 876–883. https://doi.org/10.1002/bip.22976

Carlin, L. M., Stamatiades, E. G., Auffray, C., Hanna, R. N., Glover, L., Vizcay-Barrena, G., Hedrick, C. C., Cook, H. T., Diebold, S., & Geissmann, F. (2013). Nr4a1-dependent Ly6C(low) monocytes monitor endothelial cells and orchestrate their disposal. *Cell*, *153*(2), 362–375. https://doi.org/10.1016/j.cell.2013.03.010

Catania, A., Gatti, S., Colombo, G., & Lipton, J. M. (2004). Targeting melanocortin receptors as a novel strategy to control inflammation. *Pharmacological Reviews*, *56*(1), 1–29. https://doi.org/10.1124/pr.56.1.1

Chistiakov, D. A., Grechko, A. V, Myasoedova, V. A., Melnichenko, A. A., & Orekhov, A. N. (2018). The role of monocytosis and neutrophilia in atherosclerosis. *Journal of Cellular and Molecular Medicine*, *22*(3), 1366–1382. https://doi.org/10.1111/jcmm.13462

Clark, A. J. L. (2016). 60 YEARS OF POMC: The proopiomelanocortin gene: discovery, deletion and disease. *Journal of Molecular Endocrinology*, *56*(4), T27-37. https://doi.org/10.1530/JME-15-0268

Clinicaltrial.gov. (n.d.). *Effect of Sarilumab on Atherosclerotic Disease Assessed by PET/CET in Patients With RA (SARIPET) - Full Text View - ClinicalTrials.gov*. Retrieved February 23, 2023, from https://clinicaltrials.gov/ct2/show/NCT04350216

Cole, J. E., Park, I., Ahern, D. J., Kassiteridi, C., Danso Abeam, D., Goddard, M. E., Green, P., Maffia, P., & Monaco, C. (2018). Immune cell census in murine atherosclerosis: cytometry by time of flight illuminates vascular myeloid cell diversity. *Cardiovascular Research*, *114*(10), 1360–1371. https://doi.org/10.1093/cvr/cvy109

Cone, R. D. (2005). Anatomy and regulation of the central melanocortin system. *Nature Neuroscience*, *8*(5), 571–578. https://doi.org/10.1038/nn1455

Conrad, N., Verbeke, G., Molenberghs, G., Goetschalckx, L., Callender, T., Cambridge, G., Mason, J. C., Rahimi, K., McMurray, J. J. V, & Verbakel, J. Y. (2022). Autoimmune diseases and cardiovascular risk: a population-based study on 19 autoimmune diseases and 12 cardiovascular diseases in 22 million individuals in the UK. *Lancet (London, England)*, *400*(10354), 733–743. https://doi.org/10.1016/S0140-6736(22)01349-6

Cooper, A., Robinson, S. J., Pickard, C., Jackson, C. L., Friedmann, P. S., & Healy, E. (2005). Alpha-melanocyte-stimulating hormone suppresses antigen-induced lymphocyte proliferation in humans independently of melanocortin 1 receptor gene status. *Journal of Immunology (Baltimore, Md. : 1950)*, *175*(7), 4806–4813.

D'Agostino, G., & Diano, S. (2010). Alpha-melanocyte stimulating hormone: production and degradation. *Journal of Molecular Medicine (Berlin, Germany)*, *88*(12), 1195–1201. https://doi.org/10.1007/s00109-010-0651-0

Dahlöf, B. (2010). Cardiovascular disease risk factors: epidemiology and risk assessment. *The American Journal of Cardiology*, *105*(1 Suppl), 3A-9A. https://doi.org/10.1016/j.amjcard.2009.10.007

Demidowich, A. P., Parikh, V. J., Dedhia, N., Branham, R. E., Madi, S. A., Marwitz, S. E., Roberson, R. B., Uhlman, A. J., Levi, N. J., Mi, S. J., Jun, J. Y., Broadney, M. M., Brady, S. M., & Yanovski, J. A. (2019). Associations of the melanocortin 3 receptor C17A + G241A haplotype with body composition and inflammation in African-American adults. *Annals of Human Genetics*, *83*(5), 355–360. https://doi.org/10.1111/ahg.12315

Deshmane, S. L., Kremlev, S., Amini, S., & Sawaya, B. E. (2009). Monocyte chemoattractant protein-1 (MCP-1): an overview. *Journal of Interferon & Cytokine Research : The Official Journal of the International Society for Interferon and Cytokine Research*, *29*(6), 313–326. https://doi.org/10.1089/jir.2008.0027

Diamantis, E., Kyriakos, G., Quiles-Sanchez, L. V., Farmaki, P., & Troupis, T. (2017). The Anti-Inflammatory Effects of Statins on Coronary Artery Disease: An Updated Review of the Literature. *Current Cardiology Reviews*, *13*(3), 209–216. https://doi.org/10.2174/1573403X13666170426104611

Diano, S. (2011). New aspects of melanocortin signaling: a role for PRCP in α-MSH degradation. *Frontiers in Neuroendocrinology*, *32*(1), 70–83. https://doi.org/10.1016/j.yfrne.2010.09.001

Dib, L., San-Jose, L. M., Ducrest, A.-L., Salamin, N., & Roulin, A. (2017). Selection on the Major Color Gene Melanocortin-1-Receptor Shaped the Evolution of the Melanocortin System Genes. *International Journal of Molecular Sciences*, *18*(12). https://doi.org/10.3390/ijms18122618

Dinparastisaleh, R., & Mirsaeidi, M. (2021). Antifibrotic and Anti-Inflammatory Actions of α-Melanocytic Hormone: New Roles for an Old Player. *Pharmaceuticals (Basel, Switzerland)*, *14*(1). https://doi.org/10.3390/ph14010045

Dong, Z. M., Chapman, S. M., Brown, A. A., Frenette, P. S., Hynes, R. O., & Wagner, D. D. (1998). The combined role of P- and E-selectins in atherosclerosis. *The Journal of Clinical Investigation*, *102*(1), 145–152. https://doi.org/10.1172/JCI3001

Dorr, R. T., Dvorakova, K., Brooks, C., Lines, R., Levine, N., Schram, K., Miketova, P., Hruby, V., & Alberts, D. S. (2000). Increased eumelanin expression and tanning is induced by a superpotent melanotropin [Nle4-D-Phe7]-alpha-MSH in humans. *Photochemistry and Photobiology*, *72*(4), 526–532. https://doi.org/10.1562/0031-8655(2000)072<0526:ieeati>2.0.co;2

Drechsler, M., Megens, R. T. A., van Zandvoort, M., Weber, C., & Soehnlein, O. (2010). Hyperlipidemia-triggered neutrophilia promotes early atherosclerosis. *Circulation*, *122*(18), 1837–1845. https://doi.org/10.1161/CIRCULATIONAHA.110.961714

Duewell, P., Kono, H., Rayner, K. J., Sirois, C. M., Vladimer, G., Bauernfeind, F. G., Abela, G. S., Franchi, L., Nuñez, G., Schnurr, M., Espevik, T., Lien, E., Fitzgerald, K. A., Rock, K. L., Moore, K. J., Wright, S. D., Hornung, V., & Latz, E. (2010). NLRP3 inflammasomes are required for atherogenesis and activated by cholesterol crystals. *Nature*, *464*(7293), 1357–1361. https://doi.org/10.1038/nature08938

Dutta, P., Courties, G., Wei, Y., Leuschner, F., Gorbatov, R., Robbins, C. S., Iwamoto, Y., Thompson, B., Carlson, A. L., Heidt, T., Majmudar, M. D., Lasitschka, F., Etzrodt, M., Waterman, P., Waring, M. T., Chicoine, A. T., van der Laan, A. M., Niessen, H. W. M., Piek, J. J., … Nahrendorf, M. (2012). Myocardial infarction accelerates atherosclerosis. *Nature*, *487*(7407), 325–329. https://doi.org/10.1038/nature11260

Ehtesham, S., Qasim, A., & Meyre, D. (2019). Loss-of-function mutations in the melanocortin-3 receptor gene confer risk for human obesity: A systematic review and meta-analysis. *Obesity Reviews : An Official Journal of the International Association for the Study of Obesity*, *20*(8), 1085–1092. https://doi.org/10.1111/obr.12864

Elhage, R., Maret, A., Pieraggi, M. T., Thiers, J. C., Arnal, J. F., & Bayard, F. (1998). Differential effects of interleukin-1 receptor antagonist and tumor necrosis factor binding protein on fatty-streak formation in apolipoprotein E-deficient mice. *Circulation*, *97*(3), 242–244. https://doi.org/10.1161/01.cir.97.3.242

Ericson, M. D., Lensing, C. J., Fleming, K. A., Schlasner, K. N., Doering, S. R., & Haskell-Luevano, C. (2017). Bench-top to clinical therapies: A review of melanocortin ligands from 1954 to 2016. *Biochimica et Biophysica Acta. Molecular Basis of Disease*, *1863*(10 Pt A), 2414–2435. https://doi.org/10.1016/j.bbadis.2017.03.020

Eves, P. C., MacNeil, S., & Haycock, J. W. (2006). alpha-Melanocyte stimulating hormone, inflammation and human melanoma. *Peptides*, *27*(2), 444–452. https://doi.org/10.1016/j.peptides.2005.01.027

Faggiotto, A., Ross, R., & Harker, L. (1984). Studies of hypercholesterolemia in the nonhuman primate. I. Changes that lead to fatty streak formation. *Arteriosclerosis (Dallas, Tex.)*, *4*(4), 323–340. https://doi.org/10.1161/01.atv.4.4.323

Farahi, L., Sinha, S. K., & Lusis, A. J. (2021). Roles of Macrophages in Atherogenesis. *Frontiers in Pharmacology*, *12*, 785220. https://doi.org/10.3389/fphar.2021.785220

Fernandez, D. M., Rahman, A. H., Fernandez, N. F., Chudnovskiy, A., Amir, E.-A. D., Amadori, L., Khan, N. S., Wong, C. K., Shamailova, R., Hill, C. A., Wang, Z., Remark, R., Li, J. R., Pina, C., Faries, C., Awad, A. J., Moss, N., Bjorkegren, J. L. M., Kim-Schulze, S., … Giannarelli, C. (2019). Single-cell immune landscape of human atherosclerotic plaques. *Nature Medicine*, *25*(10), 1576–1588. https://doi.org/10.1038/s41591-019-0590-4

Fredman, G., & Tabas, I. (2017). Boosting Inflammation Resolution in Atherosclerosis: The Next Frontier for Therapy. *The American Journal of Pathology*, *187*(6), 1211–1221. https://doi.org/10.1016/j.ajpath.2017.01.018

Fridmanis, D., Roga, A., & Klovins, J. (2017). ACTH Receptor (MC2R) Specificity: What Do We Know About Underlying Molecular Mechanisms? *Frontiers in Endocrinology*, *8*, 13. https://doi.org/10.3389/fendo.2017.00013

Fu, C., Chen, J., Lu, J., Yi, L., Tong, X., Kang, L., Pei, S., Ouyang, Y., Jiang, L., Ding, Y., Zhao, X., Li, S., Yang, Y., Huang, J., & Zeng, Q. (2020). Roles of inflammation factors in melanogenesis (Review). *Molecular Medicine Reports*, *21*(3), 1421–1430. https://doi.org/10.3892/mmr.2020.10950

Gallego-Colon, E., Daum, A., & Yosefy, C. (2020). Statins and PCSK9 inhibitors: A new lipid-lowering therapy. *European Journal of Pharmacology*, *878*, 173114. https://doi.org/10.1016/j.ejphar.2020.173114

Gantz, I., & Fong, T. M. (2003). The melanocortin system. *American Journal of Physiology. Endocrinology and Metabolism*, *284*(3), E468-74. https://doi.org/10.1152/ajpendo.00434.2002

Geissmann, F., Jung, S., & Littman, D. R. (2003). Blood monocytes consist of two principal subsets with distinct migratory properties. *Immunity*, *19*(1), 71–82. https://doi.org/10.1016/s1074-7613(03)00174-2

Gencer, S., Evans, B. R., van der Vorst, E. P. C., Döring, Y., & Weber, C. (2021). Inflammatory Chemokines in Atherosclerosis. *Cells*, *10*(2). https://doi.org/10.3390/cells10020226

Getting, S. J. (2006). Targeting melanocortin receptors as potential novel therapeutics. *Pharmacology & Therapeutics*, *111*(1), 1–15. https://doi.org/10.1016/j.pharmthera.2005.06.022

Getting, S. J., Christian, H. C., Flower, R. J., & Perretti, M. (2002). Activation of melanocortin type 3 receptor as a molecular mechanism for adrenocorticotropic hormone efficacy in gouty arthritis. *Arthritis and Rheumatism*, *46*(10), 2765–2775. https://doi.org/10.1002/art.10526

Getting, S. J., Lam, C. W., Chen, A. S., Grieco, P., & Perretti, M. (2006). Melanocortin 3 receptors control crystal-induced inflammation. *FASEB Journal : Official Publication of the Federation of American Societies for Experimental Biology*, *20*(13), 2234–2241. https://doi.org/10.1096/fj.06-6339com

Getting, S. J., Lam, C. W., Leoni, G., Gavins, F. N. E., Grieco, P., & Perretti, M. (2006). [D-Trp8]-gamma-melanocyte-stimulating hormone exhibits anti-inflammatory efficacy in mice bearing a nonfunctional MC1R (recessive yellow e/e mouse). *Molecular Pharmacology*, *70*(6), 1850–1855. https://doi.org/10.1124/mol.106.028878

Getting, S. J., Riffo-Vasquez, Y., Pitchford, S., Kaneva, M., Grieco, P., Page, C. P., Perretti, M., & Spina, D. (2008). A role for MC3R in modulating lung inflammation. *Pulmonary Pharmacology & Therapeutics*, *21*(6), 866–873. https://doi.org/10.1016/j.pupt.2008.09.004

Getz, G. S., & Reardon, C. A. (2016). Do the Apoe-/- and Ldlr-/- Mice Yield the Same Insight on Atherogenesis? *Arteriosclerosis, Thrombosis, and Vascular Biology*, *36*(9), 1734–1741. https://doi.org/10.1161/ATVBAHA.116.306874

Golforoush, P., Yellon, D. M., & Davidson, S. M. (2020). Mouse models of atherosclerosis and their suitability for the study of myocardial infarction. *Basic Research in Cardiology*, *115*(6), 73. https://doi.org/10.1007/s00395-020-00829-5

Gómez-SanMiguel, A. B., Villanúa, M. Á., Martín, A. I., & López-Calderón, A. (2016). D-TRP(8)-γMSH Prevents the Effects of Endotoxin in Rat Skeletal Muscle Cells through TNFα/NF-KB Signalling Pathway. *PloS One*, *11*(5), e0155645. https://doi.org/10.1371/journal.pone.0155645

Gonzalez-Rey, E., Chorny, A., & Delgado, M. (2007). Regulation of immune tolerance by anti-inflammatory neuropeptides. *Nature Reviews. Immunology*, *7*(1), 52–63. https://doi.org/10.1038/nri1984

Gonzalez-Rey, E., Chorny, A., Robledo, G., & Delgado, M. (2006). Cortistatin, a new antiinflammatory peptide with therapeutic effect on lethal endotoxemia. *The Journal of Experimental Medicine*, *203*(3), 563–571. https://doi.org/10.1084/jem.20052017

Gonzalez-Rey, E., Chorny, A., Varela, N., Robledo, G., & Delgado, M. (2006). Urocortin and adrenomedullin prevent lethal endotoxemia by down-regulating the inflammatory response. *The American Journal of Pathology*, *168*(6), 1921–1930. https://doi.org/10.2353/ajpath.2006.051104

Grieco, P., Balse, P. M., Weinberg, D., MacNeil, T., & Hruby, V. J. (2000). D-Amino acid scan of gamma-melanocyte-stimulating hormone: importance of Trp(8) on human MC3 receptor selectivity. *Journal of Medicinal Chemistry*, *43*(26), 4998–5002. https://doi.org/10.1021/jm000211e

Griffith, J. W., Sokol, C. L., & Luster, A. D. (2014). Chemokines and chemokine receptors: positioning cells for host defense and immunity. *Annual Review of Immunology*, *32*, 659–702. https://doi.org/10.1146/annurev-immunol-032713-120145

Hansson, G K, Holm, J., & Jonasson, L. (1989). Detection of activated T lymphocytes in the human atherosclerotic plaque. *The American Journal of Pathology*, *135*(1), 169–175.

Hansson, G K, Jonasson, L., Lojsthed, B., Stemme, S., Kocher, O., & Gabbiani, G. (1988). Localization of T lymphocytes and macrophages in fibrous and complicated human atherosclerotic plaques. *Atherosclerosis*, *72*(2–3), 135–141. https://doi.org/10.1016/0021-9150(88)90074-3

Hansson, Göran K. (2005). Inflammation, atherosclerosis, and coronary artery disease. *The New England Journal of Medicine*, *352*(16), 1685–1695. https://doi.org/10.1056/NEJMra043430

Hansson, Göran K, & Hermansson, A. (2011). The immune system in atherosclerosis. *Nature Immunology*, *12*(3), 204–212. https://doi.org/10.1038/ni.2001

Hansson, Göran K, & Libby, P. (2006). The immune response in atherosclerosis: a double-edged sword. *Nature Reviews. Immunology*, *6*(7), 508–519. https://doi.org/10.1038/nri1882

Harno, E., Gali Ramamoorthy, T., Coll, A. P., & White, A. (2018). POMC: The Physiological Power of Hormone Processing. *Physiological Reviews*, *98*(4), 2381–2430. https://doi.org/10.1152/physrev.00024.2017

Hartvigsen, K., Binder, C. J., Hansen, L. F., Rafia, A., Juliano, J., Hörkkö, S., Steinberg, D., Palinski, W., Witztum, J. L., & Li, A. C. (2007). A diet-induced hypercholesterolemic murine model to study atherogenesis without obesity and metabolic syndrome. *Arteriosclerosis, Thrombosis, and Vascular Biology*, *27*(4), 878–885. https://doi.org/10.1161/01.ATV.0000258790.35810.02

Hassan, M. O., Duarte, R., Dickens, C., Dix-Peek, T., Naidoo, S., Vachiat, A., Grinter, S., Manga, P., & Naicker, S. (2020). Interleukin-6 gene polymorhisms and interleukin-6 levels are associated with atherosclerosis in CKD patients. *Clinical Nephrology*, *93*(1), 82–86. https://doi.org/10.5414/CNP92S114

Herraiz, C., Martínez-Vicente, I., & Maresca, V. (2021). The α-melanocyte-stimulating hormone/melanocortin-1 receptor interaction: A driver of pleiotropic effects beyond pigmentation. *Pigment Cell & Melanoma Research*, *34*(4), 748–761. https://doi.org/10.1111/pcmr.12980

Hilgendorf, I., Swirski, F. K., & Robbins, C. S. (2015). Monocyte fate in atherosclerosis. *Arteriosclerosis, Thrombosis, and Vascular Biology*, *35*(2), 272–279. https://doi.org/10.1161/ATVBAHA.114.303565

Hilgendorf, I., Theurl, I., Gerhardt, L. M. S., Robbins, C. S., Weber, G. F., Gonen, A., Iwamoto, Y., Degousee, N., Holderried, T. A. W., Winter, C., Zirlik, A., Lin, H. Y., Sukhova, G. K., Butany, J., Rubin, B. B., Witztum, J. L., Libby, P., Nahrendorf, M., Weissleder, R., & Swirski, F. K. (2014). Innate response activator B cells aggravate atherosclerosis by stimulating T helper-1 adaptive immunity. *Circulation*, *129*(16), 1677–1687. https://doi.org/10.1161/CIRCULATIONAHA.113.006381

Holloway, P. M., Durrenberger, P. F., Trutschl, M., Cvek, U., Cooper, D., Orr, A. W., Perretti, M., Getting, S. J., & Gavins, F. N. E. (2015). Both MC1 and MC3 Receptors Provide Protection From Cerebral Ischemia-Reperfusion-Induced Neutrophil Recruitment. *Arteriosclerosis, Thrombosis, and Vascular Biology*, *35*(9), 1936–1944. https://doi.org/10.1161/ATVBAHA.115.305348

Hopper, S. E., Cuomo, F., Ferruzzi, J., Burris, N. S., Roccabianca, S., Humphrey, J. D., & Figueroa, C. A. (2021). Comparative Study of Human and Murine Aortic Biomechanics and Hemodynamics in Vascular Aging. *Frontiers in Physiology*, *12*, 746796. https://doi.org/10.3389/fphys.2021.746796

Hoseini, Z., Sepahvand, F., Rashidi, B., Sahebkar, A., Masoudifar, A., & Mirzaei, H. (2018). NLRP3 inflammasome: Its regulation and involvement in atherosclerosis. *Journal of Cellular Physiology*, *233*(3), 2116–2132. https://doi.org/10.1002/jcp.25930

Humphreys, M. H. (2004). Gamma-MSH, sodium metabolism, and salt-sensitive hypertension. *American Journal of Physiology. Regulatory, Integrative and Comparative Physiology*, *286*(3), R417-30. https://doi.org/10.1152/ajpregu.00365.2003

Ignar, D. M., Andrews, J. L., Jansen, M., Eilert, M. M., Pink, H. M., Lin, P., Sherrill, R. G., Szewczyk, J. R., & Conway, J. G. (2003). Regulation of TNF-alpha secretion by a specific melanocortin-1 receptor peptide agonist. *Peptides*, *24*(5), 709–716. https://doi.org/10.1016/s0196-9781(03)00127-x

Jagavelu, K., Tietge, U. J. F., Gaestel, M., Drexler, H., Schieffer, B., & Bavendiek, U. (2007). Systemic deficiency of the MAP kinase-activated protein kinase 2 reduces atherosclerosis in hypercholesterolemic mice. *Circulation Research*, *101*(11), 1104–1112. https://doi.org/10.1161/CIRCRESAHA.107.156075

Jakubzick, C., Gautier, E. L., Gibbings, S. L., Sojka, D. K., Schlitzer, A., Johnson, T. E., Ivanov, S., Duan, Q., Bala, S., Condon, T., van Rooijen, N., Grainger, J. R., Belkaid, Y., Ma'ayan, A., Riches, D. W. H., Yokoyama, W. M., Ginhoux, F., Henson, P. M., & Randolph, G. J. (2013). Minimal differentiation of classical monocytes as they survey steady-state tissues and transport antigen to lymph nodes. *Immunity*, *39*(3), 599–610. https://doi.org/10.1016/j.immuni.2013.08.007

Jebari-Benslaiman, S., Galicia-García, U., Larrea-Sebal, A., Olaetxea, J. R., Alloza, I., Vandenbroeck, K., Benito-Vicente, A., & Martín, C. (2022). Pathophysiology of Atherosclerosis. *International Journal of Molecular Sciences*, *23*(6). https://doi.org/10.3390/ijms23063346

Ji, L.-Q., Hong, Y., & Tao, Y.-X. (2022). Melanocortin-5 Receptor: Pharmacology and Its Regulation of Energy Metabolism. *International Journal of Molecular Sciences*, *23*(15). https://doi.org/10.3390/ijms23158727

Jia, L., Betters, J. L., & Yu, L. (2011). Niemann-pick C1-like 1 (NPC1L1) protein in intestinal and hepatic cholesterol transport. *Annual Review of Physiology*, *73*, 239–259. https://doi.org/10.1146/annurev-physiol-012110-142233

Jonasson, L., Holm, J., Skalli, O., Bondjers, G., & Hansson, G. K. (1986). Regional accumulations of T cells, macrophages, and smooth muscle cells in the human atherosclerotic plaque. *Arteriosclerosis (Dallas, Tex.)*, *6*(2), 131–138. https://doi.org/10.1161/01.atv.6.2.131

Jonasson, L., Holm, J., Skalli, O., Gabbiani, G., & Hansson, G. K. (1985). Expression of class II transplantation antigen on vascular smooth muscle cells in human atherosclerosis. *The Journal of Clinical Investigation*, *76*(1), 125–131. https://doi.org/10.1172/JCI111934

Joseph, C. G., Yao, H., Scott, J. W., Sorensen, N. B., Marnane, R. N., Mountjoy, K. G., & Haskell-Luevano, C. (2010). γ_2-Melanocyte stimulation hormone (γ_2-MSH) truncation studies results in the cautionary note that γ_2-MSH is not selective for the mouse MC3R over the mouse MC5R. *Peptides*, *31*(12), 2304–2313. https://doi.org/10.1016/j.peptides.2010.08.025

Kadekaro, A. L., Wakamatsu, K., Ito, S., & Abdel-Malek, Z. A. (2006). Cutaneous photoprotection and melanoma susceptibility: reaching beyond melanin content to the frontiers of DNA repair. *Frontiers in Bioscience : A Journal and Virtual Library*, *11*, 2157–2173. https://doi.org/10.2741/1958

Kalden, D. H., Scholzen, T., Brzoska, T., & Luger, T. A. (1999). Mechanisms of the antiinflammatory effects of alpha-MSH. Role of transcription factor NF-kappa B and adhesion molecule expression. *Annals of the New York Academy of Sciences*, *885*, 254–261.

Kaneva, M. K. (2011). *Magdalena Krasimirova Kaneva Investigation into the immuno-therapeutic*.

Kannengiesser, K., Maaser, C., Heidemann, J., Luegering, A., Ross, M., Brzoska, T., Bohm, M., Luger, T. A., Domschke, W., & Kucharzik, T. (2008). Melanocortin-derived tripeptide KPV has anti-inflammatory potential in murine models of inflammatory bowel disease. *Inflammatory Bowel Diseases*, *14*(3), 324–331. https://doi.org/10.1002/ibd.20334

Kenneth R. Feingold. (2000). *Introduction to Lipids and Lipoproteins* (et al. Feingold KR, Anawalt B, Boyce A (ed.)). Endotext.

Kim, K.-W., Ivanov, S., & Williams, J. W. (2020). Monocyte Recruitment, Specification, and Function in Atherosclerosis. *Cells*, *10*(1). https://doi.org/10.3390/cells10010015

Kirii, H., Niwa, T., Yamada, Y., Wada, H., Saito, K., Iwakura, Y., Asano, M., Moriwaki, H., & Seishima, M. (2003). Lack of interleukin-1beta decreases the severity of atherosclerosis in ApoE-deficient mice. *Arteriosclerosis, Thrombosis, and Vascular Biology*, *23*(4), 656–660. https://doi.org/10.1161/01.ATV.0000064374.15232.C3

Koenen, R. R., von Hundelshausen, P., Nesmelova, I. V, Zernecke, A., Liehn, E. A., Sarabi, A., Kramp, B. K., Piccinini, A. M., Paludan, S. R., Kowalska, M. A., Kungl, A. J., Hackeng, T. M., Mayo, K. H., & Weber, C. (2009). Disrupting functional interactions between platelet chemokines inhibits atherosclerosis in hyperlipidemic mice. *Nature Medicine*, *15*(1), 97–103. https://doi.org/10.1038/nm.1898

Koushki, K., Shahbaz, S. K., Mashayekhi, K., Sadeghi, M., Zayeri, Z. D., Taba, M. Y., Banach, M., Al-Rasadi, K., Johnston, T. P., & Sahebkar, A. (2021). Anti-inflammatory Action of Statins in Cardiovascular Disease: the Role of Inflammasome and Toll-Like Receptor Pathways. *Clinical Reviews in Allergy & Immunology*, *60*(2), 175–199. https://doi.org/10.1007/s12016-020-08791-9

Krohn, R., Raffetseder, U., Bot, I., Zernecke, A., Shagdarsuren, E., Liehn, E. A., van Santbrink, P. J., Nelson, P. J., Biessen, E. A., Mertens, P. R., & Weber, C. (2007). Y-box binding protein-1 controls CC chemokine ligand-5 (CCL5) expression in smooth muscle cells and contributes to neointima formation in atherosclerosis-prone mice. *Circulation*, *116*(16), 1812–1820. https://doi.org/10.1161/CIRCULATIONAHA.107.708016

Kumar, A., Bhandari, A., Sinha, R., Goyal, P., & Grapputo, A. (2011). Spliceosomal intron insertions in genome compacted ray-finned fishes as evident from phylogeny of MC receptors, also supported by a few other GPCRs. *PloS One*, *6*(8), e22046. https://doi.org/10.1371/journal.pone.0022046

Lam, C. W., Getting, S. J., & Perretti, M. (2005). In vitro and in vivo induction of heme oxygenase 1 in mouse macrophages following melanocortin receptor activation. *Journal of Immunology (Baltimore, Md. : 1950)*, *174*(4), 2297–2304. https://doi.org/10.4049/jimmunol.174.4.2297

Lam, C. W., Perretti, M., & Getting, S. J. (2006). Melanocortin receptor signaling in RAW264.7 macrophage cell line. *Peptides*, *27*(2), 404–412. https://doi.org/10.1016/j.peptides.2005.01.031

Lee, Y. S., Challis, B. G., Thompson, D. A., Yeo, G. S. H., Keogh, J. M., Madonna, M. E., Wraight, V., Sims, M., Vatin, V., Meyre, D., Shield, J., Burren, C., Ibrahim, Z., Cheetham, T., Swift, P., Blackwood, A., Hung, C.-C. C., Wareham, N. J., Froguel, P., … Farooqi, I. S. (2006). A POMC variant implicates beta-melanocyte-stimulating hormone in the control of human energy balance. *Cell Metabolism*, *3*(2), 135–140. https://doi.org/10.1016/j.cmet.2006.01.006

Leoni, G., Patel, H. B., Sampaio, A. L. F., Gavins, F. N. E., Murray, J. F., Grieco, P., Getting, S. J., & Perretti, M. (2008). Inflamed phenotype of the mesenteric microcirculation of melanocortin type 3 receptor-null mice after ischemia-reperfusion. *FASEB Journal : Official Publication of the Federation of American Societies for Experimental Biology*, *22*(12), 4228–4238. https://doi.org/10.1096/fj.08-113886

Libby, P, Ordovas, J. M., Auger, K. R., Robbins, A. H., Birinyi, L. K., & Dinarello, C. A. (1986). Endotoxin and tumor necrosis factor induce interleukin-1 gene expression in adult human vascular endothelial cells. *The American Journal of Pathology*, *124*(2), 179–185.

Libby, Peter. (2015). Triglycerides on the rise: should we swap seats on the seesaw? *European Heart Journal*, *36*(13), 774–776. https://doi.org/10.1093/eurheartj/ehu500

Libby, Peter. (2021). The changing landscape of atherosclerosis. *Nature*, *592*(7855), 524–533. https://doi.org/10.1038/s41586-021-03392-8

Lin, P., Ji, H.-H., Li, Y.-J., & Guo, S.-D. (2021). Macrophage Plasticity and Atherosclerosis Therapy. *Frontiers in Molecular Biosciences*, *8*, 679797. https://doi.org/10.3389/fmolb.2021.679797

Linton, M. F., Atkinson, J. B., & Fazio, S. (1995). Prevention of atherosclerosis in apolipoprotein E-deficient mice by bone marrow transplantation. *Science (New York, N.Y.)*, *267*(5200), 1034–1037. https://doi.org/10.1126/science.7863332

Lipton, B. A., Parthasarathy, S., Ord, V. A., Clinton, S. K., Libby, P., & Rosenfeld, M. E. (1995). Components of the protein fraction of oxidized low density lipoprotein stimulate interleukin-1 alpha production by rabbit arterial macrophage-derived foam cells. *Journal of Lipid Research*, *36*(10), 2232–2242.

Liu, T., Zhang, L., Joo, D., & Sun, S.-C. (2017). NF-κB signaling in inflammation. *Signal Transduction and Targeted Therapy*, *2*, 17023-. https://doi.org/10.1038/sigtrans.2017.23

Lloyd-Jones, D. M. (2010). Cardiovascular risk prediction: basic concepts, current status, and future directions. *Circulation*, *121*(15), 1768–1777. https://doi.org/10.1161/CIRCULATIONAHA.109.849166

Loser, K., Brzoska, T., Oji, V., Auriemma, M., Voskort, M., Kupas, V., Klenner, L., Mensing, C., Hauschild, A., Beissert, S., & Luger, T. A. (2010). The neuropeptide alpha-melanocyte-stimulating hormone is critically involved in the development of cytotoxic CD8+ T cells in mice and humans. *PloS One*, *5*(2), e8958. https://doi.org/10.1371/journal.pone.0008958

Louis, S. F., & Zahradka, P. (2010). Vascular smooth muscle cell motility: From migration to invasion. *Experimental and Clinical Cardiology*, *15*(4), e75-85.

Luger, T. A., Scholzen, T. E., Brzoska, T., & Böhm, M. (2003). New insights into the functions of alpha-MSH and related peptides in the immune system. *Annals of the New York Academy of Sciences*, *994*, 133–140. https://doi.org/10.1111/j.1749-6632.2003.tb03172.x

Luo, J., Yang, H., & Song, B.-L. (2020). Mechanisms and regulation of cholesterol homeostasis. *Nature Reviews. Molecular Cell Biology*, *21*(4), 225–245. https://doi.org/10.1038/s41580-019-0190-7

Maaser, C., Kannengiesser, K., Specht, C., Lügering, A., Brzoska, T., Luger, T. A., Domschke, W., & Kucharzik, T. (2006). Crucial role of the melanocortin receptor MC1R in experimental colitis. *Gut*, *55*(10), 1415–1422. https://doi.org/10.1136/gut.2005.083634

Mach, F., Baigent, C., Catapano, A. L., Koskinas, K. C., Casula, M., Badimon, L., Chapman, M. J., De Backer, G. G., Delgado, V., Ference, B. A., Graham, I. M., Halliday, A., Landmesser, U., Mihaylova, B., Pedersen, T. R., Riccardi, G., Richter, D. J., Sabatine, M. S., Taskinen, M.-R., … Wiklund, O. (2020). 2019 ESC/EAS Guidelines for the management of dyslipidaemias: lipid modification to reduce cardiovascular risk. *European Heart Journal*, *41*(1), 111–188. https://doi.org/10.1093/eurheartj/ehz455

Major, A. S., Fazio, S., & Linton, M. F. (2002). B-lymphocyte deficiency increases atherosclerosis in LDL receptor-null mice. *Arteriosclerosis, Thrombosis, and Vascular Biology*, *22*(11), 1892–1898. https://doi.org/10.1161/01.atv.0000039169.47943.ee

Markham, A. (2021). Setmelanotide: First Approval. *Drugs*, *81*(3), 397–403. https://doi.org/10.1007/s40265-021-01470-9

Masana, L., Ibarretxe, D., & Plana, N. (2020). Reasons Why Combination Therapy Should Be the New Standard of Care to Achieve the LDL-Cholesterol Targets : Lipid-lowering combination therapy. *Current Cardiology Reports*, *22*(8), 66. https://doi.org/10.1007/s11886-020-01326-w

Maurya, M., Munshi, R., & Zambre, S. (2022). Melanocortin receptors: emerging targets for the treatment of pigmentation, inflammation, stress, weight disorders and sexual dysfunction. *Current Drug Targets*. https://doi.org/10.2174/1389450124666221108143006

Mohammed, I., Haris, B., & Hussain, K. (2022). A Novel Homozygous MC2R Variant Leading to Type-1 Familial Glucocorticoid Deficiency. *Journal of the Endocrine Society*, *6*(6), bvac058. https://doi.org/10.1210/jendso/bvac058

Møller, C. L., Pedersen, S. B., Richelsen, B., Conde-Frieboes, K. W., Raun, K., Grove, K. L., & Wulff, B. S. (2015). Melanocortin agonists stimulate lipolysis in human adipose tissue explants but not in adipocytes. *BMC Research Notes*, *8*, 559. https://doi.org/10.1186/s13104-015-1539-4

Møller, C. L., Raun, K., Jacobsen, M. L., Pedersen, T. Å., Holst, B., Conde-Frieboes, K. W., & Wulff, B. S. (2011). Characterization of murine melanocortin receptors mediating adipocyte lipolysis and examination of signalling pathways involved. *Molecular and Cellular Endocrinology*, *341*(1–2), 9–17. https://doi.org/10.1016/j.mce.2011.03.010

Montero-Melendez, T., Boesen, T., & Jonassen, T. E. N. (2022). Translational advances of melanocortin drugs: Integrating biology, chemistry and genetics. *Seminars in Immunology*, *59*, 101603. https://doi.org/10.1016/j.smim.2022.101603

Montero-Melendez, T., Patel, H. B., Seed, M., Nielsen, S., Jonassen, T. E. N., & Perretti, M. (2011). The melanocortin agonist AP214 exerts anti-inflammatory and proresolving properties. *The American Journal of Pathology*, *179*(1), 259–269. https://doi.org/10.1016/j.ajpath.2011.03.042

Moore, K. J., Koplev, S., Fisher, E. A., Tabas, I., Björkegren, J. L. M., Doran, A. C., & Kovacic, J. C. (2018). Macrophage Trafficking, Inflammatory Resolution, and Genomics in Atherosclerosis: JACC Macrophage in CVD Series (Part 2). *Journal of the American College of Cardiology*, *72*(18), 2181–2197. https://doi.org/10.1016/j.jacc.2018.08.2147

Mountjoy, K. G., Robbins, L. S., Mortrud, M. T., & Cone, R. D. (1992). The cloning of a family of genes that encode the melanocortin receptors. *Science (New York, N.Y.)*, *257*(5074), 1248–1251. https://doi.org/10.1126/science.1325670

Mumtaz, S., Behera, S., & Mukhopadhyay, K. (2020). Lipidated Short Analogue of α-Melanocyte Stimulating Hormone Exerts Bactericidal Activity against the Stationary Phase of Methicillin-Resistant Staphylococcus aureus and Inhibits Biofilm Formation. *ACS Omega*, *5*(44), 28425–28440. https://doi.org/10.1021/acsomega.0c01462

Mundi, S., Massaro, M., Scoditti, E., Carluccio, M. A., van Hinsbergh, V. W. M., Iruela-Arispe, M. L., & De Caterina, R. (2018). Endothelial permeability, LDL deposition, and cardiovascular risk factors-a review. *Cardiovascular Research*, *114*(1), 35–52. https://doi.org/10.1093/cvr/cvx226

Murphy, A. J., Akhtari, M., Tolani, S., Pagler, T., Bijl, N., Kuo, C.-L., Wang, M., Sanson, M., Abramowicz, S., Welch, C., Bochem, A. E., Kuivenhoven, J. A., Yvan-Charvet, L., & Tall, A. R. (2011). ApoE regulates hematopoietic stem cell proliferation, monocytosis, and monocyte accumulation in atherosclerotic lesions in mice. *The Journal of Clinical Investigation*, *121*(10), 4138–4149. https://doi.org/10.1172/JCI57559

Murphy, A. J., & Tall, A. R. (2016). Disordered haematopoiesis and athero-thrombosis. *European Heart Journal*, *37*(14), 1113–1121. https://doi.org/10.1093/eurheartj/ehv718

Mykicki, N., Klenner, L., Baumann, C., Auriemma, M., Sternemann, C., Soeberdt, M., Elliott, G. R., Abels, C., Luger, T. A., & Loser, K. (2017). The tripeptide KdPT ameliorates ongoing psoriasis-like skin inflammation in murine and human skin. *Experimental Dermatology*, *26*(4), 328–334. https://doi.org/10.1111/exd.13145

Nakanishi, S., Inoue, A., Kita, T., Nakamura, M., Chang, A. C., Cohen, S. N., & Numa, S. (1979). Nucleotide sequence of cloned cDNA for bovine corticotropin-beta-lipotropin precursor. *Nature*, *278*(5703), 423–427. https://doi.org/10.1038/278423a0

Namjou, B., Stanaway, I. B., Lingren, T., Mentch, F. D., Benoit, B., Dikilitas, O., Niu, X., Shang, N., Shoemaker, A. H., Carey, D. J., Mirshahi, T., Singh, R., Nestor, J. G., Hakonarson, H., Denny, J. C., Crosslin, D. R., Jarvik, G. P., Kullo, I. J., Williams, M. S., & Harley, J. B. (2021). Evaluation of the MC4R gene across eMERGE network identifies many unreported obesity-associated variants. *International Journal of Obesity (2005)*, *45*(1), 155–169. https://doi.org/10.1038/s41366-020-00675-4

Nehring, S. M., Goyal, A., & Patel, B. C. (2022). *C Reactive Protein.*

Nicholls, S. J., Kastelein, J. J. P., Schwartz, G. G., Bash, D., Rosenson, R. S., Cavender, M. A., Brennan, D. M., Koenig, W., Jukema, J. W., Nambi, V., Wright, R. S., Menon, V., Lincoff, A. M., & Nissen, S. E. (2014). Varespladib and cardiovascular events in patients with an acute coronary syndrome: the VISTA-16 randomized clinical trial. *JAMA*, *311*(3), 252–262. https://doi.org/10.1001/jama.2013.282836

Nidorf, S. M., Fiolet, A. T. L., Mosterd, A., Eikelboom, J. W., Schut, A., Opstal, T. S. J., The, S. H. K., Xu, X.-F., Ireland, M. A., Lenderink, T., Latchem, D., Hoogslag, P., Jerzewski, A., Nierop, P., Whelan, A., Hendriks, R., Swart, H., Schaap, J., Kuijper, A. F. M., … Thompson, P. L. (2020). Colchicine in Patients with Chronic Coronary Disease. *The New England Journal of Medicine*, *383*(19), 1838–1847. https://doi.org/10.1056/NEJMoa2021372

Nix, M. A., Kaelin, C. B., Ta, T., Weis, A., Morton, G. J., Barsh, G. S., & Millhauser, G. L. (2013). Molecular and functional analysis of human β-defensin 3 action at melanocortin receptors. *Chemistry & Biology*, *20*(6), 784–795. https://doi.org/10.1016/j.chembiol.2013.04.015

Nus, M., Sage, A. P., Lu, Y., Masters, L., Lam, B. Y. H., Newland, S., Weller, S., Tsiantoulas, D., Raffort, J., Marcus, D., Finigan, A., Kitt, L., Figg, N., Schirmbeck, R., Kneilling, M., Yeo, G. S. H., Binder, C. J., de la Pompa, J. L., & Mallat, Z. (2017). Marginal zone B cells control the response of follicular helper T cells to a high-cholesterol diet. *Nature Medicine*, *23*(5), 601–610. https://doi.org/10.1038/nm.4315

Nuutinen, S., Ailanen, L., Savontaus, E., & Rinne, P. (2018). Melanocortin overexpression limits diet-induced inflammation and atherosclerosis in LDLR-/-mice. *The Journal of Endocrinology*, *236*(3), 111–123. https://doi.org/10.1530/JOE-17-0636

O'Donoghue, M. L., Braunwald, E., White, H. D., Lukas, M. A., Tarka, E., Steg, P. G., Hochman, J. S., Bode, C., Maggioni, A. P., Im, K., Shannon, J. B., Davies, R. Y., Murphy, S. A., Crugnale, S. E., Wiviott, S. D., Bonaca, M. P., Watson, D. F., Weaver, W. D., Serruys, P. W., … Steen, D. L. (2014). Effect of darapladib on major coronary events after an acute coronary syndrome: the SOLID-TIMI 52 randomized clinical trial. *JAMA*, *312*(10), 1006–1015. https://doi.org/10.1001/jama.2014.11061

Oesterle, A., Laufs, U., & Liao, J. K. (2017). Pleiotropic Effects of Statins on the Cardiovascular System. *Circulation Research*, *120*(1), 229–243. https://doi.org/10.1161/CIRCRESAHA.116.308537

Okyay, K. (2021). Pleiotropic effects of statins: New evidences. In *Turk Kardiyoloji Dernegi arsivi : Turk Kardiyoloji Derneginin yayin organidir* (Vol. 49, Issue 7, pp. 533–535). https://doi.org/10.5543/tkda.2021.21211

Öörni, K., & Kovanen, P. T. (2021). Aggregation Susceptibility of Low-Density Lipoproteins-A Novel Modifiable Biomarker of Cardiovascular Risk. *Journal of Clinical Medicine*, *10*(8). https://doi.org/10.3390/jcm10081769

Öörni, K., Lehti, S., Sjövall, P., & Kovanen, P. T. (2019). Triglyceride-Rich Lipoproteins as a Source of Proinflammatory Lipids in the Arterial Wall. *Current Medicinal Chemistry*, *26*(9), 1701–1710. https://doi.org/10.2174/0929867325666180530094819

Oppi, S., Lüscher, T. F., & Stein, S. (2019). Mouse Models for Atherosclerosis Research-Which Is My Line? *Frontiers in Cardiovascular Medicine*, *6*, 46. https://doi.org/10.3389/fcvm.2019.00046

Patel, H. B., Bombardieri, M., Sampaio, A. L. F., D'Acquisto, F., Gray, M., Grieco, P., Getting, S. J., Pitzalis, C., & Perretti, M. (2010). Anti-inflammatory and antiosteoclastogenesis properties of endogenous melanocortin receptor type 3 in experimental arthritis. *FASEB Journal : Official Publication of the Federation of American Societies for Experimental Biology*, *24*(12), 4835–4843. https://doi.org/10.1096/fj.10-167759

Patel, H. B., Montero-Melendez, T., Greco, K. V, & Perretti, M. (2011). Melanocortin receptors as novel effectors of macrophage responses in inflammation. *Frontiers in Immunology*, *2*, 41. https://doi.org/10.3389/fimmu.2011.00041

Pattarabanjird, T., Li, C., & McNamara, C. (2021). B Cells in Atherosclerosis: Mechanisms and Potential Clinical Applications. *JACC. Basic to Translational Science*, *6*(6), 546–563. https://doi.org/10.1016/j.jacbts.2021.01.006

Plump, A. S., & Breslow, J. L. (1995). Apolipoprotein E and the apolipoprotein E-deficient mouse. *Annual Review of Nutrition*, *15*, 495–518. https://doi.org/10.1146/annurev.nu.15.070195.002431

Plump, A. S., Smith, J. D., Hayek, T., Aalto-Setälä, K., Walsh, A., Verstuyft, J. G., Rubin, E. M., & Breslow, J. L. (1992). Severe hypercholesterolemia and atherosclerosis in apolipoprotein E-deficient mice created by homologous recombination in ES cells. *Cell*, *71*(2), 343–353. https://doi.org/10.1016/0092-8674(92)90362-g

Poznyak, A. V, Silaeva, Y. Y., Orekhov, A. N., & Deykin, A. V. (2020). Animal models of human atherosclerosis: current progress. *Brazilian Journal of Medical and Biological Research = Revista Brasileira de Pesquisas Medicas e Biologicas*, *53*(6), e9557. https://doi.org/10.1590/1414-431x20209557

Rajamäki, K., Lappalainen, J., Oörni, K., Välimäki, E., Matikainen, S., Kovanen, P. T., & Eklund, K. K. (2010). Cholesterol crystals activate the NLRP3 inflammasome in human macrophages: a novel link between cholesterol metabolism and inflammation. *PloS One*, *5*(7), e11765. https://doi.org/10.1371/journal.pone.0011765

Rattik, S., Hultman, K., Rauch, U., Söderberg, I., Sundius, L., Ljungcrantz, I., Hultgårdh-Nilsson, A., Wigren, M., Björkbacka, H., Fredrikson, G. N., & Nilsson, J. (2015). IL-22 affects smooth muscle cell phenotype and plaque formation in apolipoprotein E knockout mice. *Atherosclerosis*, *242*(2), 506–514. https://doi.org/10.1016/j.atherosclerosis.2015.08.006

Reardon, C. A., Blachowicz, L., White, T., Cabana, V., Wang, Y., Lukens, J., Bluestone, J., & Getz, G. S. (2001). Effect of immune deficiency on lipoproteins and atherosclerosis in male apolipoprotein E-deficient mice. *Arteriosclerosis, Thrombosis, and Vascular Biology*, *21*(6), 1011–1016. https://doi.org/10.1161/01.atv.21.6.1011

Rennalls, L. P., Seidl, T., Larkin, J. M. G., Wellbrock, C., Gore, M. E., Eisen, T., & Bruno, L. (2010). The melanocortin receptor agonist NDP-MSH impairs the allostimulatory function of dendritic cells. *Immunology*, *129*(4), 610–619. https://doi.org/10.1111/j.1365-2567.2009.03210.x

Renquist, B. J., Lippert, R. N., Sebag, J. A., Ellacott, K. L. J., & Cone, R. D. (2011). Physiological roles of the melanocortin MC(3) receptor. *European Journal of Pharmacology*, *660*(1), 13–20. https://doi.org/10.1016/j.ejphar.2010.12.025

Ridker, P M, Hennekens, C. H., Buring, J. E., & Rifai, N. (2000). C-reactive protein and other markers of inflammation in the prediction of cardiovascular disease in women. *The New England Journal of Medicine*, *342*(12), 836–843. https://doi.org/10.1056/NEJM200003233421202

Ridker, Paul M, Everett, B. M., Pradhan, A., MacFadyen, J. G., Solomon, D. H., Zaharris, E., Mam, V., Hasan, A., Rosenberg, Y., Iturriaga, E., Gupta, M., Tsigoulis, M., Verma, S., Clearfield, M., Libby, P., Goldhaber, S. Z., Seagle, R., Ofori, C., Saklayen, M., … Glynn, R. J. (2019). Low-Dose Methotrexate for the Prevention of Atherosclerotic Events. *The New England Journal of Medicine*, *380*(8), 752–762. https://doi.org/10.1056/NEJMoa1809798

Ridker, Paul M, Everett, B. M., Thuren, T., MacFadyen, J. G., Chang, W. H., Ballantyne, C., Fonseca, F., Nicolau, J., Koenig, W., Anker, S. D., Kastelein, J. J. P., Cornel, J. H., Pais, P., Pella, D., Genest, J., Cifkova, R., Lorenzatti, A., Forster, T., Kobalava, Z., … Glynn, R. J. (2017). Antiinflammatory Therapy with Canakinumab for Atherosclerotic Disease. *The New England Journal of Medicine*, *377*(12), 1119–1131. https://doi.org/10.1056/NEJMoa1707914

Ridker, Paul M, & Lüscher, T. F. (2014). Anti-inflammatory therapies for cardiovascular disease. *European Heart Journal*, *35*(27), 1782–1791. https://doi.org/10.1093/eurheartj/ehu203

Rinne, P., Ahola-Olli, A., Nuutinen, S., Koskinen, E., Kaipio, K., Eerola, K., Juonala, M., Kahonen, M., Lehtimaki, T., Raitakari, O. T., & Savontaus, E. (2015). Deficiency in Melanocortin 1 Receptor Signaling Predisposes to Vascular Endothelial Dysfunction and Increased Arterial Stiffness in Mice and Humans. *Arteriosclerosis, Thrombosis, and Vascular Biology*, *35*(7), 1678–1686. https://doi.org/10.1161/ATVBAHA.114.305064

Rinne, P., Nordlund, W., Heinonen, I., Penttinen, A.-M., Saraste, A., Ruohonen, S. T., Mäkelä, S., Vähätalo, L., Kaipio, K., Cai, M., Hruby, V. J., Ruohonen, S., & Savontaus, E. (2013). α-Melanocyte-stimulating hormone regulates vascular NO availability and protects against endothelial dysfunction. *Cardiovascular Research*, *97*(2), 360–368. https://doi.org/10.1093/cvr/cvs335

Rinne, P., Rami, M., Nuutinen, S., Santovito, D., van der Vorst, E. P. C., Guillamat-Prats, R., Lyytikäinen, L.-P., Raitoharju, E., Oksala, N., Ring, L., Cai, M., Hruby, V. J., Lehtimäki, T., Weber, C., & Steffens, S. (2017). Melanocortin 1 Receptor Signaling Regulates Cholesterol Transport in Macrophages. *Circulation*, *136*(1), 83–97. https://doi.org/10.1161/CIRCULATIONAHA.116.025889

Rinne, P., Silvola, J. M. U., Hellberg, S., Ståhle, M., Liljenbäck, H., Salomäki, H., Koskinen, E., Nuutinen, S., Saukko, P., Knuuti, J., Saraste, A., Roivainen, A., & Savontaus, E. (2014). Pharmacological activation of the melanocortin system limits plaque inflammation and ameliorates vascular dysfunction in atherosclerotic mice. *Arteriosclerosis, Thrombosis, and Vascular Biology*, *34*(7), 1346–1354. https://doi.org/10.1161/ATVBAHA.113.302963

Robbins, C. S., Hilgendorf, I., Weber, G. F., Theurl, I., Iwamoto, Y., Figueiredo, J.-L., Gorbatov, R., Sukhova, G. K., Gerhardt, L. M. S., Smyth, D., Zavitz, C. C. J., Shikatani, E. A., Parsons, M., van Rooijen, N., Lin, H. Y., Husain, M., Libby, P., Nahrendorf, M., Weissleder, R., & Swirski, F. K. (2013). Local proliferation dominates lesional macrophage accumulation in atherosclerosis. *Nature Medicine*, *19*(9), 1166–1172. https://doi.org/10.1038/nm.3258

Rosenfeld, M. E., Tsukada, T., Gown, A. M., & Ross, R. (1987). Fatty streak initiation in Watanabe Heritable Hyperlipemic and comparably hypercholesterolemic fat-fed rabbits. *Arteriosclerosis (Dallas, Tex.)*, *7*(1), 9–23. https://doi.org/10.1161/01.atv.7.1.9

Ross, R., & Glomset, J. A. (1976). The pathogenesis of atherosclerosis (first of two parts). *The New England Journal of Medicine*, *295*(7), 369–377. https://doi.org/10.1056/NEJM197608122950707

Sacks, D., Baxter, B., Campbell, B. C. V, Carpenter, J. S., Cognard, C., Dippel, D., Eesa, M., Fischer, U., Hausegger, K., Hirsch, J. A., Shazam Hussain, M., Jansen, O., Jayaraman, M. V, Khalessi, A. A., Kluck, B. W., Lavine, S., Meyers, P. M., Ramee, S., Rüfenacht, D. A., … Vorwerk, D. (2018). Multisociety Consensus Quality Improvement Revised Consensus Statement for Endovascular Therapy of Acute Ischemic Stroke. *International Journal of Stroke : Official Journal of the International Stroke Society*, *13*(6), 612–632. https://doi.org/10.1177/1747493018778713

Safarinejad, M. R., & Hosseini, S. Y. (2008). Salvage of sildenafil failures with bremelanotide: a randomized, double-blind, placebo controlled study. *The Journal of Urology*, *179*(3), 1066–1071. https://doi.org/10.1016/j.juro.2007.10.063

Sahm, U. G., Olivier, G. W., Branch, S. K., Moss, S. H., & Pouton, C. W. (1994). Synthesis and biological evaluation of alpha-MSH analogues substituted with alanine. *Peptides*, *15*(7), 1297–1302. https://doi.org/10.1016/0196-9781(94)90157-0

Sahm, U. G., Qarawi, M. A., Olivier, G. W., Ahmed, A. R., Branch, S. K., Moss, S. H., & Pouton, C. W. (1994). The melanocortin (MC3) receptor from rat hypothalamus: photoaffinity labelling and binding of alanine-substituted alpha-MSH analogues. *FEBS Letters*, *350*(1), 29–32. https://doi.org/10.1016/0014-5793(94)00725-x

Saigusa, R., Winkels, H., & Ley, K. (2020). T cell subsets and functions in atherosclerosis. *Nature Reviews. Cardiology*, *17*(7), 387–401. https://doi.org/10.1038/s41569-020-0352-5

Saporiti, F., Piacentini, L., Alfieri, V., Bono, E., Ferrari, F., Chiesa, M., & Colombo, G. I. (2019). Melanocortin-1 Receptor Positively Regulates Human Artery Endothelial Cell Migration. *Cellular Physiology and Biochemistry : International Journal of Experimental Cellular Physiology, Biochemistry, and Pharmacology*, *52*(6), 1339–1360. https://doi.org/10.33594/000000094

Şener, Y. Z., & Tokgözoğlu, L. (2022). Underutilisation of combination therapy in lipid lowering: A missed opportunity. *European Journal of Preventive Cardiology*. https://doi.org/10.1093/eurjpc/zwac251

Sharma, B. R., & Kanneganti, T.-D. (2021). NLRP3 inflammasome in cancer and metabolic diseases. *Nature Immunology*, *22*(5), 550–559. https://doi.org/10.1038/s41590-021-00886-5

Shimano, H., Ohsuga, J., Shimada, M., Namba, Y., Gotoda, T., Harada, K., Katsuki, M., Yazaki, Y., & Yamada, N. (1995). Inhibition of diet-induced atheroma formation in transgenic mice expressing apolipoprotein E in the arterial wall. *The Journal of Clinical Investigation*, *95*(2), 469–476. https://doi.org/10.1172/JCI117687

Simon, J. A., Kingsberg, S. A., Portman, D., Williams, L. A., Krop, J., Jordan, R., Lucas, J., & Clayton, A. H. (2019). Long-Term Safety and Efficacy of Bremelanotide for Hypoactive Sexual Desire Disorder. *Obstetrics and Gynecology*, *134*(5), 909–917. https://doi.org/10.1097/AOG.0000000000003514

Singh, J. A., Wells, G. A., Christensen, R., Tanjong Ghogomu, E., Maxwell, L., Macdonald, J. K., Filippini, G., Skoetz, N., Francis, D., Lopes, L. C., Guyatt, G. H., Schmitt, J., La Mantia, L., Weberschock, T., Roos, J. F., Siebert, H., Hershan, S., Lunn, M. P., Tugwell, P., & Buchbinder, R. (2011). Adverse effects of biologics: a network meta-analysis and Cochrane overview. *The Cochrane Database of Systematic Reviews*, *2011*(2), CD008794. https://doi.org/10.1002/14651858.CD008794.pub2

Stanisz, H., Seifert, M., Tilgen, W., Vogt, T., & Rass, K. (2011). Reciprocal responses of fibroblasts and melanocytes to α-MSH depending on MC1R polymorphisms. *Dermato-Endocrinology*, *3*(4), 259–265. https://doi.org/10.4161/derm.3.4.17454

Stary, H. C. (1989). Evolution and progression of atherosclerotic lesions in coronary arteries of children and young adults. *Arteriosclerosis (Dallas, Tex.)*, *9*(1 Suppl), I19-32.

Swirski, F. K., Libby, P., Aikawa, E., Alcaide, P., Luscinskas, F. W., Weissleder, R., & Pittet, M. J. (2007). Ly-6Chi monocytes dominate hypercholesterolemia-associated monocytosis and give rise to macrophages in atheromata. *The Journal of Clinical Investigation*, *117*(1), 195–205. https://doi.org/10.1172/JCI29950

Swirski, F. K., Nahrendorf, M., Etzrodt, M., Wildgruber, M., Cortez-Retamozo, V., Panizzi, P., Figueiredo, J.-L., Kohler, R. H., Chudnovskiy, A., Waterman, P., Aikawa, E., Mempel, T. R., Libby, P., Weissleder, R., & Pittet, M. J. (2009). Identification of splenic reservoir monocytes and their deployment to inflammatory sites. *Science (New York, N.Y.)*, *325*(5940), 612–616. https://doi.org/10.1126/science.1175202

Swirski, F. K., Pittet, M. J., Kircher, M. F., Aikawa, E., Jaffer, F. A., Libby, P., & Weissleder, R. (2006). Monocyte accumulation in mouse atherogenesis is progressive and proportional to extent of disease. *Proceedings of the National Academy of Sciences of the United States of America*, *103*(27), 10340–10345. https://doi.org/10.1073/pnas.0604260103

Tabas, I., & Bornfeldt, K. E. (2016). Macrophage Phenotype and Function in Different Stages of Atherosclerosis. *Circulation Research*, *118*(4), 653–667. https://doi.org/10.1161/CIRCRESAHA.115.306256

Tall, A. R., & Yvan-Charvet, L. (2015). Cholesterol, inflammation and innate immunity. *Nature Reviews. Immunology*, *15*(2), 104–116. https://doi.org/10.1038/nri3793

Tatro, J. B., & Sinha, P. S. (2003). The central melanocortin system and fever. *Annals of the New York Academy of Sciences*, *994*, 246–257. https://doi.org/10.1111/j.1749-6632.2003.tb03187.x

Toda, C., Santoro, A., Kim, J. D., & Diano, S. (2017). POMC Neurons: From Birth to Death. *Annual Review of Physiology*, *79*, 209–236. https://doi.org/10.1146/annurev-physiol-022516-034110

Tolani, S., Pagler, T. A., Murphy, A. J., Bochem, A. E., Abramowicz, S., Welch, C., Nagareddy, P. R., Holleran, S., Hovingh, G. K., Kuivenhoven, J. A., & Tall, A. R. (2013). Hypercholesterolemia and reduced HDL-C promote hematopoietic stem cell proliferation and monocytosis: studies in mice and FH children. *Atherosclerosis*, *229*(1), 79–85. https://doi.org/10.1016/j.atherosclerosis.2013.03.031

Toth, P. P., Worthy, G., Gandra, S. R., Sattar, N., Bray, S., Cheng, L.-I., Bridges, I., Worth, G. M., Dent, R., Forbes, C. A., Deshpande, S., Ross, J., Kleijnen, J., & Stroes, E. S. G. (2017). Systematic Review and Network Meta-Analysis on the Efficacy of Evolocumab and Other Therapies for the Management of Lipid Levels in Hyperlipidemia. *Journal of the American Heart Association*, *6*(10). https://doi.org/10.1161/JAHA.116.005367

Turner, D. L., & Farber, D. L. (2014). Mucosal resident memory CD4 T cells in protection and immunopathology. *Frontiers in Immunology*, *5*, 331. https://doi.org/10.3389/fimmu.2014.00331

Ugwu, S. O., Blanchard, J., Dorr, R. T., Levine, N., Brooks, C., Hadley, M. E., Aickin, M., & Hruby, V. J. (1997). Skin pigmentation and pharmacokinetics of melanotan-I in humans. *Biopharmaceutics & Drug Disposition*, *18*(3), 259–269. https://doi.org/10.1002/(sici)1099-081x(199704)18:3<259::aid-bdd20>3.0.co;2-x

Upadhye, A., Sturek, J. M., & McNamara, C. A. (2020). 2019 Russell Ross Memorial Lecture in Vascular Biology: B Lymphocyte-Mediated Protective Immunity in Atherosclerosis. In *Arteriosclerosis, thrombosis, and vascular biology* (Vol. 40, Issue 2, pp. 309–322). https://doi.org/10.1161/ATVBAHA.119.313064

van Wanrooij, E. J. A., Happé, H., Hauer, A. D., de Vos, P., Imanishi, T., Fujiwara, H., van Berkel, T. J. C., & Kuiper, J. (2005). HIV entry inhibitor TAK-779 attenuates atherogenesis in low-density lipoprotein receptor-deficient mice. *Arteriosclerosis, Thrombosis, and Vascular Biology*, *25*(12), 2642–2647. https://doi.org/10.1161/01.ATV.0000192018.90021.c0

Véniant, M M, Withycombe, S., & Young, S. G. (2001). Lipoprotein size and atherosclerosis susceptibility in Apoe(-/-) and Ldlr(-/-) mice. *Arteriosclerosis, Thrombosis, and Vascular Biology*, *21*(10), 1567–1570. https://doi.org/10.1161/hq1001.097780

Véniant, Murielle M, Beigneux, A. P., Bensadoun, A., Fong, L. G., & Young, S. G. (2008). Lipoprotein size and susceptibility to atherosclerosis--insights from genetically modified mouse models. *Current Drug Targets*, *9*(3), 174–189. https://doi.org/10.2174/138945008783755629

Vila, M. D. M., Remeseiro, B., Igual, L., Elosua, R., Ramos, R., Valdivielso, J. M., Martí-Lluch, R., Marrugat, J., & Grau, M. (2021). Do individuals with autoimmune disease have increased risk of subclinical carotid atherosclerosis and stiffness? *Hypertension Research : Official Journal of the Japanese Society of Hypertension*, *44*(8), 978–987. https://doi.org/10.1038/s41440-021-00655-9

W.H.O. (n.d.). *WHO reveals leading causes of death and disability worldwide: 2000-2019*. Retrieved February 16, 2023, from https://www.who.int/news/item/09-12-2020-who-reveals-leading-causes-of-death-and-disability-worldwide-2000-2019

Walker, W. P., & Gunn, T. M. (2010). Shades of meaning: the pigment-type switching system as a tool for discovery. *Pigment Cell & Melanoma Research*, *23*(4), 485–495. https://doi.org/10.1111/j.1755-148X.2010.00721.x

Wang, W., Guo, D.-Y., Lin, Y.-J., & Tao, Y.-X. (2019). Melanocortin Regulation of Inflammation. *Frontiers in Endocrinology*, *10*, 683. https://doi.org/10.3389/fendo.2019.00683

Wang, W., Lin, Y.-J., Chen, Z.-X., & Guo, D.-Y. (2021). Identification and characterization of two novel melanocortin-3 receptor mutations in Chinese obese individuals. *Biochimica et Biophysica Acta. Molecular Basis of Disease*, *1867*(6), 166107. https://doi.org/10.1016/j.bbadis.2021.166107

Wang, X., Fu, Y., Xie, Z., Cao, M., Qu, W., Xi, X., Zhong, S., Piao, M., Peng, X., Jia, Y., Meng, L., & Tian, J. (2021). Establishment of a Novel Mouse Model for Atherosclerotic Vulnerable Plaque. *Frontiers in Cardiovascular Medicine*, *8*, 642751. https://doi.org/10.3389/fcvm.2021.642751

Watson, M. G., Byrne, H. M., Macaskill, C., & Myerscough, M. R. (2018). A two-phase model of early fibrous cap formation in atherosclerosis. *Journal of Theoretical Biology*, *456*, 123–136. https://doi.org/10.1016/j.jtbi.2018.08.010

Wessells, H., Hruby, V. J., Hackett, J., Han, G., Balse-Srinivasan, P., & Vanderah, T. W. (2003). Ac-Nle-c[Asp-His-DPhe-Arg-Trp-Lys]-NH2 induces penile erection via brain and spinal melanocortin receptors. *Neuroscience*, *118*(3), 755–762. https://doi.org/10.1016/s0306-4522(02)00866-7

Westerterp, M., Bochem, A. E., Yvan-Charvet, L., Murphy, A. J., Wang, N., & Tall, A. R. (2014). ATP-binding cassette transporters, atherosclerosis, and inflammation. *Circulation Research*, *114*(1), 157–170. https://doi.org/10.1161/CIRCRESAHA.114.300738

Westerterp, M., Murphy, A. J., Wang, M., Pagler, T. A., Vengrenyuk, Y., Kappus, M. S., Gorman, D. J., Nagareddy, P. R., Zhu, X., Abramowicz, S., Parks, J. S., Welch, C., Fisher, E. A., Wang, N., Yvan-Charvet, L., & Tall, A. R. (2013). Deficiency of ATP-binding cassette transporters A1 and G1 in macrophages increases inflammation and accelerates atherosclerosis in mice. *Circulation Research*, *112*(11), 1456–1465. https://doi.org/10.1161/CIRCRESAHA.113.301086

White, H. D., Held, C., Stewart, R., Tarka, E., Brown, R., Davies, R. Y., Budaj, A., Harrington, R. A., Steg, P. G., Ardissino, D., Armstrong, P. W., Avezum, A., Aylward, P. E., Bryce, A., Chen, H., Chen, M.-F., Corbalan, R., Dalby, A. J., Danchin, N., … Wallentin, L. (2014). Darapladib for preventing ischemic events in stable coronary heart disease. *The New England Journal of Medicine*, *370*(18), 1702–1711. https://doi.org/10.1056/NEJMoa1315878

Wikberg, J. E. S., & Mutulis, F. (2008). Targeting melanocortin receptors: an approach to treat weight disorders and sexual dysfunction. *Nature Reviews. Drug Discovery*, *7*(4), 307–323. https://doi.org/10.1038/nrd2331

Winkels, H., Ehinger, E., Vassallo, M., Buscher, K., Dinh, H. Q., Kobiyama, K., Hamers, A. A. J., Cochain, C., Vafadarnejad, E., Saliba, A.-E., Zernecke, A., Pramod, A. B., Ghosh, A. K., Anto Michel, N., Hoppe, N., Hilgendorf, I., Zirlik, A., Hedrick, C. C., Ley, K., & Wolf, D. (2018). Atlas of the Immune Cell Repertoire in Mouse Atherosclerosis Defined by Single-Cell RNA-Sequencing

and Mass Cytometry. *Circulation Research*, *122*(12), 1675–1688. https://doi.org/10.1161/CIRCRESAHA.117.312513

Woollard, K. J., & Geissmann, F. (2010). Monocytes in atherosclerosis: subsets and functions. *Nature Reviews. Cardiology*, *7*(2), 77–86. https://doi.org/10.1038/nrcardio.2009.228

Xu, H., Jiang, J., Chen, W., Li, W., & Chen, Z. (2019). Vascular Macrophages in Atherosclerosis. *Journal of Immunology Research*, *2019*, 4354786. https://doi.org/10.1155/2019/4354786

Xu, Y., Guan, X., Zhou, R., & Gong, R. (2020). Melanocortin 5 receptor signaling pathway in health and disease. *Cellular and Molecular Life Sciences : CMLS*, *77*(19), 3831–3840. https://doi.org/10.1007/s00018-020-03511-0

Yang, Y. (2011). Structure, function and regulation of the melanocortin receptors. *European Journal of Pharmacology*, *660*(1), 125–130. https://doi.org/10.1016/j.ejphar.2010.12.020

Yeo, G. S. H., Chao, D. H. M., Siegert, A.-M., Koerperich, Z. M., Ericson, M. D., Simonds, S. E., Larson, C. M., Luquet, S., Clarke, I., Sharma, S., Clément, K., Cowley, M. A., Haskell-Luevano, C., Van Der Ploeg, L., & Adan, R. A. H. (2021). The melanocortin pathway and energy homeostasis: From discovery to obesity therapy. *Molecular Metabolism*, *48*, 101206. https://doi.org/10.1016/j.molmet.2021.101206

Yuan, X.-C., & Tao, Y.-X. (2022). Ligands for Melanocortin Receptors: Beyond Melanocyte-Stimulating Hormones and Adrenocorticotropin. *Biomolecules*, *12*(10). https://doi.org/10.3390/biom12101407

Yvan-Charvet, L., Ranalletta, M., Wang, N., Han, S., Terasaka, N., Li, R., Welch, C., & Tall, A. R. (2007). Combined deficiency of ABCA1 and ABCG1 promotes foam cell accumulation and accelerates atherosclerosis in mice. *The Journal of Clinical Investigation*, *117*(12), 3900–3908. https://doi.org/10.1172/JCI33372

Zhang, S. H., Reddick, R. L., Piedrahita, J. A., & Maeda, N. (1992). Spontaneous hypercholesterolemia and arterial lesions in mice lacking apolipoprotein E. *Science (New York, N.Y.)*, *258*(5081), 468–471. https://doi.org/10.1126/science.1411543

Zhou, X, Nicoletti, A., Elhage, R., & Hansson, G. K. (2000). Transfer of CD4(+) T cells aggravates atherosclerosis in immunodeficient apolipoprotein E knockout mice. *Circulation*, *102*(24), 2919–2922. https://doi.org/10.1161/01.cir.102.24.2919

Zhou, Xinghua, Robertson, A.-K. L., Hjerpe, C., & Hansson, G. K. (2006). Adoptive transfer of CD4+ T cells reactive to modified low-density lipoprotein aggravates atherosclerosis. *Arteriosclerosis, Thrombosis, and Vascular Biology*, *26*(4), 864–870. https://doi.org/10.1161/01.ATV.0000206122.61591.ff

Zhou, Y., & Cai, M. (2017). Novel approaches to the design of bioavailable melanotropins. *Expert Opinion on Drug Discovery*, *12*(10), 1023–1030. https://doi.org/10.1080/17460441.2017.1351940

Zhou, Y., Mowlazadeh Haghighi, S., Zoi, I., Sawyer, J. R., Hruby, V. J., & Cai, M. (2017). Design of MC1R Selective γ-MSH Analogues with Canonical Amino Acids Leads to Potency and Pigmentation. *Journal of Medicinal Chemistry*, *60*(22), 9320–9329. https://doi.org/10.1021/acs.jmedchem.7b01295

Appendices

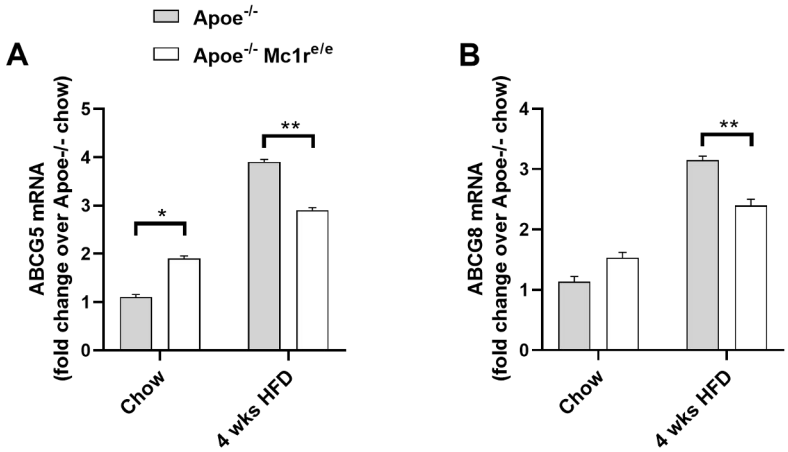

Figure 1. Hepatic expression of cholesterol transport genes in *Apoe*$^{-/-}$ and *Apoe*$^{-/-}$*Mc1r*$^{e/e}$ mice (Modified from original communication I). Quantitative RT-PCR analysis of genes involved in cholesterol transport in the liver of *Apoe*$^{-/-}$ and *Apoe*$^{-/-}$ *Mc1r*$^{e/e}$ mice fed a normal chow diet or high-fat diet (HFD) for 4 weeks. (**A**) ABCG5, ATP-binding cassette sub-family G member 5. (**B**), ABCG8, ATP-binding cassette sub-family G member 8. n=4-6 mice per group. * P<0.05 and ** P<0.01 versus *Apoe*$^{-/-}$ mice. Data are mean ± SEM by 2-way ANOVA and Bonferroni *post hoc* tests.

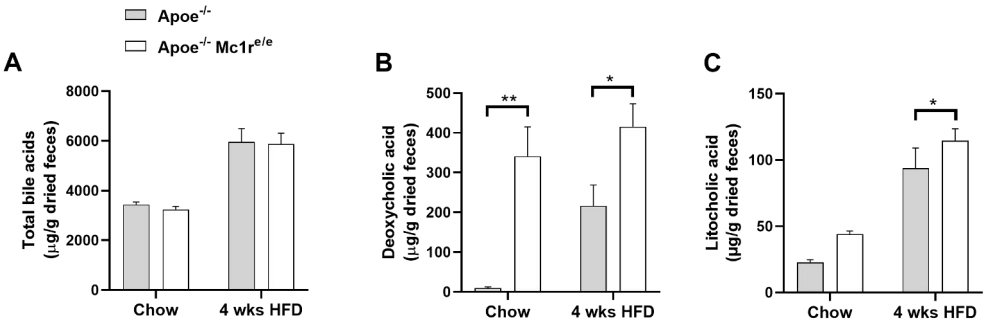

Figure 2. Composition of the fecal bile acid pool in *Apoe*$^{-/-}$ and *Apoe*$^{-/-}$*Mc1r*$^{e/e}$ mice. (Modified from original communication I). Feces were collected over 48 h and quantified for (**A**) total bile acids and (**B-C**) the secondary bile acids deoxycholic acid and litocholic acid. The results are presented as µg per g of dried feces. * P<0.05 and ** P<0.01 versus *Apoe*$^{-/-}$ mice. Data are mean ± SEM by 2-way ANOVA and Bonferroni *post hoc* tests. n=4-6 mice per group.

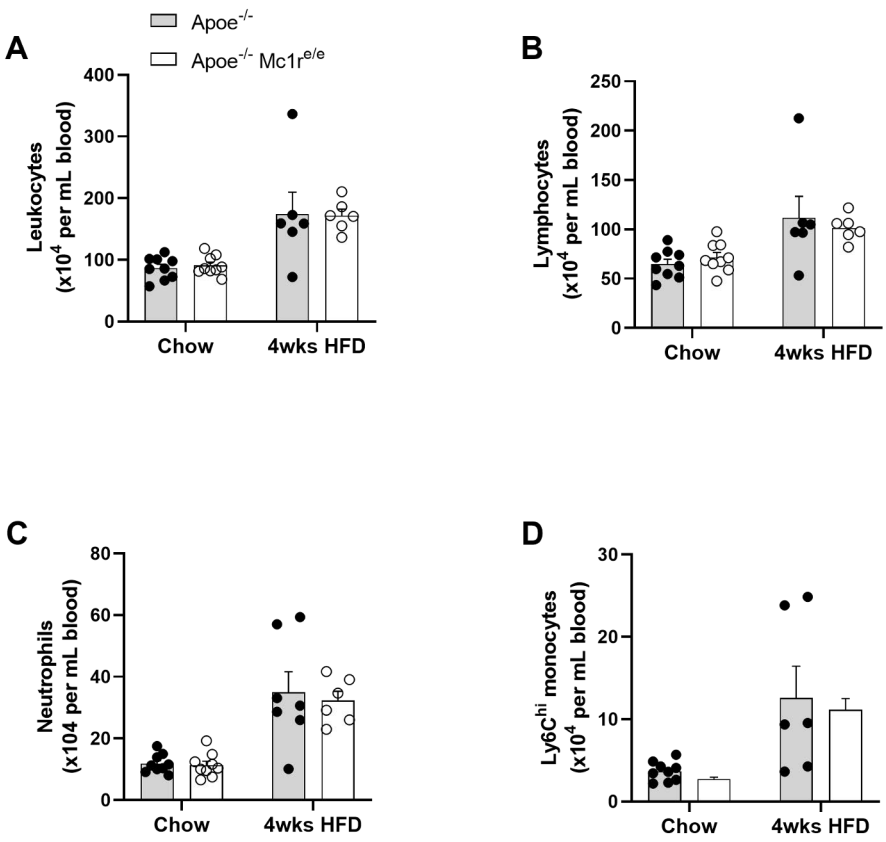

Figure 3. Quantification of total leukocytes and their subsets profiles in the blood of *Apoe*$^{-/-}$ and *Apoe*$^{-/-}$ *Mc1r*$^{e/e}$ mice. (Modified from original communication I). (**A**) Quantification of total leukocytes (CD45^{+}), (**B**) lymphocytes (CD45^{+}, CD11b^{-}), (**C**) neutrophils (CD45^{+}, CD11b^{+}, Ly6G^{+}) and (**D**) Ly6C^{high} monocytes (CD45^{+}, CD11b^{+}, CD115^{+}, Ly6C^{high}) in the blood of *Apoe*$^{-/-}$ *and Apoe*$^{-/-}$ *Mc1r*$^{e/e}$ mice fed a standard chow diet or high-fat diet (HFD) for 4 weeks. n=6 – 10 mice/group. *p<0.05 vs *Apoe*$^{-/-}$ mice. Values are mean±SEM (two-way ANOVA for diet and genotype effects). Each dot represents individual mouse.

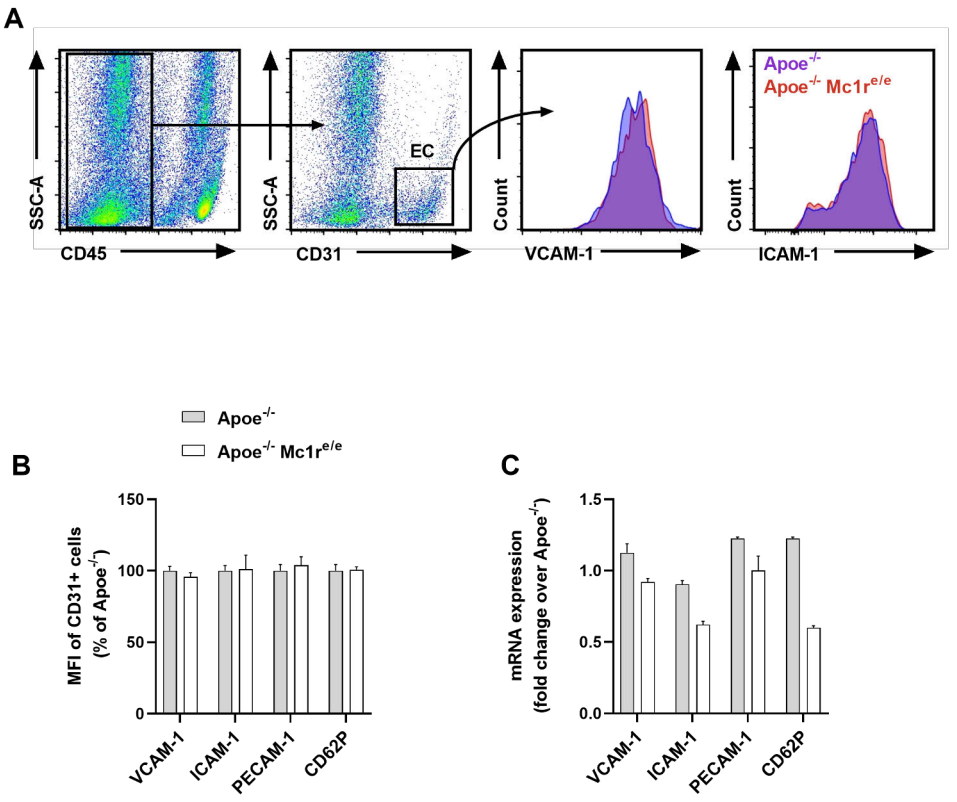

Figure 4. Deficiency in *Mc1r* does not affect adhesion molecule expression in the aortic endothelium. (Modified from original communication I). (**A**) Representative dot plots for the gating of endothelial cells ($CD45^{-}$, $CD31^{+}$) in aortic lysates and histograms for VCAM-1 (vascular cell adhesion molecule 1) and ICAM-1 (intercellular adhesion molecule 1) staining. (**B**), Mean fluorescence intensity (MFI, expressed as percentage of *Apoe*$^{-/-}$ mice) of VCAM-1, ICAM-1, PECAM-1 (platelet and endothelial cell adhesion molecule 1), and CD62P in aortic endothelial cells of chow-fed *Apoe*$^{-/-}$ and *Apoe*$^{-/-}$ *Mc1r*$^{e/e}$ mice. (**C**), Quantitative real-time-polymerase chain reaction analysis of *Vcam1*, *Icam1*, *Pecam1*, and *Cd62p* expression in the whole aorta of chow-fed *Apoe*$^{-/-}$ and *Apoe*$^{-/-}$ *Mc1r*$^{e/e}$ mice. Values are mean±SEM (Student's *t*-test for unpaired samples). n=6 to 8 mice per group in each graph.

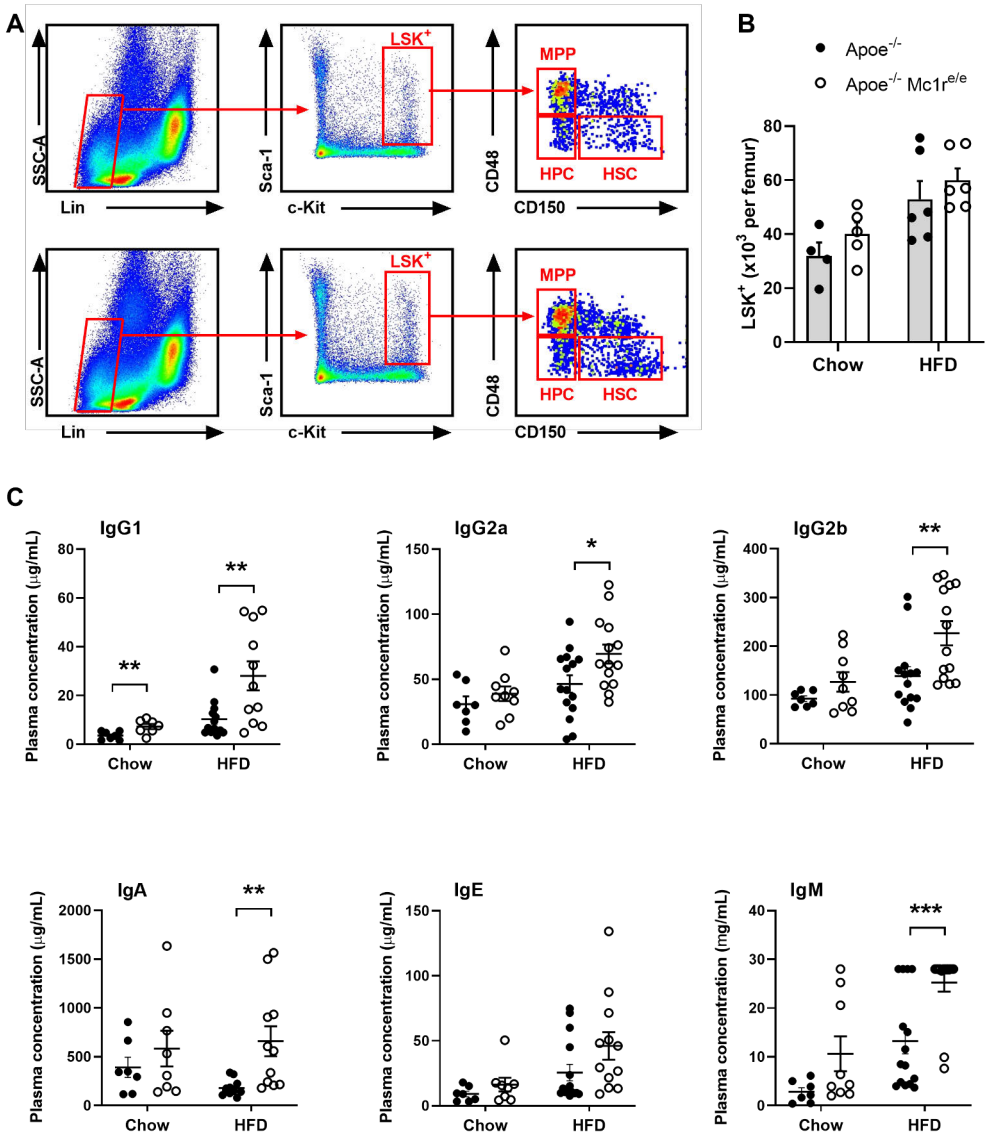

Figure 5. Hematopoietic MC1R deficiency increased hematopoietic stem cell counts in the bone marrow and plasma immunoglobulin levels of *Apoe*$^{-/-}$ recipient mice. (Modified from original communication II). (**A**) Representative dot plots for the gating of LSK^{+} (Lin^{-}, Sca-1^{+}, c-Kit^{+}), MPP (CD48^{+}, CD150^{-}), HPC (CD48^{-}, CD150^{-}), HSC (CD150^{+}, CD48^{-}) cells in the bone marrow of *Apoe*$^{-/-}$recipient mice. (**B**) Quantification of LSK^{+} cells in the bone marrow. (**C**) Quantification of plasma immunoglobulin concentrations (µg/mL) in *Apoe*$^{-/-}$ and *Apoe*$^{-/-}$ *Mc1r*$^{e/e}$ chimeric mice. Data are mean ± SEM (two-way ANOVA for diet and genotype effects on stem cells count and unpaired Student's t-test for plasma Ig expression), *P ≤ 0.05, **P < 0.01, ***P < 0.001 versus *Apoe*$^{-/-}$ mice. Each dot represents individual mouse. Lin^{-} indicates lineage-negative; Sca^{-1}, stem-cell antigen-1; c-Kit, proto-oncogene receptor tyrosin kinase; MPP, multi-potent progenitor; HSC, hematopoietic stem cell; HPC, hematopoietic progenitor cell; IgG immunoglobulin type G; IgA immunoglobulin type A; IgE immunoglobulin type E; IgM immunoglobulin type M.

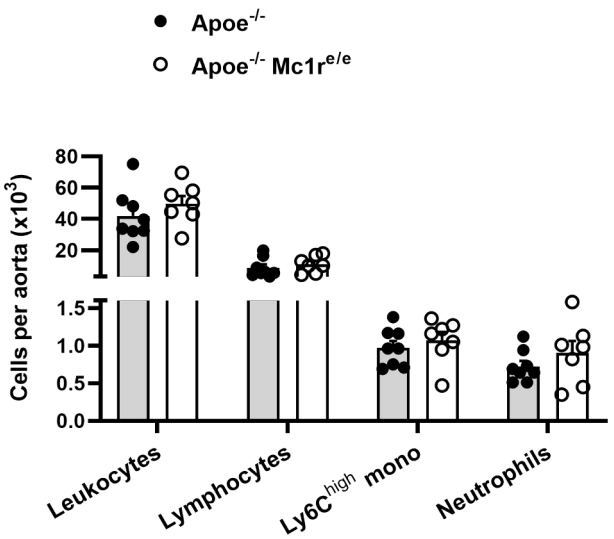

Figure 6. Hematopoietic MC1R deficiency did not alter leukocyte expression in the aorta of *Apoe*$^{-/-}$ recipient mice. (Modified from original communication II). Quantification of total leukocytes (CD45$^+$), lymphocytes (CD45$^+$, CD11b$^-$), Ly6C^{high} monocytes (CD45$^+$, CD11b$^+$, CD115$^+$, Ly6C^{high}) and neutrophils (CD45$^+$, CD11b$^+$, Ly6G$^+$) by flow cytometry in the aorta of *Apoe*$^{-/-}$ recipient mice. Data are mean ± SEM (Student's *t*-test for unpaired samples). Each dot represents individual mouse.

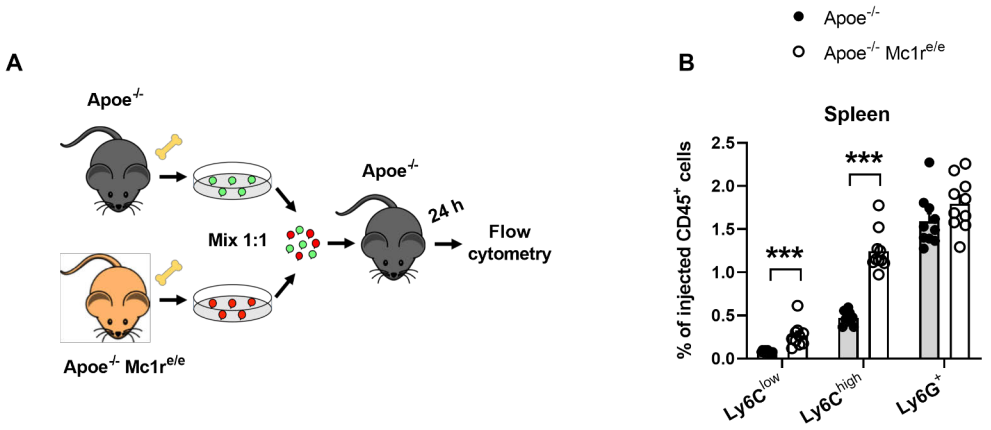

Figure 7. MC1R deficient monocytes preferentially home into the spleen. (Modified from original communication II). (**A**) Experimental setup to analyze homing of Ly6C^{high} and Ly6C^{low} monocytes and Ly6G$^+$ neutrophils to the spleen. Cells were isolated from the bone marrow of *Apoe*$^{-/-}$ and *Apoe*$^{-/-}$ *Mc1r*$^{e/e}$ mice and injected into recipient *Apoe*$^{-/-}$ mice. (**B**) Quantification of Ly6C^{low} monocytes (CD45$^+$, CD11b$^+$, CD115$^+$, Ly6C^{high}), Ly6C^{high} monocytes (CD45$^+$, CD11b$^+$, CD115$^+$, Ly6C^{low}) and neutrophils (CD45$^+$, CD11b$^+$, CD115$^-$, Ly6G$^+$) in the spleen as percentage of injected CD45$^+$ cells. Data are mean ± SEM (Student's *t*-test for unpaired samples), ***P < 0.001 versus *Apoe*$^{-/-}$ mice. Each dot represents individual mouse.

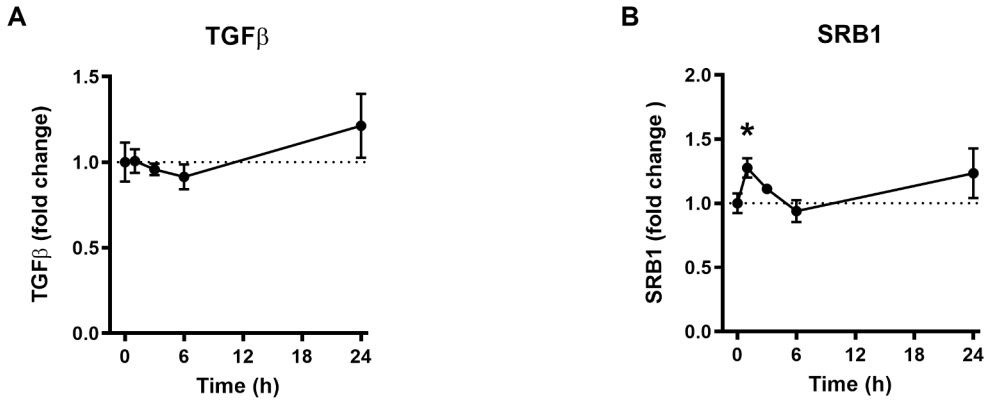

Figure 8. The effects of [D-Trp8]-γ-MSH on the expression of M1- and M2-type macrophage markers in bone marrow-derived macrophages. (Modified from original communication III). Quantitative RT-PCR analysis of transforming growth factor β (TGF-β, T*gfb*) (**A**) and scavenger receptor class B type 1 (SR-B1, *Scarb1*) (**B**) transcript expression in mouse bone marrow-derived macrophages that were treated with 1 μM [D-Trp8]-γ-MSH for 1-24 h or left untreated (control, 0 h time point). Data are mean ± S.E.M (Student's *t*-test for unpaired samples). n = 3-6 per group. *P < 0.05 versus control.

TURUN
YLIOPISTO
UNIVERSITY
OF TURKU

Painosalama, Turku, Finland 2023

ISBN 978-951-29-9242-3 (PRINT)
ISBN 978-951-29-9243-0 (PDF)
ISSN 0355-9483 (Print)
ISSN 2343-3213 (Online)